On thermo-acoustic and photo-acoustic Imaging of small absorbers

Hanin Al Jebawy

Par **Hanin AL JEBAWY**

Sur l'imagerie thermoacoustique et photoacoustique de petits absorbeurs

Thèse présentée en cotutelle pour l'obtention du grade de Docteur de l'UTC

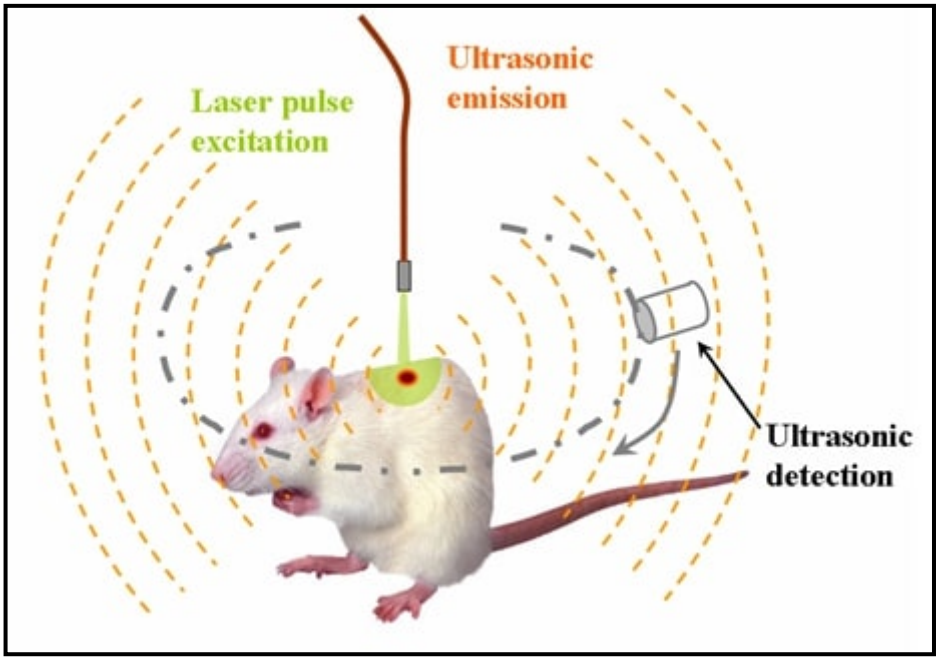

Soutenue le 22 octobre 2020
Spécialité : Mathématiques Appliquées : Laboratoire de Mathématiques Appliquées de Compiègne (Unité de recherche EA-2222)
D2588

Université Libanaise

École Doctorale
Sciences et Technologies

ALLIANCE SORBONNE UNIVERSITÉ

utc

THÈSE de doctorat en Cotutelle

Pour obtenir le grade de Docteur délivré par

L'Université Libanaise, L'École Doctorale des Sciences et Technologie

et

L'Université de Technologie de Compiègne, L'École Doctorale des Sciences pour les Ingénieries

Spécialité : Mathématiques Appliquées

Présentée et soutenue publiquement par

AL JEBAWY Hanin

22 Octobre 2020

Sur L'imagerie Thermoacoustique et Photoacoustique de petits absorbeurs

Directeurs de thèse **: EL BADIA Abdellatif- IBRAHIM Hassan**

Co-encadrement de la thèse **: NASREDDINE Elissar**

Membres du Jury

M. BONNET Marc, Professeur, École Nationale Supérieure de Techniques Avancées	Rapporteur
M. REN Kui Professeur, University of Columbia	Rapporteur
Mme ABDELAZIZ Batoul, Professeur Assistante	Examinateur
M. CHEHAB Jean-Paul, Professeur, Université de Picardie Jules Verne	Examinateur
M. DE VUYST Florian, Professeur, Université de Technologie de Compiègne	Examinateur
M. El BADIA Abdellatif, Professeur, Université de Technologie de Compiègne	Directeur
M. IBRAHIM Hassan, Professeur, Université Libanaise	Directeur
Mme. NASREDDINE Elissar, Professeur Associé, Université Libanaise	Co-Directeur

On Thermo-acoustic and Photo-acoustic Imaging of Small Absorbers

Hanin Al Jebawy

October 22, 2020

Abstract

This thesis is divided into two parts. The first part is dedicated to the study of inverse problems for wave equations and their application to medical imaging. More precisely, we focus our work on the study of the photo-acoustic and thermo-acoustic tomography techniques. They are multi-wave imaging techniques based on the photo-acoustic effect that was discovered in 1880 by Alexander Graham Bell. The inverse problem we are concerned in throughout this thesis is the problem of recovering small absorbers in a bounded domain $\Omega \subset \mathbb{R}^3$. We provide a direct reconstruction method based on the algebraic algorithm that was developed first in [34], without following the quantitative photo-acoustic tomography approach (qPAT). This algorithm allows us to reconstruct the number of the absorbers and their locations from a single Cauchy data, in addition to some information on optical parameters such as the conductivity and the absorption coefficient that can serve as an important diagnostic information in detecting tumors. The main difference between PAT and TAT is in the type of optical pulse used. In PAT, a high frequency radiation is delivered into the biological tissue to be imaged, while in TAT low frequency radiations are used, which makes some differences in the physical and mathematical setting of the problem. In this dissertation we study the both mathematical models, and propose reconstruction algorithms for the two inverse problems. The second part of this thesis is devoted to the study of non-autonomous semilinear elliptic equations. We study the existence of radial solution in $\mathbb{R}^n$ with non zero limiting behavior.

Keywords: inverse source problems, photo-acoustic tomography, thermo-acoustic tomography, algebraic algorithm, semilinear elliptic equations.

Resumé

CEtte thèse est divisée en deux parties. La première partie porte sur l'etude de problèmes inverses pour les équations des ondes et leur application à l'imagerie photoacoustique (PAT) et thermoacoustique (TAT). Ces sont des techniques d'imagerie multi-ondes basées sur l'effet photoacoustique découvert en 1880 par Alexander Graham Bell . Le problème inverse qui nous intéresse consiste à rècupèrer des petits absorbeurs dans un domaine bonrnè. On a développé un algorithme direct, en se basant sur la méthode algébrique, sans suivre l'approache d'imagerie photo-acoustique quantitative. Cet algorithme nous permet de reconstruire le nombre des absorbeurs et leur localisation à partir d'une seule observation aux bords. En plus, cet algorithme nous procure la connaissance des informations concernant les paramètres optiques tels que la conductivité et le coefficient d'absorption. Ces paramètres jouent un rôle primordial dans la détection des tumeurs. Les problèmes PAT et TAT se diffèrent principalement de type d'impulsion optique utilisée. Autrement dit, dans le PAT, on envoie une radiation à haute fréquence vers le tissue à imager. Tandis que, dans le TAT, une radiation à basse fréquence est utilisé. Ceci explique les différences dans le cadre physique et mathématique du problème. Dans cette thèse, on étudie les deux modèles mathématiques, et on propose des algorithmes de reconstruction pour les deux problèmes inverses. La deuxième partie de cette thèse consiste à étudier les équations elliptiques semi-linéaires non-autonomes. Précisément, on montre l'existence dans $\mathbb{R}^n$, des solutions radiales ne s'annulant pas à l'infini.

Mots clés: problèmes inverses, photoacoustique, thermoacoustique, méthode algébrique, équations elliptiques semi-linéaires.

List of Publications

Published Articles

- Direct algorithm for reconstructing small absorbers in thermo-acoustic tomography problem from a single data. Inverse Problems (2020). Presented in Chapter 3 (with Abdellatif EL BADIA).
- Radial and asymptotically constant solutions for nonautonomous elliptic equations. Applicable Analysis, 1-13 (2020). Presented in Chapter 5 (with Hassan IBRAHIM and Elissar NASREDDINE).

Submitted Articles

- On a photo-acoustic imaging problem for small absorbers. Presented in Chapter 4 (with Abdellatif EL BADIA)

Acknowledgments

This thesis has been accomplished with the help and support of different individuals to whom I would like to express my deep appreciation and gratitude.

First, I want to thank my supervisors Abdellatif EL BADIA and Hassan IBRAHIM for their continuous support and remarkable efforts to fulfill this work. Their expertise and knowledge added considerably to this thesis. I would like to express my deep appreciation for their guidance and motivation that highly inspired me throughout my entire years of research. I hope our collaboration will continue long after this thesis.

Also, I want to thank Professor Faouzi TRIKI for the fruitful discussions and advices that made a remarkable touch in this thesis.

I would like to thank the committee members, and Professors Marc BONNET and Kui REN for accepting to be the thesis manuscript referees. I am grateful to submit my work for such impressive reporters.

I also want to thank Walid Joumblatt foundation for university studies, ANR France and the Lebanese University for financially supporting me through my doctoral fellowship years.

Furthermore, I want to thank all the members of LMAC (Laboratoire de Mathématiques Appliquées de Compiègne): The director Florian De Vuyst, the secretary Maryline Schaefflen, and all the colleagues for being extremely friendly, helpful and supportive.

On the other hand, I want to express my deep thanks to the KALMA family (Khawarizmi Laboratory for Applied Mathematics) and all my friends there especially Rayan, Sara , Alaa, and Mohammad. Thank you for being such a special family and wonderful friends. Also I want to express my gratitude to Abir MOUKADDEM for all her guidance and help in the administrative issues. Thank you for your patience and for always helping and guiding me.

In addition, I am very thankful to the Lebanese International University (LIU), my mother university, and especially the academic director Dr. Ahmad Faraj and the head of the mathematics department Dr. Yehya Awad for all their support and advices throughout my entire years of study and career life.

No words can express my thanks and gratitude to my friends: Khawla, Darine, Saly, Boutheina, Aya, Maryam, Iman, Vivian and Bassam. Thank you for being my second family here in France,

and for all the special memories and unforgettable moments we had together. Without your presence, my journey wouldn't have been such special and amazing.

Finally, I am extremely grateful to my parents, brother and sisters for their love, caring, prayers and sacrifices that made me the person who I am today. Without your presence in my life, this journey would have never been accomplished. Thank you very much, and I will always be grateful for your love.

Last but not least, I want to thank my Mathematics teacher at the secondary school who said to me one day " I trust you, and I am sure that you will be a special mathematician one day". I always remembered your words in my hard times and they always inspired me to continue the journey.

List of Figures

Contents

Preface

Either write something worth reading or do something worth writing.

– Benjamin Franklin

1 Objective and Organization

This thesis is done under joint supervision agreement between the Lebanese University and the University of Technology of Compiègne. For this purpose, our work in this thesis is divided into two main parts. The objective of the first part, which constitutes the principal part of this thesis, is to study some inverse source problems for wave equations and their application to medical imaging. In particular, we focus our study on photo-acoustic and thermo-acoustic tomography (PAT and TAT), which are multi-wave imaging techniques based on the photo-acoustic effect (generation of sound from light). In both techniques, the object is illuminated by a laser pulse, and some of the delivered energy is absorbed by the biological tissues, which in return produce acoustic waves that propagate inside the medium until they reach the boundary. These waves are measured by transducers located at the boundary and an image is produced. The main tool of such imaging techniques is the difference in energy absorption between healthy tissues and cancerous ones.

The main difference between the two modalities is in the type of optical pulse used. In PAT a high frequency radiation is delivered into the biological tissue to be imaged, while in TAT low frequency radiations are used. This makes some differences in the mathematical context of the two problems. In this thesis, we study the two problems, and we give a direct reconstruction algorithm to resolve the inverse problem of reconstructing the locations of the tumors in both cases, in addition to some diagnostic information. This part was done under the supervision of Pr. Abdellatif EL BADIA during my stay in France.

The second part of this thesis is dedicated to the study of semilinear elliptic equations. In particular, we study the existence of radial solutions for the equation $\Delta u + g(|x|, u) = 0$ in $\mathbb{R}^n$ with non zero limiting behavior. These equations widely appear in the domain of quantum physics. In particular, solutions of semilinear elliptic equations can be viewed as stationary states for different equations such as the reaction diffusion equation, wave equation and Schrödinger equation.

This part of the thesis was done in Lebanon, under the supervision of Pr. Hassan IBRAHIM and in collaboration with Dr. Elissar NASREDDINE.

This manuscript is organized as follows.

Chapter 1 presents a general introduction to the topics discussed in this thesis. We present the idea of medical imaging, and the techniques of photo-acoustic and thermo-acoustic tomography. Moreover, we describe the difference between the two modalities and we give the mathematical derivation of both problems, then we introduce the inverse problem behind each technique. Furthermore, we illustrate the problem of semilinear elliptic equations, and we discuss the existence and behavior of solutions for such equations.

Chapter 2 is dedicated to the exact controllability problem for wave equations, which is an important tool used in our reconstruction algorithms throughout this thesis. We adapt the work of J.L. Lions in [60] on the exact controllability problem for wave equation with constant speed and we prove, following the Hilbert uniqueness method (HUM), the validity of his results in the case of variable speed.

Chapter 3 is intended to the study of the TAT problem. We introduce the inverse problem, and we provide a direct reconstruction method following the algebraic algorithm developed first in [34]. This algorithm allows us, from a single Cauchy data, to resolve the inverse problem of reconstructing the number of the absorbers (tumors) and their locations. Moreover, we provide a Hölder stability estimate.

Chapter 4 discusses the PAT problem. We follow the same algebraic algorithm used in the TAT problem, however, the high frequency radiation used in this case makes some changes in the mathematical context of the problem. More precisely, it allows us to provide our reconstruction algorithm in both cases of constant and variable acoustic speed, and with partial boundary observations. Also, we provide the corresponding stability estimate.

Chapter 5 is devoted to the second part of this thesis, which is the study of the existence of radial solution for the non-autonomous semilinear elliptic equation $\Delta u + g(|x|, u) = 0$ with non zero limiting behavior. We revisit the work of [49] on autonomous systems and we develop an ODE based method to resolve the problem. In particular we take $r = |x|$, then the radial solution $u(r)$ satisfies the ODE

$$\begin{cases} -u'' - \dfrac{N-1}{r}u' = g(r,u) \quad \text{for} \quad 0 < r < \infty \\ u(0) = \xi, \quad u'(0) = 0. \end{cases} \tag{0.1}$$

Our goal in this chapter is to study the existence of $\xi > 0$ such that the solution u satisfies $\lim_{r\to\infty} u(r) = z < \infty$, where $z \neq 0$ satisfies $g(r, z) = 0$ for every $r \geq 0$.

Notations

We define some spaces and notations that are used throughout this thesis. Let Ω be a bounded set in $\mathbb{R}^n$, for $n \geq 1$, then we define the following spaces.

- $L^\infty(\Omega)$: Set of bounded functions. More precisely, we say that $f : \Omega \longrightarrow \mathbb{R}$ is in $L^\infty(\Omega)$ if there exists $C > 0$ such that $|f(x)| \leq C$ a.e. in Ω. Moreover, we have

$$\|f\|_{L^\infty(\Omega)} = \|f\|_\infty = \inf\{C > 0 \text{ such that } |f(x)| \leq C \text{ a.e. in } \Omega\}.$$

- $L^p(\Omega) = \{f : \Omega \longrightarrow \mathbb{R} \text{ such that } \int_\Omega |f(x)|^p dx < \infty\}$, with

$$|f|_{L^p(\Omega)} = |f|_p = \left(\int_\Omega |f(x)|^p dx\right)^{\frac{1}{p}}.$$

  In particular, for $f \in L^2(\Omega)$ we define

$$|f|_2 = \left(\int_\Omega |f(x)|^2 dx\right)^{\frac{1}{2}}.$$

Now, we define the following Sobolev spaces named after the Russian mathematician Sergei Sobolev.

- $W^{m,p}(\Omega) = \{f : \Omega \longrightarrow \mathbb{R} \text{ such that } f \in L^p(\Omega) \text{ and } D^\alpha f \in L^p(\Omega) \text{ for all } |\alpha| \leq m\}$.

In particular, we have

- $H^2(\Omega) = W^{2,2}(\Omega) = \{f : \Omega \longrightarrow \mathbb{R} \text{ such that } f \in L^2(\Omega) \text{ and } D^\alpha f \in L^2(\Omega) \text{ for all } |\alpha| \leq 2\}$.
- $H^1(\Omega) = W^{1,2}(\Omega) = \{f : \Omega \longrightarrow \mathbb{R} \text{ such that } f, Df \in L^2(\Omega)\}$, with

$$\|f\|_{H^1(\Omega)} = \left(|f|_2^2 + |\nabla f|_2^2\right)^{\frac{1}{2}}.$$

- $H_0^1(\Omega) = \{f \in H^1(\Omega) \text{ such that } f|_{\partial\Omega} = 0\}$. It is the closure of the space of infinitely differentiable, compactly supported functions $C_c^\infty(\Omega)$ in $L^2(\Omega)$. Moreover, we have

$$\|f\|_{H_0^1(\Omega)} = \|f\|_0 = |\nabla f|_2.$$

- $H^{-1}(\Omega)$: The dual of $H_0^1(\Omega)$.

Finally, for $u = (u_1, u_2, \cdots, u_n) \in \mathbb{R}^n$, we define

$$\|u\|_2 = \sqrt{\sum_{i=1}^{n} |u_i|^2} \quad \text{and} \quad \|u\|_\infty = \max_{1 \le i \le n} |u_i|.$$

Moreover, for an operator $A : U \subset \mathbb{R}^n \longrightarrow \mathbb{R}^n$ we define the following induced norms

$$\|A\|_2 = \sup_{u \neq 0 \in U} \frac{\|Au\|_2}{\|u\|_2} \quad \text{and} \quad \|A\|_\infty = \sup_{u \neq 0 \in U} \frac{\|Au\|_\infty}{\|u\|_\infty}.$$

1

General Introduction

The book of nature is written in mathematical language, and the symbols are triangles, circles and other geometrical figures, without whose help it is impossible to comprehend a single word of it; without which one wanders in vain through a dark labyrinth.

– Galileo

Our work in this thesis is divided into two main parts. The first part is devoted to the study of some inverse source problems for wave equation and their application to biomedical imaging. While in the second part we concentrate our work on semi-linear elliptic equations, on which we study the existence of radial solutions for non-autonomous semi-linear elliptic equations with prescribed limiting behavior. The aim of this chapter is to provide a biological, physical and mathematical introduction to both problems.

This chapter is organized as follows:

- **Section 1** is dedicated to inverse problems and their application to photo-acoustic imaging. We first give a historical background on inverse problems and medical imaging, then we move to the techniques of photo-acoustic and thermo-acoustic tomography, on which we give the derivation of the mathematical model of each technique, the inverse problem behind each model and the methods used in literature for solving it. Finally, we end up with the drawbacks of these inverse problems.

- **Section 2** presents the problem of semi-linear elliptic equations. We start in section 2.1 by the physical background of the problem, then we give in section 2.2 the mathematical derivation of the equation. Finally, we introduce in section 2.3 several techniques used to study the existence and the behavior of the solution of these problems.

1 Introduction to Photo-acoustic Imaging

1.1 Inverse problems: historical background

An inverse problem is a mapping between certain unknown physical parameters and the acquired information about these parameters. The notion of "inverse problem" designates the best possible reconstruction of missing information in order to estimate either the loads (identification of sources or of the cause), or the value of undetermined parameters (identification of physical parameters). Unlike direct problems that usually try to calculate the observable effects of a certain physical model, the objective of inverse problems is the inversion of the physical model by means of a partial image of that model's effect. In other words, inverse maps help in determining the unknown or its distribution from the measurements that usually provide limited information about the unknown.

Even though the mathematical formulation of inverse problems has recently developed, however, inverse problems are as old as science. In fact, all natural and physical phenomenas surrounding us can be viewed in frame of inverse problems. One of the earliest examples of inverse problems was the one given by the Greek philosopher Plato in the seventh book of his *Republic*, which is known as Plato's allegory of the cave. In his experiment, Plato had a group of people chained facing a wall of a cave all their lives, on which they were allowed to watch the shadows projected on this wall from objects passing in front of a fire behind them. They had to reconstruct the external reality from the two-dimensional shadows they viewed on the wall of the cave. This is an example of inverse imaging problems that shows how such problem may lack uniqueness and stability of reconstruction, as different objects for example may have identical shadows.

The mathematical study of inverse problems was raised in 1846 by the French mathematician, Le Verrier, who predicted the existence and the position of the planet Neptune using only mathematics. In the beginning of the 19^{th} century, the most distant discovered planet was Uranus. However, when the scientists applied Newton's gravitational law on the movement of Uranus, taking into consideration only the effect of Jupiter and Saturn, the obtained position and orbit didn't match the observed ones. In 1844, Le Verrier started his calculations using inverse perturbations of physical parameters (mass, orbit, position) of the hypothetical planet assumed to cause Uranus' irregularities, and in 1846 he was able to predict the position and the orbital elements of this new planet using only mathematics.

In 1950s, the physicist Allan Cormack introduced the mathematical theory of medical imaging using inverse problems. He developed a reconstruction method of the piece-wise radially symmetric attenuation coefficient of biological tissues from measurements made external to the body. His contribution has been a breakthrough new imaging technology.

Inverse problems are now a wide range in mathematics that have applications in different do-

mains including geology, oceanography, astronomy, biomedicine and medical imaging. In this thesis, we study the application of inverse problems on medical imaging, in particular we work on the photo-acoustic and thermo-acoustic tomography problems.

1.2 Medical Imaging

Medical imaging is a continuously developing domain which involves different imaging techniques that try to image the human body for diagnostic and treatment purposes. Many techniques have been used in this field, some of them are structural techniques that try to observe only the organs, such as *X-ray* based techniques, and other techniques are more functional, that try to observe the organ and its functioning such as *Magnetic Resonance Imaging (MRI)*. Moreover, these imaging modalities can be divided into acoustic imaging techniques, such as ultrasound imaging, magnetic resonance imaging *(MRI)* and *X-ray* based techniques, that use acoustic waves and are characterized by high resolution, and optical imaging techniques such as scanning and endoscopy that use optical waves and are characterized by high contrast (optical contrast). In fact, optical contrast is very important in biological imaging due to the fact that the optical parameters (absorption and scattering coefficients) vary significantly in the biological tissues. Moreover, such imaging techniques use visible and infra-red light waves whose wavelengths coincide with the absorption spectrum of several interesting biological molecules such as hemoglobin. However, despite its high contrast, optical waves are characterized by their diffusive property, which decreases the resolution of image in depth.

Since many decades, scientists and engineers have been trying to improve these imaging techniques in order to get cheaper, faster, harmless and highly resolved results, and for this purpose, they introduced the multi-wave imaging techniques, such as photo-acoustic and thermo-acoustic tomography. These methods combine between optical and acoustic waves and thus take the advantage of high quality contrast from optical waves, and high resolution from acoustic waves.

1.3 Photo-acoustic and Thermo-acoustic Tomography

1.3.1 Photo-acoustic effect

Photo-acoustic tomography (PAT) and thermo-acoustic tomography (TAT) are multi-wave imaging techniques based on the photo-acoustic effect. It is a physical phenomenon of the generation of acoustic waves excited by the interaction of optical waves with the biological tissues, or the production of sound from light. This effect was discovered in 1880 by Alexandre Graham Bell after hearing a "pure musical tone" in a closed glass volume that had absorbed a modulated light beam, see [43] and references therein. The main tool of this phenomenon is the thermal expansion of the tissues due to the absorption of electromagnetic energy. Moreover, the advantage of such techniques is that they combine between high quality contrast from optical waves and high

resolution from acoustic waves. The goal of these methods is to reconstruct the absorption map in the biological tissues, and its main application is the detection of tumors or cancerous cells due to the high difference in absorption between healthy tissues and cancerous ones.

1.3.2 Energy absorption

Energy absorption in human body is enhanced by specific molecules such as hemoglobin, melanin, water, fats, ... etc. It is the sum of all their contributions. In particular,

$$\mu_a = \sum_i f_{v,i}\mu_{a,i},$$

where μ_a is the absorption coefficient, $f_{v,i}$ is the volumic fraction of the i^{th} absorbing component, and $\mu_{a,i}$ is the absorption coefficient of that pure component. However, hemoglobin and melanin are considered as the dominant absorbing molecules, especially for high-frequency radiations (see figures 1.1 and 1.2), and from a medical point of view, tumors are highly rich in hemoglobin (Hb), which enhance absorption in such tissues and makes photo-acoustic tomography an effective method in detecting tumors.

Studies on breast cancer [58,61] have shown that the Hb absorption coefficient in healthy women was $0.04 \pm 0.02\ cm^{-1}$, while that in abnormal blood was two times higher in pre-menopausal women and four times higher in post-menopausal women. Which indicates that knowing the absorption coefficient is very effective in detecting tumors.

Moreover, one can notice from figures 1.1 and 1.2 that the peak of absorption of hemoglobin (Hb), oxy-hemoglobin (HbO_2) and melanin is obtained at low wavelengths which correspond to high frequency radiations, such as visible and near-infrared light, that are usually used in PAT.

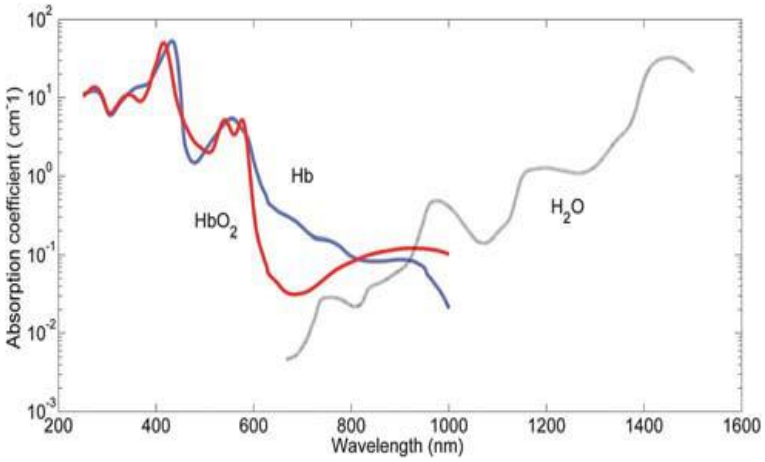

Figure 1.1: *Variation of the absorption coefficient of hemoglobin (Hb), oxy-hemoglobin (HbO_2) and water (H_2O) with the wavelength of the applied radiation*

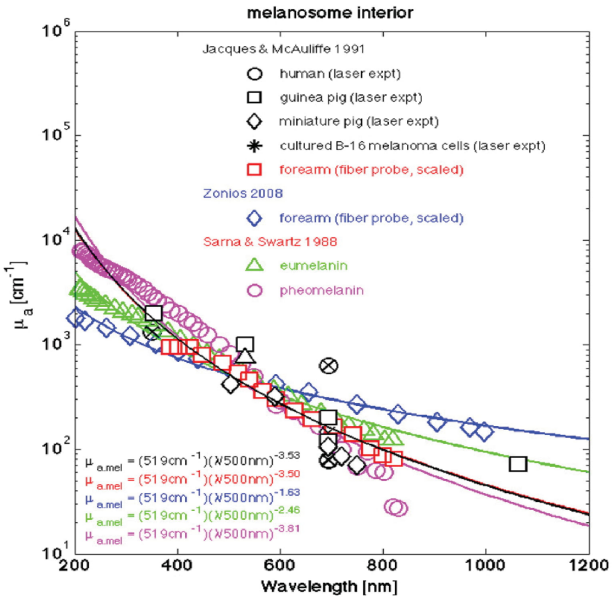

Figure 1.2: *A summary of published absorption coefficients of melanin at different wavelengths given in [52].*

1.3.3 Steps of photo-acoustic tomography

First, optical waves are applied to the object to be imaged. Then, these waves propagate inside the biological tissues which heat up due to the absorption of electromagnetic energy, causing thermal expansion of the tissues and generation of acoustic waves . These waves then propagate until they reach the boundary where they are measured and the image is produced (see figure 1.3). Thus, the steps of photo-acoustic tomography can be summarized as follows (see figure 1.4):

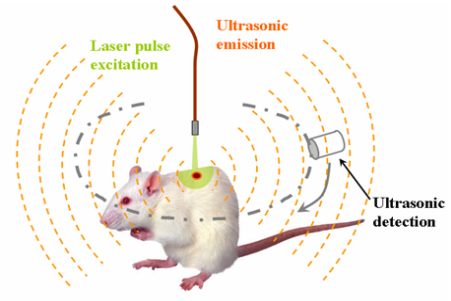

Figure 1.3: *Photo-acoustic tomography*

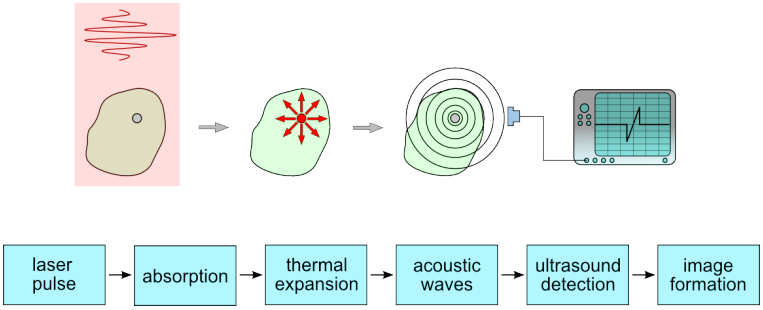

Figure 1.4: *Steps of photo-acoustic tomography*

1. Sending an optical wave into the object to be imaged;
2. Propagation of the optical waves in the biological tissue;
3. Absorption of the electromagnetic energy by the biological molecules;
4. Heating up of the absorbers;
5. Thermal expansion of the tissues;
6. Generation of the acoustic waves;
7. Propagation of the acoustic waves inside the medium;
8. Detection of these waves by transducers located at the boundary of the object and formation of the image;

1.3.4 Difference between PAT and TAT

The main difference between photo-acoustic tomography (PAT) and thermo-acoustic tomography (TAT) is in the type of optical (laser) pulse used. In PAT, a high frequency radiation is used (visible or near infrared light), while in TAT, a low frequency radiation is used (radio waves or microwaves). In fact, the wavelength of the visible light ($400\ nm - 750\ nm$) and near infrared light ($750\ nm - 2.5\ \mu m$) corresponds to the absorption spectrum of hemoglobin and oxy-hemoglobin (see figure 1.1), which makes PAT suitable for tumor imaging due to the ability to acquire hemoglobin information. On the other hand, high frequency radiations are characterized by their diffusive property, which allows low penetration of light in the biological tissues and decreases the resolution of image in depth. Moreover, for safety reasons, the laser pulse used must respect the exposure safety limits, which prevents the use of higher laser energy, and thus decreases the image depth.

However, in TAT low frequency radiations are used, which undergo less scattering, and thus

allow deeper penetration of light and increase the image depth. In fact, recent studies on the optical properties of biological tissues [52] have shown that the scattering coefficient of an optical wave in different biological tissues (skin, brain, breast, bone, etc.) is inversely proportional to its wavelength, and it is given by the formula

$$\mu'_s = a\left(\frac{\lambda}{500\ (nm)}\right)^{-b},$$

where μ'_s is the scattering coefficient, λ is the wavelength normalized by a reference wavelength (500 nm) to yield a dimensionless value, $b > 0$ is called the scattering power and $a = \mu'_s(\lambda = 500\ nm)$ is a factor that scales the wavelength-dependent term.

Thus, low frequency radiations such as radio waves and microwaves, that have higher wavelength,

$$wavelength = \frac{speed\ of\ light}{frequency},$$

undergo less scattering, and thus allow deeper penetration of light. Moreover, as explained in [87], microwaves allow penetration of several centimeters depth in the biological tissues. The penetration depths for fat and muscle tissues, for example, at 3 GHz microwave are 9 and 1.2 cm respectively.

Although the wave length of low frequency radiations used in TAT, such as radio waves ($> 10^8 nm$), may not correspond to the absorption spectrum of hemoglobin. However, as explained in [44] and [62], tumors have significantly different electrical properties from normal tissues. In fact, relatively few blood vessels can be found in the inner regions of tumors, which is responsible for lack in nutrients' supply necessary for cells' survival, and accumulation of metabolic wastes, leading to cell death and formation of scar tissues. This results in higher heterogeneity and much less uniform arrangement of cells, which leads to a significant difference in conductivity between healthy tissues and cancerous ones. Moreover, various studies show that for low frequencies, which is the case in TAT, a significant difference in conductivity is detected between healthy tissues and tumors, see figure 1.5. A study by *Smith et al.* [76] on liver tissues, for example, shows that tumor conductivity is 6-7 times higher than that of healthy liver cells. Another studies such as [44] on liver tissues, and [80] on breast cells show also a remarkable difference in conductivity between normal tissues and cancerous ones. Thus, measuring the conductivity σ would be of great importance and makes TAT an effective method in detecting tumors.

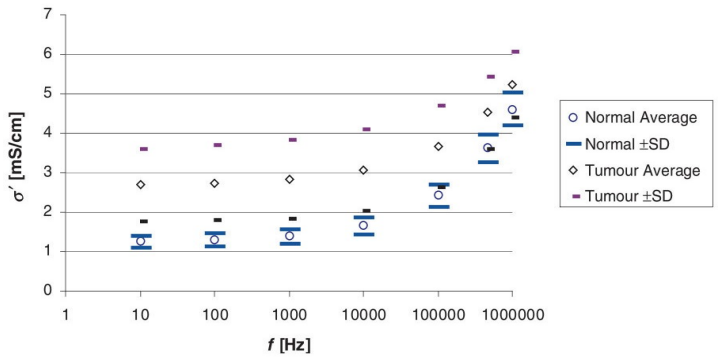

Figure 1.5: *Electrical conductivity of tumor and normal liver tissues at different frequencies based on the experiment done in [44].*

1.4 Derivation of the PAT problem

1.4.1 Modeling of the optical wave

Radiative transfer equation

As stated before, the first step in PAT is the application of optical waves into the biological tissue to be imaged. While propagating in the medium, light interacts with it. In general, this interaction is described by the equation of radiative transfer. First, we introduce the following quantities:

- Spectral Radiance L_ν: energy flow per unit normal area per unit solid angle per unit time per unit frequency.
- Radiance L: spectral radiance integrated over a narrow frequency range $[\nu, \nu + \Delta\nu]$,

$$L(\vec{r}, \vec{s}, t) = L_\nu(\vec{r}, \vec{s}, t)\Delta\nu$$

  where $\vec{r}$ is the position, $\vec{s}$ is the unit direction vector and t is the time variable.
- Fluence rate or intensity Φ: energy flow per unit area per unit time,

$$\Phi(\vec{r}, t) = \int_{4\pi} L(\vec{r}, \vec{s}, t)d\Omega,$$

  where $d\Omega$ represents the differential solid angle.
- Current density $\vec{J}$: net energy flow per unit time per unit area,

$$\vec{J}(\vec{r}, t) = \int_{4\pi} \vec{s}L(\vec{r}, \vec{s}, t)d\Omega.$$

The equation of radiative transfer is given by [31, 75]

$$\frac{1}{c_\ell}\frac{\partial L(\vec{r},\vec{s},t)}{\partial t} + \vec{s}.\nabla L(\vec{r},\vec{s},t) + (\mu_a+\mu_s)L(\vec{r},\vec{s},t) = \mu_s\int_{4\pi} L(\vec{r},\vec{s'},t)\Theta(\vec{s},\vec{s'})ds' + q(\vec{r},\vec{s},t), \quad (1.1)$$

where c_ℓ is the speed of the optical wave, q represents the electromagnetic source, μ_a and μ_s are the absorption and diffusion coefficients respectively, and $\Theta(\vec{s},\vec{s'})$ represents the probability of light traveling in the direction $\vec{s'}$ to end up traveling in the direction $\vec{s}$ if scattered.

In fact, this equation shows that the rate of change of the energy flow within a small region in a position $\vec{r}$ and traveling in direction $\vec{s}$ could be due to (1) source: q, (2) energy diverging out in the direction $\vec{s}$: $\vec{s}.\nabla L(\vec{r},\vec{s},t)$, (3) energy loss due to absorption: $\mu_a L(\vec{r},\vec{s},t)$, (4) energy loss due to scattering into another direction: $\mu_s L(\vec{r},\vec{s},t)$, and (5) energy incident and scattered into the direction $\vec{s}$ from another direction $\vec{s'}$, (given by the integral). Using expansion in spherical harmonics, the luminance L can be written as a sum of two components, the isotropic component and a component that depends on the direction $\vec{s}$,

$$L(\vec{r},\vec{s},t) = \frac{1}{4\pi}\Phi(\vec{r},t) + \frac{3}{4\pi}\vec{J}(\vec{r},t).\vec{s}.$$

We suppose that the source is isotropic, i.e. q is independent of $\vec{s}$. Then, substituting L in the radiative transfer equation (1.1) and integrating over 4π solid angle we get

$$\frac{1}{c_\ell}\frac{\partial \Phi(\vec{r},t)}{\partial t} + \mu_a\Phi(\vec{r},t) + \nabla.\vec{J}(\vec{r},t) = q(\vec{r},t). \quad (1.2)$$

On the other hand, substituting L in the radiative transfer equation (1.1), multiplying both sides by $\vec{s}$ and integrating over 4π solid angle we get

$$\frac{1}{c_\ell}\frac{\partial \vec{J}(\vec{r},t)}{\partial t} + (\mu_a+\mu_s')\vec{J}(\vec{r},t) + \frac{1}{3}\nabla\Phi(\vec{r},t) = 0, \quad (1.3)$$

where $\mu_s' = (1-g)\mu_s$ is the reduced scattering coefficient and $g \in]0,1[$ is the anisotropy factor and corresponds to cosine the average diffusion angle of the medium, see [83] for more details on the derivation of (1.2) and (1.3).

We assume that the fractional change of the current density is very small, which implies that the term $\frac{\partial \vec{J}(\vec{r},t)}{\partial t}$ in (1.3) is neglected [83]. Thus we get

$$\vec{J}(\vec{r},t) = -D\nabla\Phi(\vec{r},t),$$

where

$$D = \frac{1}{3(\mu_a+\mu_s')},$$

represents the diffusion coefficient. Therefore, substituting $\vec{J}$ in (1.2), the radiative transfer equation is thus simplified to

$$\frac{1}{c_\ell}\frac{\partial\Phi(\vec{r},t)}{\partial t} - \nabla.(D(\vec{r})\nabla\Phi(\vec{r},t)) + \mu_a(\vec{r})\Phi(\vec{r},t) = q(\vec{r},t). \tag{1.4}$$

Now, we denote by $\Omega \subset \mathbb{R}^3$ our domain of study (imaged object). We apply a laser pulse $f(\mathbf{x},t)$ at the boundary Γ of Ω. The source is thus located only at the boundary. We denote by $u(\mathbf{x},t)$ the laser fluence, then substituting u in the radiative transfer equation (1.4) we get:

$$\begin{cases} \dfrac{1}{c_\ell}\dfrac{\partial u(\mathbf{x},t)}{\partial t} - \nabla.D(\mathbf{x})\nabla u(\mathbf{x},t) + \mu_a(\mathbf{x})u(\mathbf{x},t) = 0 & \text{in } \Omega\times\mathbb{R}^+ \\ u(\mathbf{x},t) = f(\mathbf{x},t) & \text{on } \Gamma\times\mathbb{R}^+. \end{cases} \tag{1.5}$$

1.4.2 Generation of acoustic waves

Passing through the medium, the electromagnetic waves interact with it, and optical energy is absorbed. The absorbed electromagnetic energy is given by [31, 75]

$$P_V(\mathbf{x},t) = \mu_a(\mathbf{x})u(\mathbf{x},t), \tag{1.6}$$

which leads to the generation of acoustic waves. This is known as the photo-acoustic effect [43], which can occur in any absorbing medium. However, we consider here the case of liquids that constitute the principal component of the biological tissues, and that are characterized by their homogeneous acoustic and thermal properties (linear acoustic propagation), while their optical properties can vary spatially in the medium. The situation is described by the following three fundamental equations of linear acoustics [73]:

- Mass conservation equation:
$$\frac{\partial\rho}{\partial t} = -\rho_0 div(v), \tag{1.7}$$
- Momentum conservation equation:
$$\rho_0\frac{\partial v}{\partial t} = -\nabla p, \tag{1.8}$$
- Heat equation:
$$\rho_0 T\frac{\partial s}{\partial t} = div(\kappa\nabla T) + P_V \tag{1.9}$$

where ρ is the volumic mass, $p(r,t)$ is the acoustic pressure, $v(r,t)$ is the speed of acoustic displacement, $s(r,t)$ is the specific entropy, $T(r,t)$ is the temperature field, $\kappa(T)$ is the coefficient of thermal conduction and P_V represents the heat source. Moreover, as we assume a medium

of linear acoustic propagation, then the change of density in the medium is relatively small ($\frac{\rho-\rho_0}{\rho_0} \ll 1$), see [73] and references therein. We can write the two equations of state expressing the variation of density and entropy (δ_ρ, δ_s) as function of δ_p and δ_T [63, 73, 81].

$$\delta_\rho = \frac{\gamma}{c_s^2}\delta_p - \rho_0\alpha\delta_T,$$

$$\delta_s = \frac{c_p}{T}(\delta_T - \frac{\gamma-1}{\rho_0\alpha c_s^2}\delta_p),$$

where $c_p = T(\frac{\partial s}{\partial T})_p$ is the thermal capacity at constant pressure, $c_v = T(\frac{\partial s}{\partial T})_\rho$ is the thermal capacity at constant volume, $\gamma = \frac{c_p}{c_v}$, $\alpha = -\frac{1}{\rho}(\frac{\partial \rho}{\partial T})_p$ is the coefficient of thermal expansion, and c_s is the speed of thermal expansion. We thus deduce the following equations

$$\frac{\partial \rho}{\partial t} = \frac{\gamma}{c_s^2}\frac{\partial p}{\partial t} - \rho_0\alpha\frac{\partial T}{\partial t}, \tag{1.10}$$

$$\frac{\partial s}{\partial t} = \frac{c_p}{T}\left(\frac{\partial T}{\partial t} - \frac{\gamma-1}{\rho_0\alpha c_s^2}\frac{\partial p}{\partial t}\right). \tag{1.11}$$

From (1.7) and (1.8) we have

$$\frac{\partial^2 \rho}{\partial t^2} = \Delta p,$$

thus, using (1.10) we deduce that

$$\frac{\gamma}{c_s^2}\frac{\partial^2 p}{\partial t^2} - \Delta p = \rho_0\frac{\partial}{\partial t}\left(\alpha\frac{\partial T}{\partial t}\right).$$

Moreover, (1.9) and (1.11) implies that

$$\rho_0 c_p\frac{\partial T}{\partial t} = div(\kappa\nabla T) + P_V + \frac{c_p}{\alpha c_s^2}(\gamma-1)\frac{\partial p}{\partial t}.$$

Assuming that $\gamma \sim 1$, which is valid for liquids (see [73]), and $\alpha = \alpha_0$ we get

$$\frac{1}{c_s^2}\frac{\partial^2 p}{\partial t^2} - \Delta p = \rho_0\alpha_0\frac{\partial^2 T}{\partial t^2}, \tag{1.12}$$

$$\rho_0 c_p\frac{\partial T}{\partial t} = div(\kappa\nabla T) + P_V. \tag{1.13}$$

1.4.3 Stress Confinement Condition

As stated before, the optical pulse used in PAT is a high frequency radiation, which is characterized by its high speed compared to the speed of propagation of the acoustic waves, see [12] and references therein. There are two important time scales in the generation of acoustic waves: The

thermal diffusion time τ_{th}, and the stress relaxation time τ_s [92]. In order to have an effective method, the duration of this laser pulse must respect the thermal and stress confinement conditions. It must be less than the duration of thermal diffusion and stress relaxation in a way that it can be neglected. That is, the complete energy is assumed to be deposited instantaneously compared to the travel time of the acoustic waves.

In fact, the time of thermal diffusion is given by

$$\tau_{th} \simeq \frac{L_p^2}{\chi},$$

while that of stress relaxation is given by

$$\tau_s = \frac{L_p}{c_s},$$

where L_p is the spatial resolution, $\chi = \frac{\kappa}{\rho_0 c_p}$ is the thermal diffusivity ($\sim 1.4 \times 10^{-7} m^2/s$ in biological tissues) and c_s is the acoustic speed, see [92] and references therein. For a pulse of duration τ_p, the diffusion length during the pulse is estimated by $\delta_T = 2\sqrt{\chi \tau_p}$. The confinement condition is then given by $\tau_p \lll \tau_{th}, \tau_s$, see [86, 92] and references therein. Thus, under this condition, the thermal diffusion, as well as the volume expansion of the tissue can be neglected. Therefore, from (1.13) we get

$$\frac{\partial T}{\partial t} = \frac{P_V}{\rho_0 c_p}.$$

We finally write the equation of propagation of the acoustic wave

$$\frac{1}{c_s^2}\frac{\partial^2 p}{\partial t^2} - \Delta p = \frac{\beta}{c_s^2}\frac{\partial P_V}{\partial t}, \tag{1.14}$$

where $\beta = \frac{\alpha_0 c_s^2}{c_p}$ is the *Grüneisen coefficient* that measures the efficiency of convergence from optical waves into acoustic waves.

Remark 1.1. *The stress confinement condition implies that all of the thermal energy has been deposited by the electromagnetic pulse before the mass density or volume of the medium had time to change [75]. Thus in (1.10) we may assume that* $\frac{\partial \rho}{\partial t}(t=0) \simeq 0$ *and* $\rho_0 \alpha \frac{\partial T}{\partial t}(t=0) = -\frac{\rho_0}{\rho}\left(\frac{\partial \rho}{\partial T}\right)_p \frac{\partial T}{\partial t}(t=0) \simeq 0$. *Therefore we may assume, under the stress confinement condition, that* $\frac{\partial p}{\partial t}(t=0) = 0$.

For more details on the derivation of the photo-acoustic tomography problem we refer the reader to [31, 43, 53, 63, 73, 82, 86, 92] and references therein.

1.4.4 Modeling of the PAT problem under the stress confinement condition

Diffusion Equation

Under the stress confinement condition, the optical energy given in (1.6) is assumed to be absorbed initially compared to the travel time of the acoustic waves. Thus, it can be expressed in the form

$$P_V(\mathbf{x},t) = \delta_0(t)H_0(\mathbf{x}) \quad \text{where } H_0(\mathbf{x}) = \mu_a \int_{\mathbb{R}^+} u(\mathbf{x},t)\ dt,$$

where δ_0 is the Dirac delta function taken at $t = 0$, see [12]. Under this condition, and if we denote by

$$f(\mathbf{x}) = \int_{\mathbb{R}^+} f(\mathbf{x},t)\ dt \quad \text{and} \quad u(\mathbf{x}) = \int_{\mathbb{R}^+} u(\mathbf{x},t)\ dt,$$

the equation (1.5) is transformed into the following diffusion equation [12]

$$\begin{cases} -\nabla.(D(\mathbf{x})\nabla u(\mathbf{x})) + \mu_a(\mathbf{x})u(\mathbf{x}) = 0 & \text{in } \Omega \\ u(\mathbf{x}) = f(\mathbf{x}) & \text{on } \Gamma. \end{cases} \tag{1.15}$$

Wave equation

Substituting P_V in the wave equation (1.14) and taking into consideration Remark 1.1 we get

$$\frac{1}{c_s^2}p_{tt}(\mathbf{x},t) - \Delta p(\mathbf{x},t) = \frac{\beta}{c_s^2}H_0(\mathbf{x})\frac{\partial \delta_0(t)}{\partial t},$$

which is equivalent to

$$\begin{cases} \dfrac{1}{c_s^2}p_{tt}(\mathbf{x},t) - \Delta p(\mathbf{x},t) = 0 & \text{in } \Omega \times \mathbb{R}^+ \\ p(\mathbf{x},0) = p_0(\mathbf{x}) = \beta(\mathbf{x})\mu_a(\mathbf{x})u(\mathbf{x}) & \text{in } \Omega \\ p_t(\mathbf{x},0) = 0 & \text{in } \Omega. \end{cases} \tag{1.16}$$

equipped with the Neumann or Dirichlet boundary condition.

1.5 Derivation of TAT problem

As stated in the previous section, in TAT a low frequency radiation (radio wave for example) is delivered into the biological tissue to be imaged. The propagation of this radiation in the biological tissues is controlled by the 4 main physical laws that are expressed by the following Maxwell's equations:

1. **Gauss's law for electrical field**

   The electrical field produced by an electric charge diverges from the positive charge and

converges into the negative one.

$$\vec{\nabla}.\vec{E} = \frac{\rho}{\epsilon_0},$$

where E is the electric field, ρ is the electric charge density, ϵ_0 is the permittivity in free space (material's response into an electric field) and $\nabla.E$ represents the divergence of the electric field.

2. **Gauss's law for magnetic field**

   The divergence of the magnetic field at any point is zero

   $$\vec{\nabla}.\vec{B} = 0,$$

   where B is the magnetic field. This rises from the fact that magnetic poles cannot be isolated. In other words, we cannot have a north pole without a south pole and vice-versa.

3. **Faraday's law**

   A circulating electric field is produced by a magnetic field that changes with time

   $$\vec{\nabla} \times \vec{E} = -\frac{\partial \vec{B}}{\partial t}.$$

4. **Ampere's law**

   A circulating magnetic field is produced by an electric current and by an electric field that changes with time

   $$\vec{\nabla} \times \vec{B} = \alpha_0 \left(\vec{J} + \epsilon_0 \frac{\partial \vec{E}}{\partial t} \right),$$

   where α_0 is the permeability (material's response to an applied magnetic field), and $\vec{J}$ is the electric current density

From Maxwell's equations to wave equation

Using the Faraday's law, we note that

$$\vec{\nabla} \times (\vec{\nabla} \times \vec{E}) = -\frac{\partial(\vec{\nabla} \times \vec{B})}{\partial t}.$$

Moreover, $\vec{\nabla} \times (\vec{\nabla} \times \vec{E}) = \vec{\nabla}(\vec{\nabla}.\vec{E}) - \Delta\vec{E}$, and using Ampere's law we deduce that

$$\vec{\nabla}(\vec{\nabla}.\vec{E}) - \Delta\vec{E} = -\frac{\partial}{\partial t} \left(\alpha_0 \left(\vec{J} + \epsilon_0 \frac{\partial \vec{E}}{\partial t} \right) \right).$$

Finally, applying Gauss's law for electric fields we deduce that

$$\alpha_0\epsilon_0\frac{\partial^2\vec{E}}{\partial t^2} - \Delta\vec{E} + \alpha_0\frac{\partial\vec{J}}{\partial t} = -\vec{\nabla}\left(\frac{\rho}{\epsilon_0}\right).$$

We note that the value $c := \sqrt{\frac{1}{\alpha\epsilon_0}}$ is equal to the speed of light in vacuum. Moreover, Ohm's law states that

$$\vec{J} = \sigma\vec{E},$$

where σ is the material's conductivity. Therefore, we finally get in a charge free region ($\rho = 0$)

$$\frac{1}{c^2}\frac{\partial^2\vec{E}}{\partial t^2} + \alpha_0\sigma\frac{\partial\vec{E}}{\partial t} - \Delta\vec{E} = 0. \tag{1.17}$$

Furthermore, from electrodynamics [59], we know that the electromagnetic energy absorption per unit volume per unit time in biological tissues is given by

$$H(\mathbf{x}, t) = \vec{J}(\mathbf{x}, t).\vec{E}(\mathbf{x}, t).$$

Therefore, applying Ohm's law we deduce that

$$H(\mathbf{x}, t) = \sigma(\mathbf{x})|\vec{E}(\mathbf{x}, t)|^2. \tag{1.18}$$

As explained in the previous section, the absorption of electromagnetic energy leads to the generation of acoustic waves, however, in this case, low frequency radiations are used, and thus the stress confinement condition is no longer satisfied. Therefore, the acoustic waves in this case are known to satisfy a wave equation of the form

$$\begin{cases} \frac{1}{c_s^2}p_{tt}(\mathbf{x}, t) - \Delta p(\mathbf{x}, t) = \beta\frac{\partial H}{\partial t}(\mathbf{x}, t) & \text{in } \Omega \times \mathbb{R}^+ \\ p(\mathbf{x}, 0) = p_t(\mathbf{x}, 0) = 0 & \text{in } \Omega, \end{cases} \tag{1.19}$$

equipped with either the Dirichlet or the Neumann boundary condition, where the source term H is given by (1.18), see [13].

1.6 Inverse TAT/PAT Problems

In this section we introduce the inverse TAT and PAT problems and we state the main approaches used in literature for solving these problems.

1.6.1 Inverse TAT Problem

We start first by the inverse TAT problem. As stated in section 1.3.4, the low frequency radiations used in TAT reveal a high difference in conductivity between healthy tissues and cancerous ones. Thus one is interested in the reconstruction of the conductivity coefficient σ that can serve as an important tool in detecting tumors.

When the acoustic waves are generated, they propagate inside the domain Ω until they reach the boundary where they are measured by transducers located there and the image is produced. The production of the image is done in two steps. The first step is the acoustic inversion applied to the wave equation (1.19) to reconstruct the absorbed electromagnetic energy $H(\mathbf{x}, t)$ from the measurement of the acoustic pressure at the boundary. The next step is the optical inversion applied to the equation (1.17) using the previously calculated initial energy H and the relation (1.18) to reconstruct the conductivity coefficient σ. This approach is called the quantitative TAT approach (qTAT).

Acoustic Inversion

The propagation of the acoustic waves is described by the wave equation (1.19). Without loss of generality, we assume that the acoustic pressure satisfies the Neumann boundary condition

$$\left.\frac{\partial p}{\partial \nu}\right|_{\Gamma\times(0,T)} = 0.$$

The acoustic waves are then measured by transducers located at the boundary. Moreover, we consider the problem in a bounded time interval $(0, T)$ for T large enough (the value of T is discussed later in Chapter 3). We thus obtain the following equation

$$\begin{cases} \dfrac{1}{c_s^2} p_{tt}(\mathbf{x}, t) - \Delta p(\mathbf{x}, t) = \beta \dfrac{\partial H}{\partial t}(\mathbf{x}, t) & \text{in } \Omega \times (0, T) \\ p(\mathbf{x}, 0) = p_t(\mathbf{x}, 0) = 0 & \text{in } \Omega \\ \dfrac{\partial p}{\partial \nu}(\xi, t) = 0 & \text{on } \Gamma \times (0, T), \end{cases} \tag{1.20}$$

equipped with the boundary measurement

$$p(\xi, t) = f(\xi, t) \quad \text{on } \Gamma^* \times (0, T), \tag{1.21}$$

where $\Gamma^* \subsetneqq \Gamma$. The acoustic inversion is thus to reconstruct the absorbed electromagnetic energy $H(\mathbf{x}, t)$ from the measurement of the acoustic pressure at the boundary (1.21). The knowledge of H allows us to get some information about the location of the tumors due to the difference in energy absorption between healthy tissues and cancerous ones. However, one is

also interested in the knowledge of the conductivity coefficient σ which consists an important diagnostic information.

The main difficulty of this approach is that the inverse source problem for the reconstruction of the absorbed electromagnetic energy is highly ill-posed for general source term $H(\mathbf{x}, t)$, even for $\Gamma^* = \Gamma$, in particular it lacks uniqueness, see for example [35, 88] and references therein.

Optical inversion

The second step in the quantitative TAT approach (qTAT) is the optical inversion. More precisely, it is the inversion of the equation (1.17) to reconstruct the conductivity coefficient σ from the previously calculated value of H and using the relation (1.18).

1.6.2 Inverse PAT Problem

Now, we move to the inverse PAT problem. As in the previous case, the first step is the acoustic inversion applied to the wave equation (1.16) to reconstruct the initial pressure $p_0(\mathbf{x})$ from the measurement of the acoustic pressure at the boundary. The next step is the optical inversion applied to the diffusion equation (1.15) using the previously calculated initial pressure and the relation

$$p_0(\mathbf{x}) = \beta(\mathbf{x})\mu_a(\mathbf{x})u(\mathbf{x}), \tag{1.22}$$

to reconstruct the optical parameters (β, μ_a, D). This approach is called the quantitative photoacoustic tomography approach (qPAT), see figure 1.6.

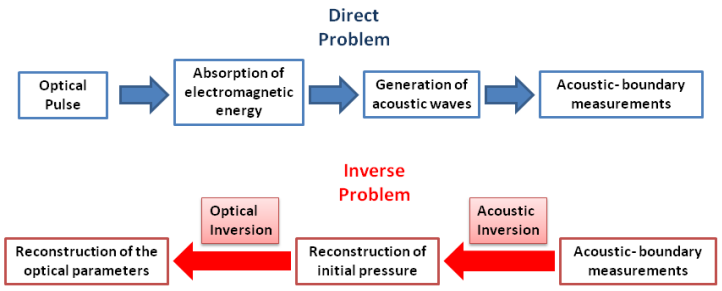

Figure 1.6: *Direct and inverse PAT problems*

Acoustic Inversion

The propagation of the acoustic waves is described by the wave equation (1.16). Without loss of generality, we consider the problem in a bounded time interval $(0, T)$ for T large enough (the value of T is discussed later in Chapter 4), and we assume that the acoustic pressure satisfies

the Dirichlet boundary condition

$$p|_{\Gamma\times(0,T)} = 0.$$

The normal derivative of these acoustic waves is then measured by transducers located at the boundary. The situation is thus described by the following equation

$$\begin{cases} \frac{1}{c_s^2} p_{tt}(\mathbf{x},t) - \Delta p(\mathbf{x},t) = 0 & \text{in } \Omega \times [0,T] \\ p(\mathbf{x},0) = p_0(\mathbf{x}) = \beta(\mathbf{x})\mu_a(\mathbf{x})u(\mathbf{x}) & \text{in } \Omega \\ p_t(\mathbf{x},0) = 0 & \text{in } \Omega \\ p(\xi,t) = 0 & \text{on } \Gamma \times [0,T], \end{cases} \tag{1.23}$$

equipped with the boundary measurements

$$\frac{\partial p}{\partial \nu}(\xi,t) = h(\xi,t) \quad \text{on } \Gamma^* \times [0,T], \tag{1.24}$$

where $\Gamma* \subsetneqq \Gamma$. The acoustic inversion is thus to reconstruct the initial pressure $p_0(\mathbf{x})$ from the boundary measurements (1.24). This step qualitatively solves the problem. In fact, the obtained initial pressure gives an idea about the structure of the biological tissue by viewing its inhomogeneities. However, from a medical point of view, this is not enough, instead it is necessary to reconstruct the optical parameters, and in particular, the absorption coefficient, that can serve as an important diagnostic information, and this can be obtained by the optical inversion.

We note that one can also consider the problem with Neumann boundary condition and by measuring the acoustic pressure p at the boundary. Both problems are considered in literature and similar inversion procedures are used, see for example [6] and references therein.

Optical Inversion

The next step in quantitative photo-acoustic tomography (qPAT) is the optical inversion. In particular, it is the inversion of the diffusion equation (1.15) to reconstruct the optical parameters D, μ_a and β from the previously calculated initial pressure $p_0(\mathbf{x})$ and using the relation (1.22)

1.7 Inversion methods used in literature

The PAT and TAT problems are highly considered in literature, and different methods are used for solving it. The main approaches used to resolve these problems are the qPAT and qTAT approaches. As explained in the previous section, these approaches involve two main steps: the acoustic inversion, and the optical inversion. In this section we give a general review on the methods used for solving both inversion problems for the qPAT approach.

1.7.1 Acoustic Inversion

The first step in the qPAT approach is the acoustic inversion whose aim is to reconstruct the initial pressure $p_0(\mathbf{x})$ in (1.23) from the boundary observations (1.24).

In case of constant sound speed c_s, Radon transform was recognized as an interesting tool in the acoustic inversion problem as it provides exact inversion formulas. In this case, the wave equation (1.23) is assumed to be verified over $\mathbb{R}^3 \times \mathbb{R}^+$ with observation surface S, then the well known Poisson-Kirchhoff formula for the solution of $3D$- wave equation states that the solution of (1.23) is given by [36]

$$p(\mathbf{x}, t) = c_s \frac{\partial}{\partial t} \left(t(Rp_0)(\mathbf{x}, c_s t) \right), \tag{1.25}$$

where p_0 is the initial pressure, and R is the spherical Radon transform operator defined on $L^1(\mathbb{R}^3)$ with values in $L^1(\mathbb{S} \times \mathbb{R}^+)$ by

$$Rf(\mathbf{x}, t) = \int_{\mathbb{S}} f(\mathbf{x} + ty) dA(y),$$

with $\mathbb{S}$ being the unit sphere in $\mathbb{R}^3$, and $dA(y)$ is the standard area element on $\mathbb{S}$.

Formula (1.25) implies that the knowledge of p on an observation surface S allows the knowledge of Rp_0 on S. Thus, if we take $R_S : f \to R_S f$ to be the restriction of R on S, then we need to determine R_S^{-1} in order to reconstruct the initial pressure p_0. Different inversion formulas were used for solving this problem, starting by the filtered back projection formulas that were developed in [37] in odd dimensions, and under the assumption that the observation surface S is a sphere. Then, a universal back projection formula in three dimensions was developed in [85]. This formula was valid for cylindrical and plane observation surfaces. Then, a generalization of this formula for general convex domains was developed in [67]. Another inversion formula for even dimensions was developed in [38]. Also, a family of inversion formulas valid for $\mathbb{R}^n$, for arbitrary $n \geq 2$ was described in [56, 69]. The drawback of these inversion formulas is that they are valid only for acoustically homogeneous media. Moreover, they are applicable for very specific observation domains: spheres, cylinders, planes, cubes and ellipsoids.

Another reconstruction techniques were developed in case of inhomogeneous media (variable acoustic speed), such as the series solutions for spherical geometry that were developed in [4] based on the eigenfunction expansion of the operator $A = -c^2(\mathbf{x})\Delta$ with zero Dirichlet condition on the boundary Γ. Also, time reversal techniques and numerical algorithms were developed based on the idea of the solution decay with time [42, 47, 48, 77]. Optimization techniques were also used in [20].

Moreover, one of the difficulties of the acoustic inversion problem is the limited boundary observations. To overcome this difficulty, different studies in literature have considered the problem with partial boundary observations. In [8] for example, the authors proposed a regularization

method to resolve the problem with limited boundary data using Radon transform. Also, in [5], the authors proposed a geometric-control approach to deal with the case of limited measurements.

1.7.2 Optical inversion

The second step in the qPAT approach is the optical inversion. It consists of reconstructing the optical parameters μ_a, D and β from the knowledge of the previously calculated initial pressure $p_0(\mathbf{x}) = \beta(\mathbf{x})\mu_a(\mathbf{x})u(\mathbf{x})$ and the diffusion equation (1.15).

In [9], G. Bal and K. Ren have proposed a reconstruction algorithm that permits us, using two different illuminations, to reconstruct two out of the three parameters provided that the third one is known. In their reconstruction method, the authors took f_1 and f_2 to be two illuminations with corresponding initial pressures p_0^1 and p_0^2 respectively, and they assumed that

1. The optical parameters $\beta, \mu_a, D \in W^{1,\infty}(\Omega)$, and are bounded by positive constants. Moreover the values of β, μ_a and D are assumed to be known on the boundary Γ.

2. The illuminations f_1 and f_2 are positive on Γ and have 3 times differentiable extensions on $\bar{\Omega}$ ($C^3(\bar{\Omega})$).

3. The vector field $\varrho = p_0^1 \nabla p_0^2 - p_0^2 \nabla p_0^1$ is a vector field in $W^{1,\infty}(\Omega)$ such that

$$|\varrho|(\mathbf{x}) \geq \alpha_0 > 0 \quad \text{almost everywhere in } \Omega.$$

Then, under the previous assumptions, they proved that

1. The knowledge of p_0^1 and p_0^2 uniquely determines the operator $\mathcal{H} : H^{\frac{1}{2}}(\Gamma) \to H^1(\Omega)$ defined by $\mathcal{H}(f) = p_0$, where $f = u(x)|_\Gamma$ is the optical pulse applied at the boundary, and p_0 is the initial pressure defined in (1.22).

2. The knowledge of the operator $\mathcal{H}$ uniquely determines two independent relations

$$R_1 = \frac{\sqrt{D}}{\beta\mu_a}(\mathbf{x}),$$

$$R_2 = -\left(\frac{\Delta\sqrt{D}}{\sqrt{D}} + \frac{\mu_a}{D}\right)(\mathbf{x}),$$

   which allow us to reconstruct two out of the three parameters provided that the third one is known.

3. These two independent relations uniquely determine p_0^1 and p_0^2. That is, no matter how many illuminations are done, the only two relations that can be established about the

coefficients β, μ_a and D are R_1 and R_2. Therefore, it is impossible to reconstruct the three parameters no matter how many illuminations are done.

Piece-wise parameters:

In [64], the authors have proved that even if $\beta(\mathbf{x})$ is known, thus the absorbed energy $\varepsilon = \mu_a u$ can be calculated from the initial pressure $p_0(\mathbf{x})$, different pairs of diffusion and absorption coefficients may lead to the same absorbed energy map ε (a detailed explanation is given in the next subsection). Moreover, they proved that if the parameters are defined piece-wisely, that is if we assume that

$$\Omega = \bigcup_{j=1}^{N} \omega_j,\ \mu_a = \sum_{j=1}^{N} \mu_j \mathbb{1}_{\omega_j},\ D = \sum_{j=1}^{N} D_j \mathbb{1}_{\omega_j},\ \beta = \sum_{j=1}^{N} \beta_j \mathbb{1}_{\omega_j},$$

then, the three parameters can be uniquely determined from the initial pressure p_0, provided that they are known in one of the inclusions.

1.8 Drawbacks of qPAT approach

The qPAT approach involves many difficulties leading to the ill-posedness of the inverse map. Different studies in literature have previously discussed the difficulties behind photo-acoustic tomography and the qPAT approach. In [29], the authors have shown that both the acoustic and the optical inversions have many limitations.

According to [29], the drawbacks of the qPAT approach can be summarized as follows.

Non-absorbing background medium

Many work on qPAT have assumed a constant acoustic speed, and a homogeneous, non absorbing background medium and proposed a reconstruction algorithm by means of spherical Radon transform and back-projection algorithms, see [8, 38, 46, 54, 55, 69] and references therein. This assumption rises from the large difference in absorption between healthy tissues and cancerous ones. However, this is not accurate and for this purpose, many works are now moving to study the case of variable acoustic speed and non-zero background absorption, see for example [4, 77] and references therein.

Spacially varying Grüneisen coefficient

The *Grüneisen* coefficient $\beta(\mathbf{x})$ is a thermodynamic property that measures the efficiency of conversion of thermal energy into acoustic waves. If β is known, then the absorbed electromagnetic energy $\varepsilon = \mu_a u$ can be directly reconstructed from the initial pressure p_0, see [6, 30], using the relation

$$p_0(\mathbf{x}) = \beta(\mathbf{x})\mu_a(\mathbf{x})u(\mathbf{x}).$$

For this purpose, most work on qPAT have assumed that β is constant and known (usually taken to be equal to 1). However, this is not accurately true. The coefficient β is a physical property that depends on other physical parameters such as the acoustic speed c_s, the thermal capacity c_p and the coefficient of thermal expansion α_0, $\beta = \frac{\alpha_0 c_s^2}{c_p}$. All these coefficients vary between different types of biological tissues, and so does β. In [91] for example, the authors have measured the Grüneisen coefficient in different tissues and the results were $\beta \sim 0.81$ for porcine subcutaneous fat tissues and $\beta \sim 0.69$ for porcine lipid at room temperature. Also, in [87] it is given that $\beta \sim 0.23$ in muscles.

Non linear dependence of the light fluence on the absorption coefficient μ_a

Another drawback of the qPAT approach is the non-linear dependence of the light fluence $u(\mathbf{x})$ on the absorption coefficient $\mu_a(\mathbf{x})$. In fact, even if the absorbed electromagnetic energy $\varepsilon = \mu_a u$ is obtained, the reconstruction of the absorption coefficient μ_a is not trivial. This rises from the fact that the light fluence u is a solution of the diffusion equation (1.15) that also depends on μ_a, see [7] and references therein.

Ill-posedness of the inverse map

Hadamard Well-posedness

The main difficulty of many inverse problems is the ill-posedness of the inverse map. That is, a small change in measurements may result in a very large change in the constructed solution. The French mathematician, Jacques Hadamard, claimed that a mathematical problem is said to be well-posed if the following three properties hold:

1. Existence: the problem admits at least one solution.
2. Uniqueness: the problem has at most one solution.
3. Stability: the solution depends continuously on the data.

Unless all these three properties hold, the problem is called an ill-posed problem.

The main difficulty of qPAT is the ill-posedness of the inverse map. In [64], the authors have proved that even if $\beta(\mathbf{x})$ is known, thus the absorbed energy $\varepsilon = \mu_a u$ can be calculated from the initial pressure $p_0(\mathbf{x})$, different pairs of diffusion and absorption coefficients may lead to the same absorbed energy map ε. Thus the reconstruction of μ_a and D from ε is not unique.

In fact, taking $f > 0$, then by maximum principle $u(D, \mu_a) > 0$ in Ω, where u is the solution of (1.15) (see [36]). Now, we fix $\varepsilon = \varepsilon(\mu_a, D) = \mu_a u(D, \mu_a)$ and we take $v(\widetilde{D})$ to be the solution of

$$\begin{cases} \nabla . \left(\widetilde{D}(\mathbf{x}) \nabla v(\mathbf{x}) \right) = \varepsilon(\mathbf{x}) & \text{in } \Omega \\ v(\mathbf{x}) = f(\mathbf{x}) & \text{on } \Gamma, \end{cases}$$

then $v(D) = u(D, \mu_a) > 0$ in Ω. Moreover, for every $\widetilde{D}$ satisfying $\|\widetilde{D} - D\|_{1,\infty} < \delta$ for some $\delta > 0$ we have

$$\nabla.\left(\widetilde{D}\nabla v(\widetilde{D})\right) = \nabla.\left(D\nabla v(D)\right) = \varepsilon(D, \mu_a),$$

where $\|\widetilde{D} - D\|_{1,\infty} = \|\widetilde{D} - D\|_\infty + \|\nabla\left(\widetilde{D} - D\right)\|_\infty$. Therefore,

$$\begin{cases} \nabla.\left(\widetilde{D}\nabla\left(v(\widetilde{D}) - v(D)\right)\right) = -\nabla.\left((\widetilde{D} - D)\nabla v(D)\right) & \text{in } \Omega \\ v(\widetilde{D}) - v(D) = 0 & \text{on } \Gamma. \end{cases} \tag{1.26}$$

Then, using the regularity results given in [36] we have

$$\|v(\widetilde{D}) - v(D)\|_\infty \leq c_1\|\nabla.\left((\widetilde{D} - D)\nabla v(D)\right)\|_\infty \leq c_2\|\widetilde{D} - D\|_{1,\infty}.$$

Thus, for δ small enough we have $v(\widetilde{D}) > 0$. Moreover, if we take $\widetilde{\mu_a} = \frac{\varepsilon(D,\mu_a)}{v(\widetilde{D})}$ then we have

$$\nabla.\left(\widetilde{D}\nabla v(\widetilde{D})\right) - \widetilde{\mu_a}v(\widetilde{D}) = 0.$$

Therefore, $v(\widetilde{D}) = u(\widetilde{D}, \widetilde{\mu_a})$ and $\varepsilon(\widetilde{D}, \widetilde{\mu_a}) = \widetilde{\mu_a}v(\widetilde{D}) = \varepsilon(D, \mu_a)$. That is, two different pairs (μ_a, D) and $(\widetilde{\mu_a}, \widetilde{D})$ lead to the same absorbed energy ε.

We finally deduce that infinitely many pairs of absorption and diffusion coefficients may lead to the same absorbed energy map. Thus the reconstruction of D and μ_a from the knowledge of the absorbed energy is an ill-posed problem. To overcome this difficulty, the authors in [64] assumed that the coefficients β, μ_a and D are defined piece wisely, then they proved that the parameters can be uniquely determined from the initial pressure provided that they are known in one of the inclusions. Moreover, to avoid the ill-posedness problem, the authors in [9] gave a reconstruction algorithm that allows us to resolve the problem using 2 laser illuminations f_1 and f_2. The algorithm they provided allows the reconstruction of 2 out of the 3 parameters β, μ_a and D provided that the third one is known, see section 1.7.2 for more details.

1.9 Problems considered in part I of this thesis

The inverse source problems studied in part I of this thesis are

1. The inverse TAT problem studied in Chapter 3, whose aim is to reconstruct the conductivity coefficient in the wave equation (1.20) from a single Cauchy data

$$p(\xi, t) = f(\xi, t), \quad \text{on} \quad \Gamma \times (0, T).$$

The conductivity coefficient in this problem is assumed to be defined piece-wisely. That

is,

$$\sigma(\mathbf{x}) = \begin{cases} \sigma_0(\mathbf{x}) & \text{in } \Omega \setminus \overline{\bigcup_{j=1}^{m} w_j} \\ \sigma_j(\mathbf{x}) & \text{in } w_j, \end{cases}$$

where σ_j are functions belonging to the spaces $L^\infty(w_j)$, and w_j are small domains representing the absorbers (tumors) and defined as follows

$$w_j = \mathbf{S}_j + \epsilon B_j \quad \text{for} \quad j = 1, \dots, m,$$

where $\mathbf{S}_j \in \Omega$ are the locations of the sub-domains w_j, and $B_j \subset \mathbb{R}^3$ are bounded domains containing the origin. The constant ϵ is the common order of magnitude of the diameters of w_j supposed to be a sufficiently small positive real number, taken without loss of generality, smaller than 1.

2. The inverse PAT problem studied in Chapter 4, whose aim is to reconstruct the absorption coefficient in the wave equation (1.23) from a single and partial boundary observation

$$\frac{\partial p}{\partial \nu}(\xi, t) = h(\xi, t) \quad \text{on } \Gamma_0 \times (0, T), \tag{1.27}$$

where $\Gamma_0 \subset \Gamma$ is a non-empty subset of the boundary of Ω, chosen to satisfy certain geometric conditions that will be specified later. Also, the absorption coefficient μ_a is assumed to be defined piece-wisely. That is,

$$\mu_a(\mathbf{x}) = \begin{cases} \mu_0(\mathbf{x}) & \text{in } \Omega \setminus \overline{\bigcup_{j=1}^{m} w_j} \\ \mu_j(\mathbf{x}) & \text{in } w_j, \end{cases}$$

where w_j are sub domains defined as in the previous problem. We study this problem in both cases of constant and variable acoustic speed.

In both problems we don't follow the qTAT or the qPAT approaches. Otherwise, we follow a direct algebraic algorithm, that was first developed in [35], which allows us to reconstruct the number of absorbers, their locations, and some information about the conductivity and the absorption coefficients directly from the wave equation using a single data and without the knowledge of the coupling *Grüneisen's* coefficient, which is assumed throughout this thesis to be spatially varying and unknown.

The reconstruction algorithm we follow in both problems requires total boundary measurements. For this purpose, we opt in the PAT problem to reconstruct the initial pressure p_0 from the partial observation (1.27) using an exact controllability problem. The data completion of $\frac{\partial p}{\partial \nu}$ on

the whole boundary Γ can then be obtained by solving (1.23). However, this doesn't work in TAT due to the ill-posedness of the inverse source problem of reconstructing the source term in (1.20), for this purpose, we assume in this case that we have total boundary observations.

One of the main tools used in the resolution of the PAT problem is the exact controllability for wave equation in both cases of constant and variable speed. For this purpose, we recall in Chapter 2 the controllability results proved by J.L. Lions in [60] and we adapt the same method he used to prove the validity of his results in case of variable speed.

2 Introduction to Semi-linear Elliptic Equations

In the second part of this thesis we focus our work on semi-linear elliptic equations. In particular, we discuss the existence of radial solutions of the equation $\Delta u + g(|x|, u) = 0$ in $\mathbb{R}^n$, with a prescribed limit $z = u(\infty) > 0$ satisfying $g(|x|, z) = 0, \forall x \in \mathbb{R}^n$.

2.1 Physical background

Definition 1.1 (Solitary waves)**.** *A solitary wave $\phi(x,t)$ is a solution of the wave equation that does not vanish with time. In other words, its maximum amplitude at time t, which is given by $\sup_x |\phi(x,t)|$, does not tend to 0 as $t \to \infty$. However, it tends to 0 in some convenient sense as $|x| \to \infty$ at each time t .*

Two particular types of solitary waves are:

1. *Traveling waves $u(x - ct)$, with constant velocity c.*

2. *Standing waves $e^{iwt}u(x)$, where w is a real constant.*

Definition 1.2 (Solitons)**.** *The term "soliton" is mostly used as a synonym of "solitary waves". However, solitons are solitary waves that maintain their shape after interaction with other waves. Moreover, as viewed by John Scott Russell, solitons are known to satisfy the following properties:*

1. *Travel over large distances in a stable manner,*

2. *The speed of propagation of a soliton depends on its size,*

3. *Does not merge with other waves,*

4. *Large waves may split into two waves of different sizes if the depth of water is low.*

Historical Background

Solitary waves were firstly discovered by the architect John Scott Russell in 1834 while conducting experiments to determine the most efficient design for canal boats. While observing the motion of a boat drawn rapidly along a narrow channel, Russell realized that when the boat suddenly stopped, a smooth, bell-shaped heap of water rolled from the front and steadily propagated with a constant speed of around eight or nine miles an hour, preserving its original shape. Russell then followed the propagating water couples of kilometers until he lost it. Scott Russell continued his experiments on solitary waves on a long narrow water tank by dropping a square block into the water, and he was able to infer different properties related to solitary waves.

The idea of solitary waves was then developed by Korteweg and de Vries in their mathematical model of shallow water, which was described by the so called KdV equation. The concept of solitary waves now appear in a wide range of physical and engineering contexts, not just water waves. The idea of having solutions that preserve their shapes and spatially vanish at ∞ is now studied in different physical domains, and for different partial differential equations such as the Klein Gordon equation.

2.2 Solitary waves and derivation of semi-linear elliptic equations

We consider the following non-linear Klein Gordon equation

$$\phi_{tt} - \Delta\phi + m^2\phi + f(\phi) = 0, \tag{1.28}$$

where $m > 0$, and f is assumed to satisfy $f(0) = 0$, and $f(re^{i\theta}) = e^{i\theta}f(r)$. Therefore, if ϕ is a standing wave $\phi(x,t) = e^{iwt}u(x)$, then (1.28) reduces to

$$-\Delta u + (m^2 - w^2)u + f(u) = 0.$$

Moreover, if ϕ is a traveling wave $\phi(x,t) = u(x - ct)$, where c is a vector with $|c| < 1$, then substituting ϕ in (1.28) we get

$$-\sum_{i,j=1}^{n} a_{ij}\frac{\partial^2 u}{\partial x_i \partial x_j} + m^2 u + f(u) = 0, \tag{1.29}$$

where $a_{ij} = \delta_{ij} - c_i c_j$. Furthermore, (a_{ij}) is a positive definite matrix as we notice that for every $\xi \in \mathbb{R}^n$ we have

$$\sum_{i,j} a_{ij}\xi_i\xi_j = |\xi|^2 - (c.\xi)^2 \geq (1 - |c|^2)|\xi|^2.$$

Therefore, applying a change of coordinates via rotation and appropriate stretching of axes we get the following equation for $x \in \mathbb{R}^n$, see [79],

$$-\Delta u + m^2 u + f(u) = 0.$$

Finally, we deduce that both the standing and traveling waves satisfy the elliptic equation

$$-\Delta u + F(u) = 0, \tag{1.30}$$

where $F(u) = f(u) + \alpha u$ for some $\alpha \in \mathbb{R}$. Since $F(0) = 0$, then 0 is a trivial solution of (1.30).

The solution of elliptic equations of the form (1.30) has attracted the attention of many authors in literature, especially solutions that vanish at ∞ $\left(\lim_{r\to\infty} u(r) = 0\right)$, which provide solitary waves for the Klein-Gordon equation (1.28). In [79], for example, the authors have shown that under some conditions on F, (1.30) admits non trivial solutions in $\mathbb{R}^n$ which are exponentially small at infinity.

Solutions of semi-linear elliptic equations can also be viewed as stationary states for the reaction diffusion equation

$$u_t - D\Delta u = f(|x|, u),$$

which is widely applicable in chemical dynamics, in particular, in studying the diffusion of the molecules of chemical species through a chemically reacting medium, where x represents the position of the molecule, t is the time, u is the spatial density, D is the diffusion coefficient and f measures the rate of change due to the reaction process. Also, they can be viewed as stationary states for nonlinear wave equations

$$u_{tt} - \Delta u = f(x, u),$$

or for the Schrödinger equation

$$iu_t + \Delta u = f(u).$$

2.3 Solution of semi-linear elliptic equations

In this section, we give a summary of the main methods provided in literature for the existence and behavior of solutions of elliptic equations in different domains. First we start by the following preliminaries that will be used throughout this section.

We consider the elliptic operator L defined by

$$Lu = -\sum_{i,j=1}^{n} a^{ij} u_i u_j + \sum_{i=1}^{n} b^i u_i + cu, \tag{1.31}$$

where the coefficients a^{ij}, b^i and c are continuous. We assume that L is uniformly elliptic, that is we assume that $\exists\, c_1, c_2 > 0$ such that for every $\xi = (\xi_1, \xi_2, \ldots, \xi_n) \in \mathbb{R}^n$

$$c_1|\xi|^2 \leq \sum_{i,j=1}^{n} a^{ij}\xi_i\xi_j \leq c_2|\xi|^2.$$

Moreover, without loss of generality, we assume that the matrix (a^{ij}) is symmetric, and the coefficients b^i and c satisfy

$$\sqrt{\sum_{i=1}^{n}(b^i)^2},\ |c| < b.$$

We assume throughout this section that Ω is an open and bounded domain of $\mathbb{R}^n$ with a C^2 boundary Γ, and $x = (x_1, x_2, \cdots, x_n) \in \Omega$. We introduce the Hopf's lemma and the maximum principle that are the main tools used in many existence results for elliptic equations.

Hopf's Lemma

Let $u \in C^2(\Omega) \cap C^1(\bar{\Omega})$ such that

$$Lu \leq 0 \text{ in } \Omega,$$

where L is defined in (1.31) with

$$c \equiv 0.$$

Suppose that there exists $x_0 \in \Gamma$ such that

$$u(x_0) > u(x) \quad \forall\ x \in \Omega.$$

Then,

$$\frac{\partial u}{\partial \nu}(x_0) > 0,$$

where ν is the outward normal vector to Γ at x_0. Moreover, if $c \geq 0$, then the same conclusion holds provided that $u(x_0) \geq 0$.

Remark 1.2. *If $u(x_0) = 0$, then no restriction is made on the sign of c.*

Maximum principle

Definition 1.3. *We say that the maximum principle holds for L in Ω if for every $u \in C^2(\Omega) \cap C(\bar{\Omega})$ with*

$$Lu \leq 0 \text{ in } \Omega,$$

and u attains a non-negative maximum over $\bar{\Omega}$ at an interior point in Ω then u is constant.

Or, if

$$Lu \geq 0 \text{ in } \Omega,$$

and u attains a non-positive minimum over $\bar{\Omega}$ at an interior point in Ω then u is constant.

According to [18], the following conditions are sufficient to apply the maximum principle.

1. $c \geq 0$;
2. Ω lies within a narrow domain $\beta < x_1 < \beta + \epsilon$, for some small enough $\epsilon > 0$.

Moreover, we admit the following proposition from [18].

Proposition 1.1. *Assume that* diam $\Omega < d$. *There exists $\delta > 0$ depending only on n, d, c_1 and b, such that the maximum principle holds for L in Ω provided that*

$$|\Omega| < \delta.$$

Now, we give the following existence results for elliptic equations

Variational method

The objective of this method is to study the existence of weak solutions for linear elliptic equations. We take L to be a uniformly elliptic operator, and we assume that the coefficients a_{ij} are C^1, then L can be rewritten in the following *divergence* form

$$Lu = -\sum_{i,j=1}^{n} (a^{ij}u_i)_j + \sum_{i=1}^{n} b^i u_i + cu.$$

We start by the simplest linear elliptic equations of the form

$$\begin{cases} Lu = f & \text{in } \Omega \\ u = 0 & \text{on } \Gamma. \end{cases} \tag{1.32}$$

where $f \in H^{-1}(\Omega)$. Now, multiplying the previous equation by $v \in H_0^1(\Omega)$ and applying Green's formula we get

$$\sum_{i,j=1}^{n} \int_\Omega a^{ij}u_i v_j \, dx + \sum_{i=1}^{n} \int_\Omega b^i u_i v \, dx + \int_\Omega cuv \, dx = < f, v >,$$

where $< ., . >$ is the application between $H^{-1}(\Omega)$ and $H_0^1(\Omega)$. If we take the bilinear form $a : H_0^1(\Omega) \times H_0^1(\Omega) \longrightarrow \mathbb{R}$ to be

$$a(u, v) = \sum_{i,j=1}^{n} \int_\Omega a^{ij}u_i v_j \, dx + \sum_{i=1}^{n} \int_\Omega b^i u_i v \, dx + \int_\Omega cuv \, dx \tag{1.33}$$

for every u and $v \in H_0^1(\Omega)$, then a weak solution of (1.32) is defined as follows.

Definition 1.4 (Weak Solution)**.** *We say that $u \in H_0^1(\Omega)$ is a weak solution of (1.32) if it satisfies*

$$a(u,v) =< f, v >$$

for every $v \in H_0^1(\Omega)$, where a is the bilinear form defined in (1.33).

The existence of weak solutions of (1.32) is given by the following theorem.

Theorem 1.1 (Lax-Milgram)**.** *Let H be a Hilbert space, and consider a bilinear mapping $a : H \times H \to \mathbb{R}$. If there exist $0 < C, \alpha < \infty$, such that*

1. $|a(u,v)| \leq C\|u\|_H\|v\|_H$ *(Continuity),*
2. $|a(u,u)| \geq \alpha\|u\|_H^2$ *(Coercivity),*

then, for every $f \in H^*$ (dual of H), there exists a unique $u \in H$ such that

$$a(u,v) =< f, v >_{H^*,H} \quad \forall\, v \in H.$$

In particular, if $H = H_0^1(\Omega)$ and a is the bilinear form given in (1.33), then if a is continuous and coercive, the problem (1.32) admits a unique weak solution. A special example of the variational problem is for L being the Laplace operator defined by

$$Lu = -\Delta u.$$

In this case, the bilinear form a is given by

$$a(u,v) = \int_\Omega \nabla u.\nabla v dx \quad \forall\ u \text{ and } v \in H_0^1(\Omega).$$

In particular,

$$a(u,u) = \int_\Omega |\nabla u|^2 dx = \|u\|^2_{H_0^1(\Omega)} \ \forall\ u \in H_0^1(\Omega).$$

Therefore, applying Lax-Milgram's theorem we deduce that for every $f \in H^{-1}(\Omega)$ there exists a unique weak solution u of the equation

$$\begin{cases} -\Delta u = f & \text{in } \Omega \\ u = 0 & \text{on } \Gamma. \end{cases}$$

Now, we move to the existence results for semilinear elliptic equations.

Method of sub and super solutions

In this method, we study the existence of solutions of the following elliptic equation in a bounded domain $\Omega \subset \mathbb{R}^n$.

$$\begin{cases} -\Delta u = g(u) & \text{in } \Omega \\ u = 0 & \text{on } \Gamma, \end{cases} \tag{1.34}$$

where g is a locally Lipschitz function in $\mathbb{R}$.

First, we define the sub and super solutions of (1.34) by:

Definition 1.5 (Super solution)**.** *A function $\overline{u} \in H^1(\Omega) \cap L^\infty(\Omega)$ is called a super solution of (1.34) if the following properties hold:*

1. *$-\Delta \overline{u} \geq g(\overline{u})$ in $H^{-1}(\Omega)$, that is, for every $v \in H_0^1(\Omega)$ we have*

$$\int_\Omega \nabla \overline{u}.\nabla v dx \geq \int_\Omega g(\overline{u}) v dx;$$

2. *$\overline{u}^- \in H_0^1(\Omega)$, where $\overline{u}^- = -\min\{u, 0\}$.*

Definition 1.6 (Sub solution)**.** *A function $\underline{u} \in H^1(\Omega) \cap L^\infty(\Omega)$ is called a sub solution of (1.34) if the following properties hold:*

1. *$-\Delta \underline{u} \leq g(\underline{u})$ in $H^{-1}(\Omega)$, that is, for every $v \in H_0^1(\Omega)$ we have*

$$\int_\Omega \nabla \underline{u}.\nabla v dx \leq \int_\Omega g(\underline{u}) v dx;$$

2. *$\underline{u}^+ \in H_0^1(\Omega)$, where $\underline{u}^+ = \max\{u, 0\}$.*

Now, the existence of solution of (1.34) is given by the following theorem given in [24]

Theorem 1.2. *Assume that $\underline{u}$ and $\overline{u}$ are sub and super solutions of (1.34) respectively, with $\underline{u} \leq \overline{u}$, then*

1. *There exist a solution $\tilde{u} \in H_0^1(\Omega) \cap L^\infty(\Omega)$ of (1.34) which is minimal with respect to $\underline{u}$. That is, if w is any super solution of (1.34) with $w \geq \underline{u}$, then $w \geq \tilde{u}$.*
2. *There exist a solution $\hat{u} \in H_0^1(\Omega) \cap L^\infty(\Omega)$ of (1.34) which is maximal with respect to $\overline{u}$. That is, if w is any sub solution of (1.34) with $w \leq \overline{u}$, then $w \leq \hat{u}$.*
3. *In particular, we have $\underline{u} \leq \tilde{u} \leq \hat{u} \leq \overline{u}$.*

Proof.
We define the positive constant M to be

$$M = \max\{\|\underline{u}\|_\infty, \|\overline{u}\|_\infty\}.$$

Since g is locally Lipschitz, then $g' \in L^\infty(-M, M)$, thus we may consider $\lambda > 0$ such that

$$\lambda > \|g'\|_{L^\infty(-M,M)}, \tag{1.35}$$

and we set for every $\lambda > 0$ the mapping g_λ defined by

$$g_\lambda(u) = g(u) + \lambda u.$$

Then, g_λ is an increasing mapping in $(-M, M)$. Now, we define the two sequences $(u_n)_{n\geq 0}$ and $(u^n)_{n\geq 0}$ where $u_0 = \underline{u}$ and $u^0 = \overline{u}$ and for every $n \in \mathbb{N}$, u_{n+1} and u^{n+1} are defined as the solutions of the following equations,

$$\begin{cases} -\Delta u_{n+1} + \lambda u_{n+1} = g_\lambda(u_n) & \text{in } \Omega \\ u_{n+1} = 0 & \text{on } \Gamma, \end{cases}$$

and

$$\begin{cases} -\Delta u^{n+1} + \lambda u^{n+1} = g_\lambda(u^n) & \text{in } \Omega \\ u^{n+1} = 0 & \text{on } \Gamma. \end{cases}$$

We will show that $u_0 \leq u_1 \leq u_2 \leq \cdots \leq u^2 \leq u^1 \leq u^0$. Moreover, $\lim\limits_{n\to\infty} u_n = \tilde{u}$ and $\lim\limits_{n\to\infty} u^n = \hat{u}$, which constitute the required solutions. We proceed in 5 steps.

Step 1: We show that $u_0 \leq u_1 \leq u^1 \leq u^0$

First, we note that since u_0 and $u^0 \in L^\infty(\Omega)$, and by regularity of g, then $g_\lambda(u_0)$ and $g_\lambda(u^0) \in L^\infty(\Omega)$. Thus, from Theorem 2.1.4 in [24], we deduce that u_1 and u^1 are well defined in $H_0^1(\Omega)$. Moreover, since u_0 is a sub solution of (1.34), then

$$-\Delta u_1 + \lambda u_1 = g_\lambda(u_0) \geq -\Delta u_0 + \lambda u_0.$$

Therefore, by maximum principle, we get $u_1 \geq u_0$. Following similar arguments, we can prove that $u^1 \leq u^0$. Moreover, since g_λ is increasing, then

$$-\Delta u^1 + \lambda u^1 = g_\lambda(u^0) \geq g_\lambda(u_0) = -\Delta u_1 + \lambda u_1.$$

Again, by maximum principle we get $u^1 \geq u_1$.

Step 2: By induction, we show that $u_{n-1} \leq u_n \leq u^n \leq u^{n-1}$.

As proved in step 1, this is true for $n = 1$. Now, we suppose that it is true for some $n \in \mathbb{N}$, then we have to show it for $n + 1$. That is, we need to show that $u_n \leq u_{n+1} \leq u^{n+1} \leq u^n$. This can be done in a similar manner to the previous step. In fact, since g_λ is increasing in $[-M, M]$,

then

$$-\Delta u_{n+1} + \lambda u_{n+1} = g_\lambda(u_n) \geq g_\lambda(u_{n-1}) = -\Delta(u_n) + \lambda(u_n),$$

then, by maximum principle, $u_{n+1} \geq u_n$. Similarly, we can show that $u^{n+1} \leq u^n$. Also, we have

$$-\Delta(u^{n+1}) + \lambda u^{n+1} = g_\lambda(u^n) \geq g_\lambda(u_n) = -\Delta u_{n+1} + \lambda(u_{n+1}).$$

By maximum principle, we deduce that $u^{n+1} \geq u_{n+1}$. Finally, up to this step we deduce that $u_0 \leq u_1 \leq u_2 \leq \cdots \leq u^2 \leq u^1 \leq u^0$.

Step 3: In this step, we show that $u_n \underset{n\to\infty}{\longrightarrow} \tilde{u}$ and $u^n \underset{n\to\infty}{\longrightarrow} \hat{u}$ which are solutions of (1.34).

Since $(u_n)_{n\geq 0}$ is an increasing sequence and bounded from above by $\overline{u}$, then $u_n \underset{n\to\infty}{\longrightarrow} \tilde{u}$. Moreover, by continuity of g, then $g_\lambda(u_n) \longrightarrow g_\lambda(\tilde{u})$ almost everywhere in Ω. Since $(u_n)_{n\geq 0}$ and g_λ are bounded, then by Lebesgue domination theorem, $g_\lambda(u_n) \longrightarrow g_\lambda(\tilde{u})$ in $L^2(\Omega)$. Moreover, since $(-\Delta + \lambda I)^{-1}$ is continuous from $L^2(\Omega)$ to $H_0^1(\Omega)$ (see theorem 2.1.4 in [24]), then

$$(-\Delta + \lambda I)^{-1} g_\lambda(u_n) \underset{n\to\infty}{\longrightarrow} v = (-\Delta + \lambda I)^{-1} g_\lambda(\tilde{u}).$$

That is, $u_n \underset{n\to\infty}{\longrightarrow} v$ in $H_0^1(\Omega)$, where v is a solution of

$$\begin{cases} -\Delta v + \lambda v = g_\lambda(\tilde{u}) & \text{in } \Omega \\ v = 0 & \text{on } \Gamma. \end{cases}$$

However, since $u_n \underset{n\to\infty}{\longrightarrow} \tilde{u}$, we deduce that $v = \tilde{u}$. Similarly, we can show that $u^n \to \hat{u}$.

Step 4: In this step, we show the independence of $\tilde{u}$ and $\hat{u}$ on λ.

In fact, if we take λ and λ' satisfying (1.35), and we define the two sequences $(u_n)_{n\geq 0}$ and $(u'_n)_{n\geq 0}$ obtained as in steps 1-3 using λ and λ' respectively, then $u_n \to \tilde{u}$ and $u'_n \to \tilde{u}'$. Moreover, we claim that $\tilde{u}' \geq u_n \ \forall n \geq 0$. This is clear for $n = 0$. By induction, we suppose that it is true for n, then, since $\tilde{u}'$ is a solution of (1.34) we deduce that

$$-\Delta \tilde{u}' + \lambda \tilde{u}' = g_\lambda(\tilde{u}') \geq g_\lambda(u_n) = -\Delta u_{n+1} + \lambda u_{n+1}.$$

By maximum principle, we deduce that $\tilde{u}' \geq u_{n+1}$. Therefore, taking the limit as $n \to \infty$ we get

$$\tilde{u}' \geq \tilde{u}.$$

Since λ and λ' are chosen randomly, we deduce that $\tilde{u}' = \tilde{u}$. Following the same arguments we can prove the result for $\hat{u}$.

Step 5: Finally, in this step we prove the minimality of $\tilde{u}$ and maximality of $\hat{u}$ with respect to

$\underline{u}$ and $\overline{u}$ respectively.

Let w be a super solution of (1.34) with $w \geq \underline{u}$, and take $M = \max\{\|\underline{u}\|_\infty, \|\overline{u}\|_\infty, \|w\|_\infty\}$, and λ as defined in (1.35). Then, since $w \geq u_0$, we proceed by induction to prove it true $\forall n \in \mathbb{N}$. Suppose that it is true for some $n \in \mathbb{N}$, then

$$-\Delta w + \lambda w \geq g_\lambda(w) \geq g_\lambda(u_n) = -\Delta u_{n+1} + \lambda u_{n+1}.$$

Then, by maximum principle we deduce that $w \geq u_{n+1}$. Now, taking the limit as $n \to \infty$ we get

$$w \geq \tilde{u}.$$

Similarly, we can show that $\hat{u}$ is maximal with respect to $\overline{u}$. ■

After studying the existence of solutions for semilinear elliptic equations in bounded domains, we move in the following section to study the behavior of these solutions.

Method of moving planes

In this part, we consider the elliptic equation

$$\begin{cases} -\Delta u = g(u) & \text{in } \Omega \\ u = 0 & \text{on } \Gamma, \end{cases} \tag{1.36}$$

where g is Lipschitz continuous. The existence of (1.36) can be viewed in context of variational methods and the method of sub and super solutions, as explained in the previous sections. However, the goal of this section is to study the behavior of this solution which is described by the following theorem.

Theorem 1.3. *Let Ω be an arbitrary bounded domain in $\mathbb{R}^n$, which is convex in the x_1 direction and symmetric with respect to the plane $x_1 = 0$. Let $u \in W^{2,n}_{loc}(\Omega) \cap C(\bar{\Omega})$ be a positive solution of (1.36), where g is Lipschitz continuous. Then, u is symmetric with respect to x_1 and $u_{x_1} < 0$ for $x_1 > 0$ in Ω.*

Proof.
The proof is done using the method of moving planes. Let $x = (x_1, y) \in \Omega$. We prove that

$$\begin{aligned} &u_{x_1} > 0 && \text{if } x_1 < 0, \\ &u(x_1, y) < u(x_1', y) && \text{for } x_1 < x_1' \text{ and } x_1 + x_1' < 0. \end{aligned} \tag{1.37}$$

Taking the limit as $x_1' \to -x_1$ we get

$$u(x_1, y) \leq u(-x_1, y) \quad \text{if } x_1 < 0. \tag{1.38}$$

In fact, since Ω is symmetric with respect to the plane $x_1 = 0$, then we can apply (1.37) and (1.38) on $v(x_1, y) = u(-x_1, y)$, which reveals the symmetry of u.

Let $(-a, a)$ be the projection of Ω on the x_1 axis, and for every $\lambda \in (-a, 0)$, let T_λ be the plane $x_1 = \lambda$, and

$$\Sigma(\lambda) = \{x \in \Omega \text{ such that } x_1 < \lambda\}.$$

For every $x \in \Sigma(\lambda)$ we define $v(x_1, y) = u(2\lambda - x_1, y)$ and $w(x, \lambda) = v(x) - u(x)$. Since g is Lipschitz, then w satisfies an equation of the form

$$\begin{cases} \Delta w + c(x, \lambda) w = 0 & \text{in } \Sigma(\lambda) \\ w \underset{\not\equiv}{\geq} 0 & \text{on } \partial\Sigma(\lambda). \end{cases}$$

where $c(x, \lambda)$ is bounded ($|c| < b$). Now, if $\Sigma(\lambda)$ is narrow in the x_1 direction ($0 < \lambda + a$ is small enough), we deduce from the maximum principle that

$$w(x, \lambda) > 0 \text{ on } \Sigma(\lambda). \tag{1.39}$$

That is, $u(2\lambda - x_1, y) > u(x_1, y)$ $\forall (x_1, y) \in \Sigma(\lambda)$. Moreover, since $w = 0$ on $T_\lambda \cap \Omega$, then by Hopf's lemma we deduce that $w_{x_1} = -2u_{x_1} < 0$ on $T_\lambda \cap \Omega$. Therefore, $u_{x_1}(\lambda, y) > 0$ on $T_\lambda \cap \Omega$.

Now, if we can prove that the previous results remain true for every $\lambda \in (-a, 0)$, then we deduce that (1.37) and (1.38) are verified. In fact, if we take $(-a, \mu)$ to be the maximal interval on which (1.39) is verified, then we claim that $\mu = 0$. We argue by contradiction. Suppose that $\mu < 0$, then $w(x, \mu) > 0$ in $\Sigma(\mu)$. Since Ω is bounded and $\forall \lambda \in (-a, 0)$, diam $\Sigma(\lambda) <$ diam Ω, and $|c(x, \lambda)| < b$, then $\Sigma(\lambda)$ and $c(x, \lambda)$ are changing in a way that n, d, c_1 and b defined in Proposition 1.1 remain the same, so we may fix $\delta > 0$, as in Proposition 1.1, small enough so that the maximum principle holds. Let K be a closed set in $\Sigma(\mu)$ such that

$$|\Sigma(\mu) \setminus K| \leq \frac{\delta}{2}.$$

Then $w(x, \mu) > 0$ in K. Moreover, by continuity of w it follows that for $\epsilon > 0$, small enough, we have $|\Sigma(\mu + \epsilon) \setminus K| \leq \delta$ and $w(x, \mu + \epsilon) > 0$ in K. Now, we take $\widetilde{\Sigma} = \Sigma(\mu + \epsilon) \setminus K$, then we have

$$\begin{cases} \Delta w + c(x, \mu + \epsilon) w = 0 & \text{in } \widetilde{\Sigma} \\ w \underset{\not\equiv}{\geq} 0 & \text{on } \partial\widetilde{\Sigma}. \end{cases}$$

Since $|\widetilde{\Sigma}| < \delta$, then applying the maximum principle we get

$$w(x, \mu + \epsilon) > 0 \text{ on } \widetilde{\Sigma}.$$

Therefore, $w(x, \mu + \epsilon) > 0$ on $\Sigma(\mu + \epsilon)$ which contradicts the maximality of μ. ■

After addressing the problem in bounded domains, we move now to the study of semilinear elliptic equations in the whole space $\mathbb{R}^n$. More precisely, we study the existence of radial solutions for such equations and the behavior of these solutions at ∞.

ODE based method

In this method, we study the existence of solution of elliptic equations in the whole space $\mathbb{R}^n$, $n \geq 2$. In particular, we take u to be a solution of

$$-\Delta u = g(u) \quad \text{in } \mathbb{R}^n, \tag{1.40}$$

with

$$\lim_{|x|\to\infty} u(x) = 0,$$

where g is a locally Lipschitz function in $\mathbb{R}$. Taking $r = |x|$, then the previous equation reduces to

$$u''(r) + \frac{n-1}{r}u'(r) + g(u(r)) = 0 \quad r \in \mathbb{R}^+, \tag{1.41}$$

with

$$\lim_{r\to\infty} u(r) = 0. \tag{1.42}$$

Theorem 1.4. *For every $u_0 > 0$, there exists a unique solution $u \in C^2([0, r_m))$ of (1.41) with $u(0) = u_0$ and $u'(0) = 0$, where $[0, r_m)$ is the maximal interval after which u satisfies the blow up alternative. More precisely, either $r_m = \infty$, or $\lim_{r\to r_m}(|u| + |u'|) = \infty$.*

Proof.
We give here a sketch of the proof for the convinience of the reader. Multiplying (1.41) by r^{n-1}, we notice that

$$(r^{n-1}u')' = -r^{n-1}g(u).$$

Therefore, if u exists, then it satisfies

$$u(r) = u_0 - \int_0^r s^{1-n}\int_0^s \sigma^{n-1}g(u(\sigma))\, d\sigma ds.$$

Now, we take $r_m > 0$ and we define $I_{r_m} = (0, r_m)$ and $X_{r_m,R} = \{u \in C(I_{r_m}) \text{ such that } \|u - u_0\|_\infty < R\}$, where R is chosen such that g is Lipschitz in $B_R(u_0)$. That is, there exists $K > 0$ such that for every $u, v \in B_R(u_0)$ we have $|g(u) - g(v)| < K|u - v|$. Consider the operator T such that

$$T(u)(r) = u_0 - \int_0^r s^{1-n}\int_0^s \sigma^{n-1}g(u(\sigma))\, d\sigma ds.$$

We claim that $T : X_{r_m,R} \longrightarrow X_{r_m,R}$ is a contraction for some $r_m > 0$ to be determined. First, we note that for every $u \in X_{r_m,R}$, then by regularity of g, $Tu \in C(I_{r_m})$. Moreover, for every $r \in I_{r_m}$ we have

$$\begin{aligned} |Tu(r) - u_0| &= \left| \int_0^r \int_0^s \frac{\sigma^{n-1}}{s^{n-1}} g(u(\sigma))\, d\sigma \right| \\ &\leq r_m^2 \|g\|_{L^\infty(B_R(u_0))}. \end{aligned}$$

Therefore, if r_m is chosen such that

$$r_m^2 \|g\|_{L^\infty(B_R)} < R, \tag{1.43}$$

then $Tu \in X_{r_m,R}$. Furthermore, for every $u, v \in X_{r_m,R}$ we have

$$\begin{aligned} |Tu - Tv| &= \left| \int_0^r \int_0^s \frac{\sigma^{n-1}}{s^{n-1}} (g(v(\sigma)) - g(u(\sigma)))\, d\sigma \right| \\ &\leq r_m^2 K \|v - u\|_\infty \end{aligned}$$

Therefore, if $r_m^2 K < 1$, that is

$$r_m < \frac{1}{\sqrt{K}}, \tag{1.44}$$

then T is a contraction. Therefore, by Banach fixed point theorem we deduce that T has a unique fixed point $u \in X_{r_m,R}$ satisfying $Tu(r) = u(r)\ \forall r \in I_{r_m}$.

Finally, we deduce that if r_m is chosen such that (1.43) and (1.44) are verified, then there exists a unique $u \in X_{r_m,R}$ such that

$$u(r) = u_0 - \int_0^r s^{1-n} \int_0^s \sigma^{n-1} g(u(\sigma))\, d\sigma ds,$$

for every $r \in I_{r_m}$. This interval can be extended to a maximal interval after which u satisfies the blow up alternative. ■

The previous theorem ensures the existence of solution of (1.41). In particular, it proves that $u(0)$ and $u'(0)$ uniquely determines u in a maximal interval $(0, r_m)$. Moreover, the condition (1.42), that is, the existence of solutions of (1.41) that vanish at infinity has attracted the attention of different authors in literature (see [16, 17, 19, 24, 28, 68, 74] and references therein). In [24] for example, the authors have shown that for a specific class of functions g, for example for

$$g(u) = -\lambda u + \mu |u|^{p-1} u,$$

where $\lambda, \mu > 0$ and $(n-2)p < (n+2)$, then there exists $u_0 > 0$ such that the solution u of (1.41)

with $u(0) = u_0$ and $u'(0) = 0$ is defined for all $r > 0$, that is $r_m = \infty$. Moreover, u is strictly positive and decreasing in r with $\lim_{r\to\infty} u(r) = 0$.

However, the existence of solutions of (1.40) non vanishing at ∞, in other words, the existence of solutions of (1.40) with $\lim_{|x|\to\infty} u(x) = z < \infty$ $(z \neq 0)$ was rarely discussed in literature. In [70], the authors have studied the existence of positive radial solutions of (1.40). They proved, under some conditions on the function g, the existence of oscillating solutions that converge to a positive root α of g. In particular, they applied their results on functions of the form $g(u) = -u + u^p$, $p > 1$. Yet, and up to our knowledge, none of the aforementioned works investigates the existence of monotonically varying solutions with non zero limiting behavior. In [49], the author has addressed this idea. He provided an ODE-based method to study the existence of positive, radial and monotonically increasing solutions of (1.40) with non zero limit related to the roots of the nonlinearity g.

In this thesis, we revisit the work of [49], however, we consider a more general case. In our work, we follow an algorithm similar to that used by the authors in [49] to study semi-linear elliptic equations of the form $\Delta u + g(|x|, u) = 0$ on $\mathbb{R}^n$. Given a suitable positive z satisfying $g(r, z) = 0$, $\forall r \in \mathbb{R}^+$, we discuss the existence of positive radial solutions u with $u(\infty) = z$.

2.4 Problems considered in part II of this thesis

In the second part of this thesis, presented in Chapter 5, we consider semi-linear elliptic equations of the form

$$\Delta u + g(|x|, u) = 0 \quad \text{in } \mathbb{R}^N.$$

Given a suitable positive z satisfying $g(r, z) = 0$ $\forall r \in \mathbb{R}^+$, we discuss the existence of positive radial solutions u with $u(\infty) = z$.

We develop an ODE based method similar to that used by the author in [49]. In fact, if we take $r = |x|$, then our equation is transformed into the following ODE

$$\begin{cases} -u'' - \dfrac{N-1}{r}u' = g(r, u) \quad \text{for} \quad 0 < r < \infty \\ u(0) = \xi, \quad u'(0) = 0. \end{cases} \tag{1.45}$$

Our goal thus is to determine $\xi > 0$, so that the solution u satisfies

$$\lim_{r\to\infty} u(r) = z. \tag{1.46}$$

We prove the following existence result.

Theorem 1.5. *Let g be a function defined on $\mathbb{R}^+ \times \mathbb{R}^+ = [0, \infty[\times[0, \infty[$, locally Lipschitz for the second variable and increasing for the first variable, satisfying (5.5), such that $g(r, 0) =$*

$g(r,z) = 0,\ \forall r \geq 0$ *where* $z > 0$ *satisfying the conditions* (5.6)–(5.14)*, see figure 5.1. Then there exists* $\xi \in]0, \xi_0[$ *and a solution* $u \in C^2(\mathbb{R}^+)$ *of* (5.3) *and* (5.4)*, with* $u(r) < z$ *for* $r \in [0, \infty[$ *and* $u'(r) > 0$ *for* $r \in]0, \infty[$.

Part I

Inverse problems and application to medical imaging of small absorbers

2

Exact controllability for wave equation

Jacques-Louis Lions was a scientist of remarkable prescience and immense energy. He understood that mathematics can make a great contribution to science, and he worked to see this goal realized.

– Roger Temam

One of the main tools used in our work throughout this thesis for the resolution of inverse source problems for wave equations is the exact controllability problem. In this chapter, we recall some preliminary results on the exact controllability problem for wave equation given by Lions [60]. Moreover, we focus on the controllability problem for wave equation with variable speed. In particular, we consider the following wave equation

$$\begin{cases} \dfrac{1}{c^2(\mathbf{x})} y_{tt}(\mathbf{x},t) - \Delta y(\mathbf{x},t) = 0 & \text{in } \Omega \times (0,T) \\ y(\mathbf{x},0) = y_0(\mathbf{x}) \quad y_t(\mathbf{x},0) = y_1(\mathbf{x}) & \text{in } \Omega \\ y(\sigma,t) = v(\sigma,t) & \text{on } \Sigma_T^0 = \Gamma_0 \times (0,T) \\ y(\sigma,t) = 0 & \text{on } \Sigma_T^1 = \Gamma_1 \times (0,T), \end{cases} \tag{2.1}$$

where $\Omega \subset \mathbb{R}^n$ is an open bounded domain with a smooth boundary Γ, Γ_0 is a subset of Γ with non-empty interior, and $\Gamma_1 = \Gamma \setminus \Gamma_0$.

We assume that the speed $c(\mathbf{x}) \in C^1(\bar{\Omega})$ with

$$c_{\min} \leq c(\mathbf{x}) \leq c_{\max}, \tag{2.2}$$

for some $c_{\min}, c_{\max} > 0$, and we denote by

$$s_1 = \|\nabla c\|_{L^\infty(\bar{\Omega})}. \tag{2.3}$$

The objective of this chapter is to study the existence of a control function v such that the

solution y of (2.1) satisfies

$$y(.,T) = y_t(.,T) = 0.$$

Exact controllability problem for wave equation was highly considered in literature, however, and up to our knowledge, non of the previous work has directly addressed equations of the form (2.1). For this purpose, in this chapter, we adapt the work done by Lions in [60] for the case of constant speed $c = 1$, and we follow the same steps to prove the convenience of his results in case of variable speed $c(\mathbf{x})$, which will be the case in the PAT problem studied in Chapter 4.

This chapter is organized as follows:

- **Section 1** recalls the work of Lions on the exact controllability results for wave equation with constant speed $c = 1$.

- **Section 2** provides an adaptation of the work of Lions to the case of variable speed $c = c(\mathbf{x})$. In section 2.1 we give the results with an L^2 boundary control. We follow the Hilbert uniqueness method, and we prove under some geometric-time conditions the existence of $v \in L^2(\Sigma_T^0)$ such that the controllability problem is verified. Then, in section 2.2 we discuss the existence of higher regularity results. In particular we study the existence of a control $v \in H_0^1((0,T), L^2(\Gamma_0))$.

1 Exact Controllability for wave equation with constant speed

We recall in this section the exact controllability results given by Lions in [60] for the wave equation with constant speed $c(\mathbf{x}) = c$, taken without loss of generality $c = 1$. In particular, we consider the problem

$$\begin{cases} y_{tt}(\mathbf{x},t) - \Delta y(\mathbf{x},t) = 0 & \text{in } \Omega \times (0,T) \\ y(\mathbf{x},0) = y_0(\mathbf{x}) \quad y_t(\mathbf{x},0) = y_1(\mathbf{x}) & \text{in } \Omega \\ y(\sigma,t) = v(\sigma,t) & \text{on } \Sigma_T^0 = \Gamma_0 \times (0,T) \\ y(\sigma,t) = 0 & \text{on } \Sigma_T^1 = \Gamma_1 \times (0,T), \end{cases} \tag{2.4}$$

The objective of this section is to study the existence of a control function v such that the solution y of (2.4) satisfies

$$y(.,T) = y_t(.,T) = 0. \tag{2.5}$$

First, we define for $\mathbf{x}_0$ in $\mathbb{R}^n$

$$\Gamma(\mathbf{x}_0) = \{\mathbf{x} \in \Gamma \text{ such that } (\mathbf{x} - \mathbf{x_0}).\nu > 0\},$$

and we take

$$R(\mathbf{x}_0) = \sup_{\mathbf{x}\in\bar{\Omega}} |\mathbf{x} - \mathbf{x}_0|.$$

Then, we recall the following results proved by Lions in [60].

Theorem 2.6. [**[60], Theorem 6.1**] *Let Ω be a bounded domain in $\mathbb{R}^n$, with a C^2 boundary Γ. Suppose that $\exists\ \mathbf{x}_0 \in \mathbb{R}^n$ such that*

$$\Gamma_0 = \Gamma(\mathbf{x}_0).$$

If $T > 2R(\mathbf{x}_0)$, then for every $(y_0, y_1) \in L^2(\Omega) \times H^{-1}(\Omega)$, there exists $v \in L^2(\Sigma_T^0)$ such that the solution y of (2.4) satisfies (2.5).

Another controllability result, with higher regularity control was also proved in the following theorem given in [60].

Theorem 2.7. [**[60], Theorem 6.4**] *Under the assumptions of the previous theorem, and for $T > 2R(\mathbf{x}_0)$, then for every $(y_0, y_1) \in H_0^1(\Omega) \times L^2(\Omega)$ there exists $v \in H_0^1((0,T), L^2(\Gamma_0))$ such that the solution y of (2.4) satisfies (2.5).*

2 Exact controllability for wave equation with variable speed

In this section we adjust the work of Lions to the case of variable speed $c = c(\mathbf{x})$.

2.1 Controllability results with L^2 boundary control

First, we give the following regularity result for the wave equation (2.1) based on the work of [57].

Lemma 2.1. *For every $(y_0, y_1) \in L^2(\Omega) \times H^{-1}(\Omega)$ and $v \in L^2(\Sigma_T^0)$, (2.1) admits a unique solution*

$$y \in C((0,T), L^2(\Omega)) \cap C^1((0,T), H^{-1}(\Omega)).$$

Our goal now is to find a suitable function $v \in L^2(\Sigma_T^0)$ such that the solution of (2.1) satisfies

$$y(.,T) = y_t(.,T) = 0.$$

For this purpose we follow the same approach followed by Lions in [60] in case of constant speed ($c = 1$), on which the Hilbert uniqueness method (HUM) is our main tool.

Hilbert Uniqueness Method (HUM)

First, we take ϕ to be a solution of the following wave equation

$$\begin{cases} \dfrac{1}{c^2(\mathbf{x})}\phi_{tt}(\mathbf{x},t) - \Delta\phi(\mathbf{x},t) = 0 & \text{in } \Omega \times (0,T) \\ \phi(\mathbf{x},0) = \phi_0(\mathbf{x}) \quad \phi_t(\mathbf{x},0) = \phi_1(\mathbf{x}) & \text{in } \Omega \\ \phi(\sigma,t) = 0 & \text{on } \Sigma_T = \Gamma \times (0,T). \end{cases} \tag{2.6}$$

Then, for every $(\phi_0, \phi_1) \in H_0^1(\Omega) \times L^2(\Omega)$, (2.6) admits a unique solution

$$\phi \in C((0,T), H_0^1(\Omega)) \cap C^1((0,T), L^2(\Omega)),$$

with

$$\frac{\partial\phi}{\partial\nu} \in L^2(\Sigma_T),$$

where ν is the outward normal vector on Γ, see [57].

Remark 2.1. *The quantity*

$$E(t) = \frac{1}{2}\int_\Omega \left(|\nabla\phi(\mathbf{x},t)|^2 + \frac{1}{c^2(\mathbf{x})}|\phi_t(\mathbf{x},t)|^2 \right) d\mathbf{x}$$

represents the energy of the system at time t, which is conserved in time. That is, $\forall\ t \in (0,T)$ we have $E(t) = E_0$ where

$$E_0 = E(0) = \frac{1}{2}\int_\Omega \left(|\nabla\phi_0|^2 + \frac{1}{c^2(\mathbf{x})}|\phi_1|^2 \right) d\mathbf{x}.$$

In fact, at each time t we have

$$\frac{dE}{dt} = \int_\Omega \left(\nabla\phi\nabla\phi_t + \frac{1}{c^2(\mathbf{x})}\phi_{tt}\phi_t \right) d\mathbf{x}.$$

On the other hand, multiplying (2.6) by ϕ_t and integrating over Ω we get

$$\int_\Omega \frac{1}{c^2(\mathbf{x})}\phi_{tt}\ \phi_t\ d\mathbf{x} - \int_\Omega \Delta\phi\ \phi_t\ d\mathbf{x} = 0,$$

thus,

$$\int_\Omega \frac{1}{c^2(\mathbf{x})}\phi_{tt}\ \phi_t\ d\mathbf{x} + \int_\Omega \nabla\phi\nabla\phi_t\ d\mathbf{x} = 0.$$

Therefore,

$$\frac{dE}{dt} = 0.$$

Moreover, the following estimate holds.

Lemma 2.2. *For every $(\phi_0, \phi_1) \in H_0^1(\Omega) \times L^2(\Omega)$, the solution ϕ of (2.6) satisfies*

$$\left|\frac{\partial \phi}{\partial \nu}\right|^2_{L^2(\Sigma_T)} \leq C(T, n, c) E_0, \tag{2.7}$$

for some $C(T, n, c) > 0$.

Proof.

The regularity of Ω allows us to take $q \in (C^1(\bar{\Omega}))^n$ such that $q = \nu$ on Γ. Then, multiplying (2.6) by $q.\nabla\phi$ and integrating over $\Omega \times (0, T)$ we get

$$\int_0^T \int_\Omega \frac{1}{c^2(\mathbf{x})} \phi_{tt}(q.\nabla\phi)\, d\mathbf{x}\, dt - \int_0^T \int_\Omega \Delta\phi(q.\nabla\phi)\, d\mathbf{x}\, dt = 0.$$

Moreover,

$$\begin{aligned}\int_0^T \int_\Omega \frac{1}{c^2(\mathbf{x})} \phi_{tt}(q.\nabla\phi)\, d\mathbf{x}\, dt =& \frac{1}{2}\int_0^T \int_\Omega \frac{1}{c^2(\mathbf{x})} |\phi_t|^2 \operatorname{div} q\, d\mathbf{x}\, dt + \frac{1}{2}\int_0^T \int_\Omega \nabla\left(\frac{1}{c^2}\right).q\ |\phi_t|^2 d\mathbf{x}\, dt \\ &+ \int_\Omega \frac{1}{c^2(\mathbf{x})} \phi_t(\mathbf{x}, T)\,(q.\nabla\phi(\mathbf{x}, T))\, d\mathbf{x} - \int_\Omega \frac{1}{c^2(\mathbf{x})} \phi_1(q.\nabla\phi_0)\, d\mathbf{x}.\end{aligned} \tag{2.8}$$

In fact,

$$\begin{aligned}\int_0^T \int_\Omega \frac{1}{c^2(\mathbf{x})} \phi_{tt}(q.\nabla\phi)\, d\mathbf{x}\, dt &= -\int_0^T \int_\Omega \frac{1}{c^2(\mathbf{x})} \phi_t(q.\nabla\phi_t)\, d\mathbf{x}\, dt + \int_\Omega \frac{1}{c^2(\mathbf{x})} \phi_t(q.\nabla\phi)\, d\mathbf{x}\Big|_0^T \\ &= -\int_0^T \int_\Omega \frac{1}{c^2(\mathbf{x})} \phi_t(q.\nabla\phi_t)\, d\mathbf{x}\, dt + \int_\Omega \frac{1}{c^2(\mathbf{x})} \phi_t(\mathbf{x}, T)(q.\nabla\phi(\mathbf{x}, T))\, d\mathbf{x} \\ &\quad - \int_\Omega \frac{1}{c^2(\mathbf{x})} \phi_1(q.\nabla\phi_0)\, d\mathbf{x}.\end{aligned}$$

Furthermore,

$$\begin{aligned}\int_0^T \int_\Omega \frac{1}{c^2(\mathbf{x})} \phi_t(q.\nabla\phi_t)\, d\mathbf{x}\, dt =& -\int_0^T \int_\Omega \frac{1}{c^2(\mathbf{x})} (\nabla\phi_t.q)\phi_t\, d\mathbf{x}\, dt - \int_0^T \int_\Omega \frac{1}{c^2(\mathbf{x})} |\phi_t|^2 \operatorname{div} q\, d\mathbf{x}\, dt \\ &- \int_0^T \int_\Omega \nabla\left(\frac{1}{c^2}\right).q\ |\phi_t|^2 d\mathbf{x}\, dt + \int_{\Sigma_T} \frac{1}{c^2(\sigma)} |\phi_t|^2 d\sigma dt.\end{aligned}$$

However, $\phi_t = \phi = 0$ on Γ. Thus,

$$\int_\Omega \frac{1}{c^2(\mathbf{x})} \phi_t(q.\nabla\phi_t)\, d\mathbf{x} = -\frac{1}{2}\int_\Omega \frac{1}{c^2(\mathbf{x})} |\phi_t|^2 \operatorname{div} q\, d\mathbf{x} - \frac{1}{2}\int_0^T \int_\Omega \nabla\left(\frac{1}{c^2}\right).q\ |\phi_t|^2 d\mathbf{x}\, dt,$$

which implies (2.8). On the other hand,

$$-\int_0^T\int_\Omega \Delta\phi(q.\nabla\phi)\,d\mathbf{x}\,dt = -\frac{1}{2}\int_0^T\int_\Omega |\nabla\phi|^2 \operatorname{div} q\,d\mathbf{x}\,dt + \int_0^T\int_\Omega (\nabla q)\nabla\phi.\nabla\phi\,d\mathbf{x}\,dt - \frac{1}{2}\int_0^T\int_\Omega \left|\frac{\partial\phi}{\partial\nu}\right|^2 d\sigma dt. \tag{2.9}$$

In fact,

$$\begin{aligned}-\int_0^T\int_\Omega \Delta\phi(q.\nabla\phi)\,d\mathbf{x}\,dt &= \int_0^T\int_\Omega \nabla\phi.\nabla(q.\nabla\phi)\,d\mathbf{x}\,dt - \int_0^T\int_\Gamma \frac{\partial\phi}{\partial\nu} q.\nabla\phi\,d\sigma dt\\ &= \int_0^T\int_\Omega \nabla\phi.\nabla(q.\nabla\phi)\,d\mathbf{x}\,dt - \int_0^T\int_\Gamma \left|\frac{\partial\phi}{\partial\nu}\right|^2 d\sigma dt.\end{aligned}$$

Moreover, by simple calculations one can see that

$$\int_Q \nabla\phi.\nabla(q.\nabla\phi)\,d\mathbf{x}dt = \int_Q (\nabla q)\nabla\phi.\nabla\phi\,d\mathbf{x}\,dt - \frac{1}{2}\int_Q \operatorname{div} q\,|\nabla\phi|^2\,d\mathbf{x}\,dt + \frac{1}{2}\int_0^T\int_\Gamma |\nabla\phi|^2\,d\sigma dt,$$

where (∇q) is the $n\times n$ matrix defined by

$$(\nabla q) = (\nabla q_1\ \nabla q_2\ \cdots\ \nabla q_n)^T.$$

Consequently,

$$\begin{aligned}-\int_0^T\int_\Omega \Delta\phi\,(q.\nabla\phi)\,d\mathbf{x}dt &= \int_Q (\nabla q)\nabla\phi.\nabla\phi\,d\mathbf{x}\,dt - \frac{1}{2}\int_Q \operatorname{div} q\,|\nabla\phi|^2\,d\mathbf{x}\,dt\\ &\quad + \frac{1}{2}\int_0^T\int_\Gamma |\nabla\phi|^2\,d\sigma dt - \int_0^T\int_\Gamma \left|\frac{\partial\phi}{\partial\nu}\right|^2 d\sigma dt.\end{aligned}$$

Moreover, since ϕ satisfies the Dirichlet boundary condition $\phi|_{\Sigma_T}=0$, then we have

$$\nabla\phi = \frac{\partial\phi}{\partial\nu}\nu \quad \text{on } \Sigma_T,$$

which implies (2.9). Combining (2.8) and (2.9) we get

$$\begin{aligned}\frac{1}{2}\int_0^T\int_\Gamma \left|\frac{\partial\phi}{\partial\nu}\right|^2 d\sigma dt &= \frac{1}{2}\int_0^T\int_\Omega \left(\frac{1}{c^2(\mathbf{x})}|\phi_t|^2 - |\nabla\phi|^2\right)\operatorname{div} q\,d\mathbf{x}\,dt\\ &\quad + \int_\Omega \frac{1}{c^2(\mathbf{x})}\phi_t(\mathbf{x},T)(q.\nabla\phi(\mathbf{x},T))\,d\mathbf{x} - \int_\Omega \frac{1}{c^2(\mathbf{x})}\phi_1(q.\nabla\phi_0)\,d\mathbf{x}\\ &\quad + \int_0^T\int_\Omega (\nabla q)\nabla\phi.\nabla\phi\,d\mathbf{x}\,dt + \frac{1}{2}\int_0^T\int_\Omega \nabla\left(\frac{1}{c^2}\right).q\ |\phi_t|^2 d\mathbf{x}\,dt.\end{aligned}$$

Therefore,

$$\begin{aligned}\frac{1}{2}\int_0^T\int_\Gamma\left|\frac{\partial\phi}{\partial\nu}\right|^2 d\sigma dt \leq{}& \frac{||\operatorname{div} q||_\infty}{2}\int_0^T\int_\Omega\left(|\nabla\phi|^2+\frac{1}{c^2(\mathbf{x})}|\phi_t|^2\right)d\mathbf{x}\,dt\\ &+\frac{n||q||_\infty}{2c_{\min}}\int_\Omega\left(|\nabla\phi(\mathbf{x},T)|^2+\frac{1}{c^2(\mathbf{x})}|\phi_t(\mathbf{x},T)|^2\right)d\mathbf{x}\\ &+\frac{n||q||_\infty}{2c_{\min}}\int_\Omega\left(|\nabla\phi_0|^2+\frac{1}{c^2(\mathbf{x})}|\phi_1|^2\right)d\mathbf{x}+\int_0^T\int_\Omega(\nabla q)\nabla\phi.\nabla\phi\,d\mathbf{x}\,dt\\ &+\frac{ns_1\|q\|_\infty}{c_{\min}}\int_0^T\int_\Omega\frac{1}{c^2(\mathbf{x})}|\phi_t|^2 d\mathbf{x}\,dt.\end{aligned}$$

Also,

$$\int_0^T\int_\Omega(\nabla q)\nabla\phi.\nabla\phi\,d\mathbf{x}dt\leq\int_0^T|(\nabla q)\nabla\phi|_2|\nabla\phi|_2\,dt.$$

However,

$$\begin{aligned}|(\nabla q)\nabla\phi|_2^2&=\int_\Omega|(\nabla q)\nabla\phi|^2\,dx\\ &\leq\int_\Omega||(\nabla q)||_2^2|\nabla\phi|^2dx\\ &\leq n||(\nabla q)||_\infty^2|\nabla\phi|_2^2.\end{aligned}$$

Therefore,

$$\begin{aligned}\int_0^T\int_\Omega(\nabla q)\nabla\phi.\nabla\phi\,d\mathbf{x}\,dt&\leq\int_0^T\sqrt{n}||(\nabla q)||_\infty|\nabla\phi|_2^2\,dt\\ &\leq\sqrt{n}||(\nabla q)||_\infty\int_0^T\int_\Omega|\nabla\phi|^2\,d\mathbf{x}\,dt\\ &\leq\sqrt{n}||(\nabla q)||_\infty\int_0^T\int_\Omega\left(|\nabla\phi|^2+\frac{1}{c^2(\mathbf{x})}|\phi_t|^2\right)d\mathbf{x}\,dt.\end{aligned}$$

Consequently,

$$\begin{aligned}\int_{\Sigma_T}\left|\frac{\partial\phi}{\partial\nu}\right|^2 d\sigma dt &\leq ||\operatorname{div} q||_\infty \int_0^T\int_\Omega \left(|\nabla\phi|^2+\frac{1}{c^2(\mathbf{x})}|\phi_t|^2\right) d\mathbf{x}\, dt\\ &+\frac{n||q||_\infty}{c_{\min}}\int_\Omega\left(|\nabla\phi(\mathbf{x},T)|^2+\frac{1}{c^2(\mathbf{x})}|\phi_t(\mathbf{x},T)|^2\right) d\mathbf{x}\\ &+\frac{n||q||_\infty}{c_{\min}}\int_\Omega\left(|\nabla\phi_0|^2+\frac{1}{c^2(\mathbf{x})}|\phi_1|^2\right) d\mathbf{x}\\ &+2\sqrt{n}||(\nabla q)||_\infty\int_0^T\int_\Omega(|\nabla\phi|^2+\frac{1}{c^2(\mathbf{x})}|\phi_t|^2)\, d\mathbf{x}\, dt\\ &+2\frac{ns_1\|q\|_\infty}{c_{\min}}\int_0^T\int_\Omega\frac{1}{c^2(\mathbf{x})}|\phi_t|^2 d\mathbf{x}\, dt\\ &\leq C(T,n,c)E_0,\end{aligned}$$

where we have used the conservation of energy given in Remark 2.1 in the last line. ■

The inequality (2.7) implies that the mapping $(\phi_0,\phi_1)\longrightarrow\frac{\partial\phi}{\partial\nu}$ is a continuous map from $H_0^1(\Omega)\times L^2(\Omega)$ to $L^2(\Sigma_T)$. Having ϕ in hands, we can now consider the following system:

$$\begin{cases}\dfrac{1}{c^2(\mathbf{x})}\psi_{tt}-\Delta\psi=0 & \text{in}\quad \Omega\times(0,T)\\ \psi=\dfrac{\partial\phi}{\partial\nu} & \text{on}\quad \Gamma_0\times(0,T)\\ \psi=0 & \text{on}\quad \Gamma_1\times(0,T)\\ \psi(.,T)=\psi_t(.,T)=0 & \text{in}\quad \Omega.\end{cases}\tag{2.10}$$

Applying the change of variables $t'=T-t$, we get a system similar to (2.1). Thus, the problem (2.10) admits a unique solution $\psi\in C((0,T);L^2(\Omega))\cap C^1((0,T);H^{-1}(\Omega))$, see [57], which implies that $\psi(.,0)$ and $\psi_t(.,0)$ are well defined in $L^2(\Omega)$ and $H^{-1}(\Omega)$ respectively. Now, if we can find $(\phi_0,\phi_1)\in H_0^1(\Omega)\times L^2(\Omega)$ such that

$$\psi(.,0)=y_0\quad\text{and}\quad\psi_t(.,0)=y_1,$$

then the controllability problem is solved with $v=\frac{\partial\phi}{\partial\nu}$ and $y=\psi$. For this purpose, we define the following map

$$\begin{aligned}\Lambda: H_0^1(\Omega)\times L^2(\Omega)&\longrightarrow H^{-1}(\Omega)\times L^2(\Omega)\\ (\phi_0,\phi_1)&\longrightarrow(\psi_t(.,0),-\psi(.,0)).\end{aligned}\tag{2.11}$$

Thus, if we can prove that Λ is an isomorphism between $H_0^1(\Omega)\times L^2(\Omega)$ and $H^{-1}(\Omega)\times L^2(\Omega)$, then the controllability problem is solved. First we note that for every (ϕ_0,ϕ_1) and $(\widetilde{\phi}_0,\tilde{\phi}_1)\in$

$H_0^1(\Omega) \times L^2(\Omega)$ we have

$$\left\langle \Lambda(\phi_0, \phi_1), \frac{1}{c^2}(\widetilde{\phi}_0, \tilde{\phi}_1) \right\rangle = \int_\Omega \frac{1}{c^2(\mathbf{x})} \psi_t(., 0)\tilde{\phi}_0 \, d\mathbf{x} - \int_\Omega \frac{1}{c^2(\mathbf{x})} \psi(., 0)\tilde{\phi}_1 \, d\mathbf{x}.$$

where $\langle ., . \rangle$ is the duality product between $H^{-1}(\Omega) \times L^2(\Omega)$ and $H_0^1(\Omega) \times L^2(\Omega)$. If we denote by ϕ, $\tilde{\phi}$ the solutions of (2.6) corresponding the initial conditions (ϕ_0, ϕ_1) and $(\tilde{\phi}_0, \tilde{\phi}_1)$ respectively, then multiplying (2.10) by $\tilde{\phi}$ and integrating over $\Omega \times (0, T)$, we get

$$\left\langle \Lambda(\phi_0, \phi_1), \frac{1}{c^2}(\widetilde{\phi}_0, \tilde{\phi}_1) \right\rangle = \int_0^T \int_{\Gamma_0} \frac{\partial \phi}{\partial \nu} \frac{\partial \tilde{\phi}}{\partial \nu} d\sigma dt. \tag{2.12}$$

In particular,

$$\left\langle \Lambda(\phi_0, \phi_1), \frac{1}{c^2}(\phi_0, \phi_1) \right\rangle = \int_0^T \int_{\Gamma_0} \left(\frac{\partial \phi}{\partial \nu} \right)^2 d\sigma dt.$$

Now, to prove that Λ is an isomorphism we proceed in two steps. First, we prove in the following lemma the continuity of Λ

Lemma 2.3. *The operator Λ defined in (2.11) is continuous.*

Proof.

The continuity of Λ can be obtained from (2.12) along with (2.7). In fact, for every (ϕ_0, ϕ_1) and $(\widetilde{\phi}_0, \tilde{\phi}_1) \in H_0^1(\Omega) \times L^2(\Omega)$ we have

$$\begin{aligned} \left| \left\langle \Lambda(\phi_0, \phi_1), \frac{1}{c^2}(\widetilde{\phi}_0, \tilde{\phi}_1) \right\rangle \right| &= \left| \int_0^T \int_{\Gamma_0} \frac{\partial \phi}{\partial \nu} \frac{\partial \tilde{\phi}}{\partial \nu} d\sigma dt \right| \\ &\leq \left| \frac{\partial \phi}{\partial \nu} \right|_{L^2(\Sigma_T)} \left| \frac{\partial \tilde{\phi}}{\partial \nu} \right|_{L^2(\Sigma_T)} \\ &\leq C \|(\phi_0, \phi_1)||_{1,2} \, ||(\tilde{\phi}_0, \tilde{\phi}_1)||_{1,2}, \end{aligned}$$

where $\| \cdot \|_{1,2}$ is the norm in $H_0^1(\Omega) \times L^2(\Omega)$. However, the regularity of the speed ($c \in C^1(\bar{\Omega})$), along with (2.2) implies that for every $(\widetilde{\phi}_0, \tilde{\phi}_1) \in H_0^1(\Omega) \times L^2(\Omega)$ we have

$$\left| \left\langle \Lambda(\phi_0, \phi_1), (\widetilde{\phi}_0, \tilde{\phi}_1) \right\rangle \right| \leq C \|(\phi_0, \phi_1)||_{1,2} \, ||(\tilde{\phi}_0, \tilde{\phi}_1)||_{1,2},$$

which implies the continuity of Λ. ■

Now, to prove the isomorphism it is enough to have the following observability inequality satisfied

$$| \langle \Lambda(\phi_0, \phi_1), (\phi_0, \phi_1) \rangle | \geq C \|(\phi_0, \phi_1)\|_{1,2}^2.$$

In other words, we need to prove that for every $(\phi_0, \phi_1) \in H_0^1(\Omega) \times L^2(\Omega)$ we have

$$\int_0^T \int_{\Gamma_0} \left(\frac{\partial \phi}{\partial \nu} \right)^2 d\sigma dt \geq C E_0. \tag{2.13}$$

In the following theorem, we give a sufficient condition to obtain the observability inequality (2.13).

Theorem 2.8. *Suppose that* $\exists\, \mathbf{x}_0 \in \mathbb{R}^n$ *such that*

$$\Gamma_0 = \Gamma(\mathbf{x}_0) = \{\mathbf{x} \in \Gamma \text{ such that } (\mathbf{x} - \mathbf{x}_0).\nu > 0\}. \tag{2.14}$$

Consider the following constants,

$$R(\mathbf{x}_0) = \sup_{x \in \bar{\Omega}} |\mathbf{x} - \mathbf{x}_0|, \tag{2.15}$$

and

$$r(\mathbf{x}_0) = \sup_{x \in \Gamma(\mathbf{x}_0)} (\mathbf{x} - \mathbf{x}_0).\nu\ . \tag{2.16}$$

Take

$$T_0 = 2\frac{(s_1 + 1)}{c_{\min}} R(\mathbf{x}_0), \tag{2.17}$$

where $c_{\min}$ *and* s_1 *are defined in* (2.2) *and* (2.3) *respectively. Then, for every* $T > T_0$*, the observability inequality* (2.13) *is satisfied.*

Following the previous theorem, we finally we end up with the following controllability result.

Theorem 2.9. *Under the assumptions of Theorem 2.8, if* $T > T_0$ *then for every* $(y_0, y_1) \in L^2(\Omega) \times H^{-1}(\Omega)$ *there exits* $v \in L^2(\Sigma_T^0)$ *such that the solution of* (2.1) *satisfies*

$$y(., T) = y_t(., T) = 0.$$

Moreover, there exists $C > 0$ *such that*

$$|v|_{L^2(\Sigma_T^0)} \leq C \|(y_0, y_1)\|_{L^2(\Omega) \times H^{-1}(\Omega)}.$$

Proof of Theorem 2.8

Let $q \in (W^{1,\infty})^n$. Multiplying (2.6) by $q.\nabla\phi$ and integrating we get

$$\int_0^T \int_\Omega \frac{1}{c^2(\mathbf{x})} \phi_{tt}(q.\nabla\phi) d\mathbf{x} dt - \int_0^T \int_\Omega \Delta\phi(q.\nabla\phi) d\mathbf{x} dt = 0.$$

Moreover, following the same steps of Lemma 2.2 we obtain

$$\frac{1}{2}\int_0^T\int_\Gamma\left|\frac{\partial\phi}{\partial\nu}\right|^2 q.\nu\, d\sigma dt = \frac{1}{2}\int_0^T\int_\Omega\left(\frac{1}{c^2(\mathbf{x})}|\phi_t|^2-|\nabla\phi|^2\right)\operatorname{div} q\, d\mathbf{x}dt+\left(\frac{1}{c^2}\phi_t, q.\nabla\phi\right)\Big|_0^T + \int_0^T\int_\Omega(\nabla q)\nabla\phi.\nabla\phi\, d\mathbf{x}dt+\frac{1}{2}\int_0^T\int_\Omega\nabla\left(\frac{1}{c^2}\right).q\ |\phi_t|^2 d\mathbf{x}dt,$$

where $(.,.)$ is the inner product in $L^2(\Omega)$. In particular, for $q=\mathbf{x}-\mathbf{x}_0$ we have

$$\frac{1}{2}\int_0^T\int_\Gamma\left|\frac{\partial\phi}{\partial\nu}\right|^2(\mathbf{x}-\mathbf{x}_0).\nu\, d\sigma dt = \frac{n}{2}\int_0^T\int_\Omega\left(\frac{1}{c^2(\mathbf{x})}|\phi_t|^2-|\nabla\phi|^2\right)d\mathbf{x}\,dt+\left(\frac{1}{c^2}\phi_t, q.\nabla\phi\right)\Big|_0^T + \int_0^T\int_\Omega|\nabla\phi|^2\, d\mathbf{x}\,dt+\frac{1}{2}\int_0^T\int_\Omega\nabla\left(\frac{1}{c^2}\right).q\ |\phi_t|^2 d\mathbf{x}\,dt. \tag{2.18}$$

On the other hand, multiplying (2.6) by ϕ and integrating over $\Omega\times(0,T)$ we get

$$\int_0^T\int_\Omega\left(\frac{1}{c^2(\mathbf{x})}|\phi_t|^2-|\nabla\phi|^2\right)d\mathbf{x}\,dt=\left(\frac{1}{c^2}\phi_t,\phi\right)\Big|_0^T. \tag{2.19}$$

Multiplying (2.19) by $\frac{n-1}{2}$ and adding to (2.18) we get

$$\frac{1}{2}\int_0^T\int_\Gamma\left|\frac{\partial\phi}{\partial\nu}\right|^2(\mathbf{x}-\mathbf{x}_0).\nu\, d\sigma dt = \left(\frac{1}{c^2}\phi_t, q.\nabla\phi+\frac{n-1}{2}\phi\right)\Big|_0^T + \frac{1}{2}\int_0^T\int_\Omega\left(\frac{1}{c^2(\mathbf{x})}|\phi_t|^2+|\nabla\phi|^2\right)d\mathbf{x}\,dt + \frac{1}{2}\int_0^T\int_\Omega\nabla\left(\frac{1}{c^2}\right).q\ |\phi_t|^2 d\mathbf{x}\,dt.$$

Moreover, using the conservation of energy we deduce that

$$\frac{1}{2}\int_0^T\int_\Gamma\left|\frac{\partial\phi}{\partial\nu}\right|^2(\mathbf{x}-\mathbf{x}_0).\nu\, d\sigma dt = \left(\frac{1}{c^2}\phi_t, q.\nabla\phi+\frac{n-1}{2}\phi\right)\Big|_0^T + TE_0 + \frac{1}{2}\int_0^T\int_\Omega\nabla\left(\frac{1}{c^2}\right).q\ |\phi_t|^2 d\mathbf{x}\,dt. \tag{2.20}$$

Now, to obtain the observability inequality (2.13), one should bound each of the terms in the previous equation. In fact, for every $t\in(0,T)$ we have

$$\left|\left(\frac{1}{c^2}\phi_t, q.\nabla\phi+\frac{n-1}{2}\phi\right)\right|\le\left|\frac{1}{c^2}\phi_t\right|_2\left|q.\nabla\phi+\frac{n-1}{2}\phi\right|_2$$

In addition, since $\phi|_\Gamma=0$, we have

$$(q.\nabla\phi,\phi)=\int_\Omega(q.\nabla\phi)\phi\, d\mathbf{x}=-\int_\Omega q\phi.\nabla\phi\, dx-\int_\Omega\operatorname{div} q\,|\phi|^2\, d\mathbf{x},$$

thus,

$$(q.\nabla\phi,\phi) = -\frac{1}{2}\int_\Omega \operatorname{div} q\,|\phi|^2\,dx = -\frac{n}{2}|\phi|_2^2.$$

Therefore,

$$\begin{aligned}\left|q.\nabla\phi + \frac{(n-1)}{2}\phi\right|_2^2 &= |q.\nabla\phi|_2^2 + (n-1)(q.\nabla\phi,\phi) + \frac{(n-1)^2}{4}|\phi|_2^2\\ &= |q.\nabla\phi|_2^2 - \frac{n(n-1)}{2}|\phi|_2^2 + \frac{(n-1)^2}{4}|\phi|_2^2\\ &= |q.\nabla\phi|_2^2 - \frac{(n^2-1)}{4}|\phi|_2^2\\ &\le |q.\nabla\phi|_2^2.\end{aligned}$$

Moreover,

$$\begin{aligned}|q.\nabla\phi|_2 &= |(\mathbf{x}-\mathbf{x}^0).\nabla\phi|_2\\ &\le R(\mathbf{x}^0)|\nabla\phi|_2,\end{aligned}$$

where $R(\mathbf{x}^0)$ is defined in (2.15). Therefore,

$$\begin{aligned}\left|\left(\frac{1}{c^2}\phi_t, q.\nabla\phi + \frac{n-1}{2}\phi\right)\right| &\le \frac{1}{c_{\min}}\left|\frac{1}{c}\phi_t\right|_2\left|q.\nabla\phi + \frac{n-1}{2}\phi\right|_2\\ &\le \frac{1}{c_{\min}}\left|\frac{1}{c}\phi_t\right|_2|q.\nabla\phi|_2\\ &\le \frac{1}{c_{\min}}R(\mathbf{x}_0)\left|\frac{1}{c}\phi_t\right|_2|\nabla\phi|_2\\ &\le \frac{R(\mathbf{x}_0)}{c_{\min}}\left(\frac{1}{2}\left|\frac{1}{c}\phi_t\right|_2^2 + \frac{1}{2}|\nabla\phi|_2^2\right)\\ &\le \frac{R(\mathbf{x}_0)}{c_{\min}}E_0,\end{aligned}$$

where $c_{\min}$ is defined in (2.2). Finally, we deduce that

$$\left|\left(\frac{1}{c^2}\phi_t, q.\nabla\phi + \frac{n-1}{2}\phi\right)\Big|_0^T\right| \le 2\frac{R(\mathbf{x}_0)}{c_{\min}}E_0. \tag{2.21}$$

Furthermore,

$$\begin{aligned}\left|\frac{1}{2}\int_0^T\int_\Omega \nabla\left(\frac{1}{c^2}\right).q\ |\phi_t|^2 d\mathbf{x}\ dt\right| &\leq \frac{1}{2}\left|\int_0^T\int_\Omega -2\frac{\nabla c(\mathbf{x})}{c^3(\mathbf{x})}.q\ |\phi_t|^2 d\mathbf{x}\right| \\ &\leq 2\frac{s_1}{c_{\min}}R(\mathbf{x}_0)\left(\frac{1}{2}\int_0^T\int_\Omega \frac{1}{c^2(\mathbf{x})}|\phi_t|^2 d\mathbf{x}\right) \\ &\leq 2\frac{s_1}{c_{\min}}R(\mathbf{x}_0)E_0,\end{aligned} \tag{2.22}$$

where s_1 is defined in (2.3). Combining (2.20), (2.21) and (2.22) we obtain

$$\begin{aligned}\left(T-2\frac{(s_1+1)}{c_{\min}}R(\mathbf{x}_0)\right)E_0 &\leq \frac{1}{2}\int_0^T\int_\Gamma \left|\frac{\partial\phi}{\partial\nu}\right|^2(\mathbf{x}-\mathbf{x}_0).\nu\, d\sigma dt \\ &\leq \frac{1}{2}\int_0^T\int_{\Gamma_0} \left|\frac{\partial\phi}{\partial\nu}\right|^2(\mathbf{x}-\mathbf{x}_0).\nu\, d\sigma dt \\ &\leq \frac{r(\mathbf{x}_0)}{2}\int_0^T\int_{\Gamma_0} \left|\frac{\partial\phi}{\partial\nu}\right|^2 d\sigma dt,\end{aligned}$$

where $r(\mathbf{x}_0)$ is defined in (2.16). Now, if $T > T_0 = 2\frac{(s_1+1)}{c_{\min}}R(\mathbf{x}_0)$ we get

$$E_0 \leq \frac{r(\mathbf{x}_0)}{2(T-T_0)}\int_0^T\int_{\Gamma_0}\left|\frac{\partial\phi}{\partial\nu}\right|^2 d\sigma dt,$$

which is equivalent to (2.13).

■

Proof of Theorem 2.9

According to Theorem 2.8, if $\Gamma = \Gamma(\mathbf{x}_0)$ and $T > T_0$, then we know that the observability inequality (2.13) is verified. That is, the operator Λ is an isomorphism between $H_0^1(\Omega)\times L^2(\Omega)$ and $H^{-1}(\Omega)\times L^2(\Omega)$, which implies that for every $(y_0, y_1) \in L^2(\Omega)\times H^{-1}(\Omega)$, there exists $(\phi_0,\phi_1)\in H_0^1(\Omega)\times L^2(\Omega)$ such that

$$\Lambda(\phi_0,\phi_1) = (y_1, -y_0).$$

Therefore, the controllability problem is solved with $v = \frac{\partial\phi}{\partial\nu}$ and $y = \psi$, where ϕ and ψ are the solutions of (2.6) and (2.10) respectively.

Moreover, from the regularity of the wave equation (2.6) and the estimate given in Lemma 2.2 we know that

$$\left|\frac{\partial\phi}{\partial\nu}\right|_{L^2(\Sigma_T^0)} \leq C(T,n,c)\|(\phi_0,\phi_1)\|_{1,2}.$$

However, since Λ is an isomorphism, we deduce that

$$\begin{aligned}\|(\phi_0,\phi_1)\|_{1,2} &\leq C\|\Lambda(\phi_0,\phi_1)\|_{H^{-1}(\Omega)\times L^2(\Omega)}\\ &\leq C\|(y_1,-y_0)\|_{H^{-1}(\Omega)\times L^2(\Omega)}.\end{aligned}$$

Therefore,

$$|v|_{L^2(\Sigma_T^0)} = \left|\frac{\partial\phi}{\partial\nu}\right|_{L^2(\Sigma_T^0)} \leq C\|(y_1,-y_0)\|_{H^{-1}(\Omega)\times L^2(\Omega)}.$$

■

2.2 Higher regularity results

In this section we study the exact controllability problem of (2.1) with higher regularity control. In particular, we prove the following theorem.

Theorem 2.10. *Suppose that the observation boundary Γ_0 satisfies the geometric condition (2.14), and $T > T_0$ defined in (2.17). Then, for every $(y_0,y_1) \in H_0^1(\Omega)\times L^2(\Omega)$, there exists $v \in H_0^1((0,T),L^2(\Gamma_0))$ such that the solution of (2.1) satisfies*

$$y(.,T) = y_t(.,T) = 0.$$

Before doing the proof of this theorem, we take ϕ to be a solution of (2.6), then the following regularity result is verified.

Lemma 2.4. *For every $(\phi_0,\phi_1) \in L^2(\Omega)\times H^{-1}(\Omega)$, the solution ϕ of (2.6) satisfies*

$$\phi \in C((0,T),L^2(\Omega)) \cap C^1((0,T),H^{-1}(\Omega)).$$

Moreover,

$$\frac{\partial\phi}{\partial\nu} \in H^{-1}((0,T),L^2(\Gamma)),$$

and the mapping $(\phi_0,\phi_1) \longrightarrow \frac{\partial\phi}{\partial\nu}$ is continuous from $L^2(\Omega)\times H^{-1}(\Omega)$ to $H^{-1}((0,T),L^2(\Gamma))$.

Proof.
The regularity of ϕ is obtained by following the work of [57]. To prove the regularity of $\frac{\partial\phi}{\partial\nu}$ we take $\Psi \in H_0^1(\Omega)$ to be a solution of

$$\Delta\Psi = \frac{1}{c^2(\mathbf{x})}\phi_1. \tag{2.23}$$

Now we define

$$w(\mathbf{x},t) = \int_0^t \phi(\mathbf{x},s)ds + \Psi(\mathbf{x}). \tag{2.24}$$

Then, w is a solution of

$$\begin{cases} \dfrac{1}{c^2(\mathbf{x})} w_{tt} - \Delta w = 0 & \text{in } \Omega \times (0,T) \\ w(\mathbf{x},0) = \Psi(\mathbf{x}) \quad w_t(\mathbf{x},0) = \phi_0 & \text{in } \Omega \\ w(\sigma,t) = 0 & \text{on } \Gamma \times (0,T). \end{cases} \tag{2.25}$$

Moreover, since $(\phi_0, \phi_1) \in L^2(\Omega) \times H^{-1}(\Omega)$, then $(\Psi, \phi_0) \in H_0^1(\Omega) \times L^2(\Omega)$, which implies that

$$w \in C((0,T), H_0^1(\Omega)) \cap C^1((0,T), L^2(\Omega)),$$

and

$$\frac{\partial w}{\partial \nu} \in L^2(\Sigma_T),$$

with

$$\left| \frac{\partial w}{\partial \nu} \right|_{L^2(\Sigma_T)} \leq C \|(\Psi, \phi_0)\|_{1,2} \leq C \|(\phi_0, \phi_1)\|_{L^2(\Omega) \times H^{-1}(\Omega)}. \tag{2.26}$$

Furthermore, formula (2.24) implies that $\phi(\mathbf{x}, t) = w_t(\mathbf{x}, t)$, thus

$$\frac{\partial \phi}{\partial \nu} = \frac{\partial}{\partial t} \left(\frac{\partial w}{\partial \nu} \right) \in H^{-1}((0,T), L^2(\Gamma)).$$

The continuity of the mapping $(\phi_0, \phi_1) \longrightarrow \frac{\partial \phi}{\partial \nu}$ is directly obtained from (2.26). ■

Proof of Theorem 2.10

We first take ϕ to be a solution of (2.6) for $(\phi_0, \phi_1) \in L^2(\Omega) \times H^{-1}(\Omega)$. Then, as proved in the previous lemma, we have

$$\frac{\partial \phi}{\partial \nu} \in H^{-1}((0,T), L^2(\Gamma)),$$

with

$$\left\| \frac{\partial \phi}{\partial \nu} \right\|_{H^{-1}((0,T), L^2(\Gamma))} \leq C \|(\phi_0, \phi_1)\|_{L^2(\Omega) \times H^{-1}(\Omega)}.$$

Let $G = H^{-1}((0,T), L^2(\Gamma_0))$, then the dual of G is given by $G' = H_0^1((0,T), L^2(\Gamma_0))$. We define the operator $L : G \to G'$ to be the isomorphism between G and G', then for every $(\phi_0, \phi_1) \in L^2(\Omega) \times H^{-1}(\Omega)$, we have $L\left(\frac{\partial \phi}{\partial \nu}\right) \in G'$ with

$$\left\| L\left(\frac{\partial \phi}{\partial \nu} \right) \right\|_{G'} \leq \left\| \frac{\partial \phi}{\partial \nu} \right\|_{G} \leq C \|(\phi_0, \phi_1)\|_{L^2(\Omega) \times H^{-1}(\Omega)}. \tag{2.27}$$

Now, we take ψ to be a solution of

$$\begin{cases} \dfrac{1}{c^2(\mathbf{x})}\psi_{tt} - \Delta\psi = 0 & \text{in } \Omega \times (0,T) \\ \psi(.,T) = \psi_t(.,T) = 0 & \text{in } \Omega \\ \psi(\sigma,t) = L\left(\dfrac{\partial\phi}{\partial\nu}\right) & \text{on } \Gamma_0 \times (0,T) \\ \psi(\sigma,t) = 0 & \text{on } \Gamma_1 \times (0,T). \end{cases} \tag{2.28}$$

As in the previous section, if we can find $(\phi_0, \phi_1) \in L^2(\Omega) \times H^{-1}(\Omega)$ such that

$$\psi(.,0) = y_0 \quad \text{and} \quad \psi_t(.,0) = y_1,$$

then the controllability problem is solved with $y = \psi$ and $v = L\left(\frac{\partial\psi}{\partial\nu}\right)$. Again, we define the operator $\Lambda : L^2(\Omega) \times H^{-1}(\Omega) \to L^2(\Omega) \times H_0^1(\Omega)$, where

$$\Lambda(\phi_0, \phi_1) = (\psi_t(.,0), -\psi(.,0)).$$

Then, taking $\phi, \tilde{\phi}$ to be the solutions of (2.6) with initial conditions (ϕ_0, ϕ_1) and $(\tilde{\phi_0}, \tilde{\phi_1})$ respectively, and multiplying (2.28) by $\tilde{\phi}$ and integrating over $\Omega \times (0,T)$ we get

$$\left\langle \frac{1}{c^2(\mathbf{x})}(\tilde{\phi_0}, \tilde{\phi_1}),\ \Lambda(\phi_0, \phi_1) \right\rangle = \left\langle \frac{\partial\tilde{\phi}}{\partial\nu}, L\left(\frac{\partial\phi}{\partial\nu}\right) \right\rangle_{G,G'} \tag{2.29}$$

where, $\langle ., . \rangle_{G,G'}$ is the application between G and G'. In particular, we have

$$\left\langle \frac{1}{c^2(\mathbf{x})}(\phi_0, \phi_1),\ \Lambda(\phi_0, \phi_1) \right\rangle = \left\langle \frac{\partial\phi}{\partial\nu}, L\left(\frac{\partial\phi}{\partial\nu}\right) \right\rangle_{G,G'} = \int_0^T \int_\Gamma \left| L\left(\frac{\partial\phi}{\partial\nu}\right) \right|^2 d\sigma dt. \tag{2.30}$$

Our goal again is to prove that Λ is an isomorphism. First we note that from (2.27) and (2.29) one can see that Λ is continuous from $L^2(\Omega) \times H^{-1}(\Omega)$ to $L^2(\Omega) \times H_0^1(\Omega)$. Moreover, (2.30) implies that it is enough to prove that the mapping $(\phi_0, \phi_1) \to L\left(\frac{\partial\phi}{\partial\nu}\right)$ is an isomorphism.

Now, for every $(\phi_0, \phi_1) \in L^2(\Omega) \times H^{-1}(\Omega)$ we take $\Psi \in H_0^1(\Omega)$ to be a solution of (2.23), and w as defined in (2.24) solution of (2.25). Then, as proved in the previous section, if Γ_0 is assumed to satisfy the geometric condition (2.14), and for $T > T_0$, the mapping $(\Psi, \phi_0) \to \frac{\partial w}{\partial\nu}$ is an isomorphism from $H_0^1(\Omega) \times L^2(\Omega)$ to $L^2((0,T), L^2(\Gamma_0))$. Therefore, $(\phi_0, \phi_1) \to \frac{\partial w}{\partial\nu}$ is an isomorphism from $L^2(\Omega) \times H^{-1}(\Omega)$ to $L^2((0,T), L^2(\Gamma_0))$.

Furthermore, from (2.24) we notice that $\phi = \frac{\partial w}{\partial t}$, that is $\frac{\partial\phi}{\partial\nu} = \frac{\partial}{\partial t}\left(\frac{\partial w}{\partial\nu}\right)$. Therefore, the mapping

$$(\phi_0, \phi_1) \to \frac{\partial\phi}{\partial\nu},$$

is an isomorphism from $L^2(\Omega) \times H^{-1}(\Omega)$ to $H^{-1}((0,T), L^2(\Gamma_0))$. Moreover, since L is an isomorphism from G to G' we deduce that

$$(\phi_0, \phi_1) \to L\left(\frac{\partial \phi}{\partial \nu}\right),$$

is an isomorphism from $L^2(\Omega) \times H^{-1}(\Omega)$ to $H_0^1((0,T), L^2(\Gamma_0))$, which ends the proof.

■

3

Inverse TAT problem

Scientific inquiry starts with observation. The more one can see, the more one can investigate. Indeed, we often mark our progress in science by improvements in imaging.

– Martin Chalfie

This chapter deals with the inverse thermo-acoustic tomography (TAT) problem. It is a biomedical, multi-wave imaging technique, based on the photo-acoustic effect (generation of sound from light) that was discovered in 1880 by Alexander Graham Bell. The inverse problem we are concerned in is the inverse source problem of recovering small absorbers in a bounded domain $\Omega \subset \mathbb{R}^3$ without following the quantitative thermo-acoustic tomography approach. In our work, we follow a direct algebraic algorithm, that was first developed in [35], which allows us to reconstruct the number of absorbers, their locations, and some information about the conductivity coefficient directly from the wave equation with constant sound speed, and using a single data, without the knowledge of the coupling *Grüneisen's* coefficient measuring the strength of the photo-acoustic effect. Finally, we establish the corresponding Hölder stability result.

This chapter is organized as follows:

- **Section 1** introduces the main problem of this chapter and states the inverse problem behind it. Furthermore, we give a general review on the methods used in literature for solving this inverse problem, and finally we end up by introducing the technique that we shall use in our work.
- **Section 2** is dedicated to the solution of the inverse problem, and the reconstruction algorithm. We give a detailed explanation of the idea of *reciprocity gap functional*, then we derive the algebraic relations required for our algorithm. Finally, we end up with a 4-step reconstruction algorithm that uniquely determines the number of absorbers, their locations and some information about the conductivity coefficient.
- **Section 3** provides a generalization of the algebraic algorithm we follow to higher dimensions $\mathbb{R}^n$ for $n \in \mathbb{N}$.

- **Section 4** finally provides a Hölder stability result for the reconstruction of the centers of the absorbers using specific wave functions and suitable inequalities estimates.

1 Introduction and statement of the problem

In this chapter, we consider the inverse TAT problem, whose aim is to reconstruct the conductivity coefficient in the biological tissues. As stated in Chapter 1, in TAT, a low frequency radiation (radio waves for example) is delivered into the biological tissue to be imaged. The propagation of this electromagnetic radiation in the biological tissue is modeled by the wave equation

$$\begin{cases} \dfrac{1}{c^2}u_{tt}(\mathbf{x},t) + \sigma\alpha u_t(\mathbf{x},t) - \Delta u(\mathbf{x},t) = 0 & \text{in } \Omega\times(0,T) \\ u(\mathbf{x},0) = u_t(\mathbf{x},0) = 0 & \text{in } \Omega \\ u(\xi,t) = w(\xi,t) & \text{on } \Gamma\times(0,T), \end{cases} \tag{3.1}$$

where Ω is an open, bounded and connected domain in $\mathbb{R}^3$, with a smooth boundary Γ; c is the light speed; α is the permeability; $\sigma = \sigma(\mathbf{x})$ is the conductivity to be determined; and the incoming data w is the source radiation. Some of the delivered energy is absorbed by the underlying medium and converted into heat, which in turn generates acoustic waves. The absorbed radiation by the underlying medium is given by [59],

$$H(\mathbf{x},t) = \sigma(\mathbf{x})|u(\mathbf{x},t)|^2. \tag{3.2}$$

Then, using ultrasonic transducers, the acoustic signal is measured at the boundary in order to localize the absorbing subregions. The acoustic wave generated is described by the pressure p that satisfies the boundary value problem

$$\begin{cases} \dfrac{1}{c_s^2}p_{tt}(\mathbf{x},t) - \Delta p(\mathbf{x},t) = \beta(\mathbf{x})\dfrac{\partial H}{\partial t}(\mathbf{x},t) & \text{in } \Omega\times(0,T) \\ p(\mathbf{x},0) = p_t(\mathbf{x},0) = 0 & \text{in } \Omega \\ \dfrac{\partial p}{\partial \nu}(\xi,t) = 0 & \text{on } \Sigma = \Gamma\times(0,T), \end{cases} \tag{3.3}$$

equipped with the observation

$$p(\xi,t) = f(\xi,t), \quad \text{on} \quad \Gamma\times(0,T), \tag{3.4}$$

where c_s is the acoustic speed, chosen to be constant, and $\beta(\mathbf{x})$ is the *Grüneisen's* coefficient that measures the efficiency of conversion from radio waves into acoustic waves. The boundary observation (3.4) is measured by transducers located at the boundary of the imaged object.

Objective: The main objective of this inverse problem is to propose a reconstruction algorithm that allows us to uniquely determine the conductivity coefficient $\sigma(\mathbf{x})$ from a single Cauchy data.

1.1 Methods used in literature

This problem is highly considered in literature, and different methods are used for solving it (see [27, 55] and references therein), in which the main tool used is the quantitative thermo-acoustic tomography approach (qTAT) [6, 7, 13, 39]. Furthermore, different studies in literature have proposed numerical algorithms to solve the problem. In [15], for example, the authors have considered the TAT problem in $\mathbb{R}^n$ with variable sound speed, and proposed a numerical reconstruction method based on the back projection algorithms. Also, TAT was studied through spherical or circular Radon transform, see for example [46, 54].

Quantitative thermo-acoustic tomography (qTAT)

The qTAT approach is divided into two main steps: The first step is solving the inverse source problem for the wave equation (3.3) to reconstruct the absorbed electromagnetic energy $H(x,t)$, and the second step is to reconstruct the conductivity coefficient σ using the relation (3.2) and equations (3.1). The main difficulty of this approach is that the inverse source problem for the reconstruction of the absorbed electromagnetic energy is highly ill-posed for general source term $H(\mathbf{x},t)$, in particular it lacks uniqueness, see for example [35, 88] and references therein. For this purpose, many studies consider the source term H to be separable, that is $H(\mathbf{x},t) = H_0(\mathbf{x})\Phi(\mathbf{x},t)$, where Φ is known and H_0 is the unknown function that shall be determined (see [88, 89]). Also, in the quantitative photo-acoustic tomography problem, for example, the source term is assumed to satisfy $H(\mathbf{x},t) = H_0(\mathbf{x})\delta(t)$, where δ is the Dirac delta function (see [11, 13, 45] and references therein). Moreover, the coefficient β is often assumed to be constant and known.

Algebraic methods

In our work, we don't follow the qPAT approach, yet we develop a reconstruction algorithm based on the algebraic method. This method was first developed by El Badia and H.Doung in [34]. It consists in developing a system of algebraic relations based on the idea of the so called *Reciprocity gap functional* and Green's formula. The idea behind this algorithm is the projection of the problem onto well chosen test functions, which allows the reconstruction of the unknowns from a single boundary data. The main advantage of this method is that it does not require any a priori information about the unknown. In other words, compared to other iterative methods, the algebraic algorithm doesn't require the knowledge of an initial solution.

In [34], the authors developed the algebraic algorithm to solve the inverse source problem for elliptic equations. Later, they used this algorithm in [35] to study the inverse source problem for wave equation with point sources. Their algorithm was based on the construction of a Hankel matrix H from the boundary observations, then the number of point sources can be reconstructed as the rank of this matrix, and the locations of these sources are the eigenvalues of a companion matrix that is also built using the boundary measurements. This algorithm was later used in several works such as [1, 25, 26, 65, 66], and it was recently used in [2] for the problem of reconstructing small electromagnetic inhomogeneities in the framework of Helmoltz's and Maxwell's equations.

1.2 Conductivity coefficient

In this chapter, we consider the inverse thermo-acoustic problem of recovering the conductivity coefficient σ, defined piece-wisely. That is

$$\sigma(\mathbf{x}) = \begin{cases} \sigma_0(\mathbf{x}) & \text{in } \Omega \setminus \overline{\bigcup_{j=1}^{m} \omega_j} \\ \sigma_j(\mathbf{x}) & \text{in } \omega_j, \end{cases}$$

where σ_j are functions belonging to the spaces $L^\infty(\omega_j)$, and $\omega_j \subset \Omega$ are small domains representing the absorbers (tumors) and defined as follows

$$\omega_j = \mathbf{S}_j + \epsilon B_j \quad \text{for} \quad j = 1, \dots, m, \tag{3.5}$$

where $\mathbf{S}_j \in \Omega$ are the locations of the sub-domains ω_j, and $B_j \subset \mathbb{R}^3$ are bounded domains containing the origin. The constant ϵ is the common order of magnitude of the diameters of ω_j supposed to be a sufficiently small positive real number, taken without loss of generality, smaller than 1.

Moreover, the domains ω_j are assumed to be far from the boundary Γ and their centers are supposed to be mutually distinct. We denote by

$$\omega_0 = \Omega \setminus \overline{\bigcup_{j=1}^{m} \omega_j},$$

the background medium.

The difference in conductivity between healthy tissues and cancerous ones allows us to assume that the conductivity coefficient σ_0 in the background medium ω_0 is very small compared to that in the absorbers $\{\omega_j\}_{j=1,\dots,m}$. More precisely, $\sigma_0 = O(\epsilon^\kappa)$ for some $\kappa > 0$. This is an important assumption that we will use in our reconstruction algorithm later. The inverse problem we are

interested in, consists in determining the number of absorbers m, the centers $\mathbf{S}_j$, and some characteristics related to ω_j, using only one acoustic boundary measurement $p_{\Gamma\times(0,T)}$.

2 Identification Algorithm

In this section, we present our identification algorithm of the number of sub-domains ω_j and their centers $\mathbf{S}_j$ based on the idea of the so called *reciprocity gap functional* and by using specific test functions that allow us to get the desired results.

2.1 Reciprocity gap formula

First, we set

$$h(\mathbf{x},t) = \beta(\mathbf{x})\frac{\partial H}{\partial t}(\mathbf{x},t),$$

where H is given in (3.2), and we consider the adjoint problem

$$\frac{1}{c_s^2}v_{tt} - \Delta v = 0 \quad \text{in} \quad \Omega\times(0,T). \tag{3.6}$$

Then, multiplying equation (3.3) by v, and integrating by parts, we obtain using Green's formula

$$\begin{aligned}\int_0^T\int_\Omega h(\mathbf{x},t)v(\mathbf{x},t)d\mathbf{x}dt = \int_\Sigma f(\xi,t)\frac{\partial v}{\partial \nu}(\xi,t)\ d\xi dt \\ + \frac{1}{c_s^2}\int_\Omega [p_t(\mathbf{x},T)v(\mathbf{x},T) - p(\mathbf{x},T)v_t(\mathbf{x},T)]\ d\mathbf{x}.\end{aligned} \tag{3.7}$$

We note that

$$h(\mathbf{x},t) = \beta(\mathbf{x})\frac{\partial H}{\partial t}(\mathbf{x},t) = \beta(\mathbf{x})\sigma(\mathbf{x})\frac{\partial}{\partial t}|u(\mathbf{x},t)|^2.$$

Let

$$g(\mathbf{x},t) := \beta(\mathbf{x})\frac{\partial}{\partial t}|u(\mathbf{x},t)|^2,$$

then

$$h(\mathbf{x},t) = \sigma(\mathbf{x})g(\mathbf{x},t) = \sum_{j=0}^{m}\sigma_j(\mathbf{x})g(\mathbf{x},t)\chi_{\omega_j}.$$

If we denote the so called *reciprocity gap functional* by

$$\mathcal{R}(f,v) = \int_\Sigma f(\xi,t)\frac{\partial v}{\partial \nu}(\xi,t)\ d\xi dt + \frac{1}{c_s^2}\int_\Omega [p_t(\mathbf{x},T)v(\mathbf{x},T) - p(\mathbf{x},T)v_t(\mathbf{x},T)]\ d\mathbf{x}, \tag{3.8}$$

then, from (3.7), we get

$$\mathcal{R}(f,v)=\sum_{j=0}^{m}\int_0^T\int_{\omega_j}\sigma_j(\mathbf{x})g(\mathbf{x},t)v(\mathbf{x},t)\;d\mathbf{x}\;dt.$$

Furthermore, the large difference in conductivity between healthy tissues and cancerous ones, see [31, 44, 62, 75], permits us to assume that $\sigma_0 = O(\epsilon^\kappa)$ for some $\kappa > 0$, assumed in our work to be $\kappa > 4$. Consequently, we have

$$\mathcal{R}(f,v)=\sum_{j=1}^{m}\int_0^T\int_{\omega_j}\sigma_j(\mathbf{x})g(\mathbf{x},t)v(\mathbf{x},t)\;d\mathbf{x}\;dt+O(\epsilon^\kappa). \tag{3.9}$$

To solve our inverse problem, we need to know the values of $p(\mathbf{x},T)$ and $p_t(\mathbf{x},T)$, unless we impose that the solution v of (3.6) satisfies

$$v(\mathbf{x},T)=v_t(\mathbf{x},T)=0\quad\text{in}\quad\Omega. \tag{3.10}$$

To overcome this difficulty, and for a source term of the form $\sum_{j=1}^{N}\lambda_j(t)\delta_{\mathbf{S}_j}$, the authors in [35] opted for the determination of the values of the unknowns $p_t(\mathbf{x},T)$ and $p(\mathbf{x},T)$ using the fact that the intensities $\lambda_j(t)$ become null after a certain time $T^* < T$ and by applying the exact controllability approach. In here, this approach is not employed where we opt for the choice of the condition (3.10). Indeed, we introduce what one calls test functions, the solutions of (3.6) verifying the condition (3.10).

2.2 Algebraic relations

In the following, we will show how an appropriate choice of test functions unveils the desired information. The general idea behind our identification method is the projection of the problem onto well chosen test functions. This idea is not new, but our approach employs a specific family of functions that allows a practical solution.

Let $\alpha_i, \beta_i, \gamma_i \in \mathbb{R}$, for $i = 1, 2$ such that

$$\Omega \subset [\alpha_1,\alpha_2]\times[\beta_1,\beta_2]\times[\gamma_1,\gamma_2].$$

Consider now the one-dimensional wave equation,

$$\begin{cases} \frac{1}{c_s^2}\rho_{tt}(z,t)-\rho_{zz}(z,t) &= 0 \quad \text{in} \quad (\gamma_1,\gamma_2)\times(0,T)\\ \rho(z,T)=\rho_t(z,T) &= 0 \quad \text{in} \quad (\gamma_1,\gamma_2). \end{cases} \tag{3.11}$$

Then, employing the test functions

$$v_n^a(x,y,z,t) = \rho(z,t)(x+iy)^n,\ n \in \mathbb{N}, \tag{3.12}$$

the relation (3.9) becomes

$$\mathcal{R}(f, v_n^a) = \sum_{j=1}^{m} \int_0^T \int_{\omega_j} \sigma_j(\mathbf{x}) g(\mathbf{x},t) \rho(z,t)(x+iy)^n d\mathbf{x}\ dt + O(\epsilon^\kappa) \quad \text{for all} \quad n \in \mathbb{N}. \tag{3.13}$$

Thus, using the change of variables $\mathbf{x} = \mathbf{S}_j + \epsilon\boldsymbol{\tau}$ with $\boldsymbol{\tau} = (\tau_1, \tau_2, \tau_3)$, one obtains

$$\mathcal{R}(f, v_n^a) = \sum_{j=1}^{m} \int_0^T \int_{B_j} \epsilon^3 \gamma_j(\boldsymbol{\tau}, t) \rho(z_j + \epsilon\tau_3, t)[x_j + iy_j + \epsilon(\tau_1 + i\tau_2)]^n d\boldsymbol{\tau}\ dt + O(\epsilon^\kappa), \tag{3.14}$$

where

$$\gamma_j(\boldsymbol{\tau}, t) = \sigma_j(\mathbf{S}_j + \epsilon\boldsymbol{\tau}) g(\mathbf{S}_j + \epsilon\boldsymbol{\tau}, t), \tag{3.15}$$

and consequently,

$$\mathcal{R}(f, v_n^a) = \sum_{j=1}^{m} \sum_{k=0}^{n} \nu_j^{k,a} \binom{n}{k} (P_j^a)^{n-k} + O(\epsilon^\kappa), \quad \text{for all} \quad n \in \mathbb{N}, \tag{3.16}$$

where

$$\nu_j^{k,a} = \epsilon^{3+k} \int_0^T \int_{B_j} \gamma_j(\boldsymbol{\tau}, t) \rho(z_j + \epsilon\tau_3, t)[\tau_1 + i\tau_2]^k d\boldsymbol{\tau}\ dt, \tag{3.17}$$

$$P_j^a = x_j + iy_j,$$

and

$$\binom{n}{k} = \begin{cases} \frac{n!}{k!(n-k)!} & \text{if } n \geq k \\ 0 & \text{if } n < k. \end{cases}$$

Our goal now is to solve the equations (3.16) for the reconstruction of the unknown coefficients $\nu_j^{k,a}$ and the centers P_j^a.

We observe that $\forall n_0 \in \mathbb{N}$, the system (3.16), with $n = 0, \cdots, n_0$, has $n_0 + 1$ equations and $m(n_0 + 2)$ unknowns ($\nu_j^{k,a}, P_j^a$ for $j = 1, , \ldots, m$ and $k = 0, \ldots, n_0$). Then, the number of unknowns is variable with n_0, and it increases with the increase of the number of equations. Thus, it is impossible to uniquely reconstruct the unknowns no matter how many equations are taken. To overcome this difficulty, we will truncate these equations from a small error. First, for a given positive $\epsilon < 1$, we choose a fixed positive integer K such that $K < \kappa - 4$ and ϵ^{K+4} is small enough, and we set

$$\alpha_n^a = \sum_{j=1}^{m} \sum_{k=0}^{K} \nu_j^{k,a} \binom{n}{k} (P_j^a)^{n-k}, \quad \text{for all} \quad n \in \mathbb{N}. \tag{3.18}$$

Then, according to (3.16), we can see that for $n \leq K$ one has

$$\mathcal{R}(f, v_n^a) = \alpha_n^a + O(\epsilon^\kappa),$$

and for $n > K$,

$$\mathcal{R}(f, v_n^a) = \alpha_n^a + O(\epsilon^{K+4}), \tag{3.19}$$

where

$$O(\epsilon^{K+4}) = \sum_{j=1}^{m} \sum_{k=K+1}^{n} \nu_j^{k,a} \binom{n}{k} (P_j^a)^{n-k}.$$

From (3.18), we notice that the number of unknowns is now fixed at $m(K+2)$. Thus, we can increase the number of equations, by taking n large enough, to be able to uniquely determine the unknowns. This is the objective of the next subsection.

Remark 3.1. *Assuming that the observation time T is large enough, $T > \frac{\operatorname{diam}\,\Omega}{c_s}$, then a special solution of (3.11) would be*

$$\rho(z,t) = \rho_\varepsilon \left(t + \frac{z}{c_s} - \theta \right),$$

where $\rho_\varepsilon \in C_0^\infty(\mathbb{R})$ is a mollifier function supported in the interval $[-\varepsilon, \varepsilon]$ and satisfying

$$\int_{\mathbb{R}} \rho_\varepsilon(s) ds = 1,$$

and $\theta \in [\theta_{\min} + \varepsilon, \theta_{\max} - \varepsilon]$ with

$$\theta_{\min} = \frac{\gamma_2}{c_s}, \quad \theta_{\max} = T + \frac{\gamma_1}{c_s}.$$

It is obvious that for every θ and ε fixed, the function ρ belongs to the functional space $C^\infty((\gamma_1, \gamma_2) \times (0,T))$. Moreover, for each z fixed, $\rho(z,t)$ is supported in the time interval $\left[\theta - \frac{z}{c_s} - \varepsilon, \theta - \frac{z}{c_s} + \varepsilon\right]$. Therefore, taking $\theta \in [\theta_{\min} + \varepsilon, \theta_{\max} - \varepsilon]$ we get $\rho(.,T) = \rho_t(.,T) = 0$.

The mollifier function ρ was used by the authors in [71] for solving the inverse problem of reconstruction of time-varying point sources for wave equation.

Before solving the equations (3.16), we need to know if the projections P_j^a are mutually distinct, which is necessary in order to use the algebraic method proposed below. Indeed, one can remark that there is only a finite number of planes containing the origin such that at least two points among $\mathbf{S}_j$, are projected onto the same point on this plane. So, if a basis is chosen randomly, one is almost sure that the points $\mathbf{S}_j$ are projected onto distinct points on every coordinate plane. Therefore, without loss of generality, we assume that:

(H) The projections onto the xy, yz and xz-planes of the points $\mathbf{S}_j$ are mutually distinct.

2.3 Reconstruction algorithm

Before presenting our identification algorithm we introduce, for simplicity, some notations and definitions that are used throughout this subsection.

First, denote by P_j^b and P_j^c, the projections of $\mathbf{S}_j$ onto the yz and xz-complex planes respectively. Then, using in (3.9), the following test functions

$$v_n^b = (y+iz)^n \rho_1(x,t) \quad \text{and} \quad v_n^c = (x+iz)^n \rho_2(y,t) \tag{3.20}$$

where ρ_1, and ρ_2 are the solutions of (3.11) with the space variable z being replaced by x and y respectively, leads to the following algebraic quantities

$$\alpha_n^b = \sum_{j=1}^{m} \sum_{k=0}^{K} \nu_j^{k,b} \binom{n}{k} (P_j^b)^{n-k} \quad \text{for all} \quad n \in \mathbb{N} \tag{3.21}$$

and

$$\alpha_n^c = \sum_{j=1}^{m} \sum_{k=0}^{K} \nu_j^{k,c} \binom{n}{k} (P_j^c)^{n-k} \quad \text{for all} \quad n \in \mathbb{N}, \tag{3.22}$$

where

$$\nu_j^{k,b} = \epsilon^{3+k} \int_0^T \int_{B_j} \gamma_j(\boldsymbol{\tau}, t) \rho_1(x_j + \epsilon\tau_1, t) [\tau_2 + i\tau_3]^k d\boldsymbol{\tau}\ dt$$

and

$$\nu_j^{k,c} = \epsilon^{3+k} \int_0^T \int_{B_j} \gamma_j(\boldsymbol{\tau}, t) \rho_2(y_j + \epsilon\tau_2, t) [\tau_1 + i\tau_3]^k d\boldsymbol{\tau}\ dt.$$

Finally, bringing together the equations (3.18), (3.21) and (3.22), we can write

$$\alpha_n^r = \sum_{j=1}^{m} \sum_{k=0}^{K} \nu_j^{k,r} \binom{n}{k} (P_j^r)^{n-k}, \quad \text{for} \quad r = a, b, c \quad \text{and} \quad n \in \mathbb{N}. \tag{3.23}$$

On the other hand, we assume that we know an upper bound M of the number of sources m, then $\bar{J} = M(K+1)$ is an upper bound of the number $J = m(K+1)$. We define for $r = a, b, c$, and $k = 0, \ldots, K$, the complex vectors

$$\xi_n^r = (\alpha_n^r, \cdots, \alpha_{\bar{J}+n-1}^r)^t, \quad \Lambda_k^r = (\nu_1^{k,r}, \cdots, \nu_m^{k,r})^t \text{ and } \Lambda^r = ((\Lambda_0^r)^t, (\Lambda_1^r)^t, \cdots, (\Lambda_K^r)^t)^t,$$

of sizes $\bar{J}, m$ and J respectively, and consider, for all $n \in \mathbb{N}$, the complex matrices A_n^r of size $\bar{J} \times J$,

$$A_n^r = (V_n^{0,r}, \cdots, V_n^{K,r}), \tag{3.24}$$

where, for $k \in \{0, \cdots, K\}$, $V_n^{k,r}$ are the confluent $\bar{J} \times m$ Vandermonde matrices

$$V_n^{k,r} = \begin{pmatrix} \binom{n}{k}(P_1^r)^{n-k} & \cdots & \binom{n}{k}(P_m^r)^{n-k} \\ \binom{n+1}{k}(P_1^r)^{n-k+1} & \cdots & \binom{n+1}{k}(P_m^r)^{n-k+1} \\ \vdots & \ddots & \vdots \\ \binom{\bar{J}+n-1}{k}(P_1^r)^{n-k+\bar{J}-1} & \cdots & \binom{\bar{J}+n-1}{k}(P_m^r)^{n-k+\bar{J}-1} \end{pmatrix}.$$

Now, let us introduce the Hankel matrix

$$H_{\bar{J}}^r = \begin{pmatrix} \alpha_0^r & \alpha_1^r & \cdots & \alpha_{\bar{J}-1}^r \\ \alpha_1^r & \alpha_2^r & \cdots & \alpha_{\bar{J}}^r \\ \vdots & \vdots & \vdots & \vdots \\ \alpha_{\bar{J}-1}^r & \alpha_{\bar{J}}^r & \cdots & \alpha_{2\bar{J}-2}^r \end{pmatrix} \tag{3.25}$$

and the following multi-diagonal matrix

$$L^r = \begin{pmatrix} \nu^{0,r} & \nu^{1,r} & \cdots & \nu^{K,r} \\ \vdots & \vdots & \iddots & \vdots \\ \nu^{K-1,r} & \nu^{K,r} & \cdots & 0 \\ \nu^{K,r} & 0 & \cdots & 0 \end{pmatrix}, \tag{3.26}$$

where

$$\nu^{k,r} = diag(\nu_1^{k,r}, \cdots, \nu_m^{k,r}).$$

We propose an identification processes in four steps.

1. **Step 1:** We determine the absorbers' number m using the Hankel matrix defined in (3.25).
2. **Step 2:** We obtain the projections P_j^r using a companion matrix.
3. **Step 3:** We get the coefficients $\nu_j^{k,r}$ as a solution of a linear system via the Hankel matrix H_J^r.
4. **Step 4:** We reconstruct the final locations $\mathbf{S}_j$ by solving a similar linear system and using the coefficients $\nu_j^{k,r}$.

Step 1: Determination of the number of absorbers

The first step consists in determining the number of sources by means of the following theorem.

Theorem 3.11. *Let $H^r_{\bar{J}}$ be the Hankel matrix defined in (3.25) where $\bar{J}$ is a known upper bound of $J = m(K+1)$. Assume that, for $r = a, b, c$, the projected points P^r_j of $\boldsymbol{S}_j$ are mutually distinct, then we have*

$$rank\left(H^r_{\bar{J}}\right) = m(K+1) \quad \text{if and only if} \quad \nu^{K,r}_j \neq 0 \quad \text{for } j = 1, ..., m.$$

The proof of this theorem is similar to that of Theorem 2.8 in [1]. It is based on the decomposition of the Hankel matrix $H^r_{\bar{J}}$ given in Lemma 2.9 in [1]. For the convenience of the reader, we recall this lemma here for which we present a sketch of the proof.

Lemma 3.1. *Let $H^r_{\bar{J}}$ be the Hankel matrix defined in (3.25), L^r the multi-diagonal matrix defined in (3.26), A^r_0 the Vandermonde matrix defined in (3.24), and $(A^r_0)^t$ its transpose matrix. Then,*

$$H^r_{\bar{J}} = A^r_0 L^r (A^r_0)^t. \tag{3.27}$$

Proof.
Indeed, from (3.24), we notice that

$$A^r_n \Lambda^r = \sum_{k=0}^{K} V^{k,r}_n \Lambda^r_k.$$

Moreover,

$$V^{k,r}_n \Lambda^r_k = \begin{pmatrix} \sum_{j=1}^{m} \binom{n}{k} (P^r_j)^{n-k} \nu^{k,r}_j \\ \vdots \\ \sum_{j=1}^{m} \binom{\bar{J}+n-1}{k} (P^r_j)^{n-k+\bar{J}-1} \nu^{k,r}_j \end{pmatrix}.$$

Therefore, the algebraic relation (3.23) can be rewritten in a matrix form as

$$\xi^r_n = A^r_n \Lambda^r, \qquad \forall n \in \mathbb{N}. \tag{3.28}$$

Furthermore, if we denote by T^r the block $J \times J$ upper triangular complex matrix

$$T^r = \begin{pmatrix} D^r_p & I & \cdots & 0 \\ 0 & \ddots & \ddots & \vdots \\ \vdots & \ddots & D^r_p & I \\ 0 & \cdots & 0 & D^r_p \end{pmatrix}, \tag{3.29}$$

with

$$D^r_p = diag(P^r_1, \cdots, P^r_m) \quad \text{and} \quad I = diag(1, \cdots, 1),$$

then, using the Pascal formula $\binom{n}{j-1} + \binom{n}{j} = \binom{n+1}{j}$, it follows that

$$V_{n+1}^{k,r} = V_n^{k-1,r} + V_n^{k,r} D_p^r, \quad \forall\, n \in \mathbb{N}, \quad k = 1, \ldots, K$$

and

$$V_{n+1}^{0,r} = V_n^{0,r} D_p^r, \quad \forall\, n \in \mathbb{N}.$$

From the definition of the matrix A_n^r, we obtain

$$A_{n+1}^r = A_n^r T^r = A_0^r (T^r)^{n+1}, \quad \forall n \in \mathbb{N},$$

and therefore, from (3.28), one gets

$$\xi_n^r = A_0^r (T^r)^n \Lambda^r, \qquad \forall n \in \mathbb{N}. \tag{3.30}$$

Now, thanks to (3.30), one can verify by a simple calculation the following relationship

$$H_{\bar{J}}^r = A_0^r [\Lambda^r, T^r \Lambda^r, ..., (T^r)^{\bar{J}-1} \Lambda^r] = A_0^r L^r (A_0^r)^t,$$

which ends the proof of Lemma 3.1. ■

Proof of Theorem 3.11.
We can easily check that $rank(A_0^r) = rank(A_0^r)^t = J$ if and only if the projections P_j^r are mutually distinct, for $j = 1, \cdots, m$. Moreover, the matrix L^r is nonsingular if and only if $\nu_j^{K,r} \neq 0\ \forall j = 1, \ldots, m$. Therefore, under the hypothesis **(H)**, and assuming that the coefficients $\nu_j^{K,r} \neq 0$, we deduce that $A_0^r L^r$ is surjective and therefore we have $rank(A_0^r L^r (A_0^r)^t) = rank(A_0^r)^t = J$, which leads to the desired result. ■

Step 2: Reconstruction of the projections P_j^r

The second step consists in determining the projections onto the xy-, xz- and yz-complex planes of the centers $\mathbf{S}_j$.

Henceforth, we replace $\bar{J}$ by J in the quantities defined above. Thus, from (3.30), we can easily derive that

$$\xi_{n+1}^r = B^r \xi_n^r, \qquad \forall n \in \mathbb{N},$$

where we have set

$$B^r = A_0^r T^r (A_0^r)^{-1}. \tag{3.31}$$

Here, the matrix A_0^r is invertible since the projected points P_j^r are assumed distinct. Moreover, since $rank(H_J^r) = J$, the family $(\xi_n^r)_{n=0,\ldots,J-1}$ forms a basis of $\mathbb{C}^J$, so the $J \times J$ complex matrix

B^r is given explicitly by

$$B^r = \begin{pmatrix} 0 & 1 & \cdots & 0 & 0 \\ 0 & 0 & 1 & \cdots & 0 \\ \vdots & \vdots & \ddots & \ddots & 0 \\ \vdots & \vdots & \ddots & \ddots & 1 \\ c_0^r & c_1^r & \cdots & \cdots & c_{J-1}^r \end{pmatrix}, \tag{3.32}$$

where the vector $C^r = (c_0^r, ..., c_{J-1}^r)^t$ is obtained by solving the linear system

$$H_J^r C^r = \xi_J^r. \tag{3.33}$$

Indeed, as the family $(\xi_n^r)_{n=0,...,J-1}$ forms a basis of $\mathbb{C}^J$, given ξ_J, there exists a vector $C^r = (c_0^r, ..., c_{J-1}^r)^t$ such that

$$\xi_J^r = \sum_{n=0}^{J-1} c_n^r \xi_n^r,$$

which is equivalent to (3.33) since the matrix $H_J^r = (\xi_0^r, ..., \xi_{J-1}^r)$.

Finally, the projections P_j^r are given by the following theorem.

Theorem 3.12. *Let B^r, for $r = a, b, c$, be the companion matrices defined in (3.32). Assume that the projected points P_j^r of $\boldsymbol{S}_j$ are distinct and away from the origin and that $\nu_j^{K,r} \neq 0$ for $j = 1, ..., m$. Then,*

1. *B^r admits m eigenvalues of multiplicity $K + 1$;*
2. *The m eigenvalues of multiplicity $K + 1$ are the projections P_j^r of the point sources $\boldsymbol{S}_j$.*

Proof.
The proof of this theorem follows from (3.29) and (3.31). ■

Remark 3.2. *We know according to formulas (3.29), (3.31) and hypothesis (H), that the matrix B^r admits m distinct eigenvalues having the same multiplicity $K + 1$, where K is given. Then, numerically, one should obtain m distinct eigenvalues, m obtained from the rank of the Hankel matrix $H_{\bar{J}}^r$ defined in (3.25). The rank of $H_{\bar{J}}^r$ can be obtained numerically as the number of its non-zero singular values.*

Step 3: Determination of the vectors Λ^r

In this step, we shall determine the quantities $\nu_j^{k,r}$, which we will use later to reconstruct the locations $\mathbf{S}_j$. In fact, in order to determine $\nu_j^{k,r}$, it is sufficient to solve the linear systems

$$A_0^r \Lambda^r = \xi_0^r. \tag{3.34}$$

Step 4: Complete reconstruction of locations $\mathbf{S}_j$

In step 2, we were able to reconstruct modulo ϵ^{K+4} the projections of the centers $\mathbf{S}_j$ on the xy-, yz- and xz-planes. However, this is not enough. In fact, the combination of different projections doesn't uniquely determine the centers $\mathbf{S}_j$, see Remark 3.3. For this purpose, we fix $r = a$ and we reconstruct, modulo ϵ, the third components z_j that correspond to the previously calculated projections P_j^a, on which we need that the coefficients $\nu_j^{0,a}$ calculated in the previous step to satisfy

$$\nu_j^{0,a} \neq 0 \text{ for } j = 1, ..., m. \tag{3.35}$$

We propose an algorithm for the reconstruction of the components z_j using specific wave functions. For this purpose, for $n \in \mathbb{N}$, we take v_n^a defined in (3.12) and we consider the following wave functions,

$$g_n^a(\mathbf{x}, t) = -\frac{\partial}{\partial z} v_n^a(\mathbf{x}, t) = -\rho_z(z, t)(x + iy)^n, \tag{3.36}$$

$$\begin{aligned} h_n^a(\mathbf{x}, t) &= z\left(\frac{\partial}{\partial x} - i\frac{\partial}{\partial y}\right) v_n^a(\mathbf{x}, t) - (x - iy)\frac{\partial}{\partial z} v_n^a(\mathbf{x}, t) \\ &= 2nz\rho(z, t)(x + iy)^{n-1} - \rho_z(z, t)(x - iy)(x + iy)^n, \end{aligned} \tag{3.37}$$

which are solutions of (3.6) satisfying the condition (3.10). Therefore, substituting g_n^a in (3.9) we get

$$\begin{aligned} R(f, g_n^a) &= \sum_{j=1}^{m} \int_0^T \int_{\omega_j} \sigma_j(\mathbf{x}) g(\mathbf{x}, t) g_n^a(\mathbf{x}, t) d\mathbf{x}\, dt + O(\epsilon^\kappa) \\ &= -\sum_{j=1}^{m} \int_0^T \int_{\omega_j} \sigma_j(\mathbf{x}) g(\mathbf{x}, t) \rho_z(z, t)(x + iy)^n d\mathbf{x}\, dt + O(\epsilon^\kappa) \\ &= \sum_{j=1}^{m} \sum_{k=1}^{n} \binom{n}{k} \widetilde{\nu}_j^{k,a} (P_j^a)^{n-k} + O(\epsilon^\kappa), \end{aligned}$$

where for every $j = 1, \cdots, m$ and $k = 1, \cdots, K$,

$$\widetilde{\nu}_j^{k,a} = -\epsilon^{3+k} \int_0^T \int_{B_j} \sigma_j(\mathbf{S}_j + \epsilon\boldsymbol{\tau}) g(\mathbf{S}_j + \epsilon\boldsymbol{\tau}, t) \rho_z(z_j + \epsilon\tau_3, t)(\tau_1 + i\tau_2)^k d\boldsymbol{\tau}\, dt. \tag{3.38}$$

Similar to the previous section, we have for $n \leq K$

$$R(f, g_n^a) = \sum_{j=1}^{m} \sum_{k=0}^{K} \binom{n}{k} \widetilde{\nu}_j^{k,a} (P_j^a)^{n-k} + O(\epsilon^\kappa), \tag{3.39}$$

and for $n > K$

$$R(f, g_n^a) = \sum_{j=1}^{m} \sum_{k=0}^{K} \binom{n}{k} \widetilde{\nu}_j^{k,a} (P_j^a)^{n-k} + O(\epsilon^{K+4}). \tag{3.40}$$

Now, if we choose for $n \in \mathbb{N}$

$$\widetilde{\alpha}_n^a = \sum_{j=1}^{m} \sum_{k=0}^{K} \binom{n}{k} \widetilde{\nu}_j^{k,a} (P_j^a)^{n-k}, \tag{3.41}$$

and we define the following quantities

$$\widetilde{\xi}_n^a = (\widetilde{\alpha}_n^a, \cdots, \widetilde{\alpha}_{J+n-1}^a)^t,$$

$$\widetilde{\Lambda}_k = \left(\widetilde{\nu}_1^{k,a}, \cdots, \widetilde{\nu}_m^{k,a}\right)^t \quad \text{for } k = 0, \ldots, K$$

and

$$\widetilde{\Lambda} = \left((\widetilde{\Lambda}_0)^t, \cdots, (\widetilde{\Lambda}_K)^t\right)^t,$$

where $J = m(K+1)$, we get using the formula (3.41) the following system of equations

$$A_0^a \widetilde{\Lambda} = \widetilde{\xi}_0^a, \tag{3.42}$$

where A_0^a is defined in (3.24), and $\widetilde{\xi}_0^a$ can be approximated using the equations (3.39) and (3.40). Under the assumption that the projections P_j^a are mutually distinct, then A_0^a is invertible, and system (3.42) admits a unique solution. By solving this system, we can reconstruct the quantities $\widetilde{\nu}_j^{k,a}$. On the other hand, if we substitute h_n^a in (3.9) we get

$$\begin{aligned} R(f, h_n^a) &= \sum_{j=1}^{m} \int_0^T \int_{\omega_j} \sigma_j(\mathbf{x}) g(\mathbf{x}, t) h_n^a(\mathbf{x}, t) d\mathbf{x}\, dt + O(\epsilon^\kappa) \\ &= 2n \sum_{j=1}^{m} \int_0^T \int_{\omega_j} \sigma_j(\mathbf{x}) g(\mathbf{x}, t) \rho(z, t) z (x+iy)^{n-1} d\mathbf{x}\, dt \\ &\quad - \sum_{j=1}^{m} \int_0^T \int_{\omega_j} \sigma_j(\mathbf{x}) g(\mathbf{x}, t) \rho_z(z, t) (x-iy)(x+iy)^n d\mathbf{x}\, dt + O(\epsilon^\kappa). \end{aligned}$$

Applying the change of variables $\omega_j = \mathbf{S}_j + \epsilon B_j$ one gets,

$$\begin{aligned} R(f, h_n^a) = 2n \sum_{j=1}^{m} \epsilon^3 \int_0^T \int_{B_j} \gamma_j(\boldsymbol{\tau}, t) \rho(z_j + \epsilon\tau_3, t)(z_j + \epsilon\tau_3)(P_j^a + \epsilon(\tau_1 + i\tau_2))^{n-1} d\boldsymbol{\tau}\, dt \\ - \sum_{j=1}^{m} \epsilon^3 \int_0^T \int_{B_j} \gamma_j(\boldsymbol{\tau}, t) \rho_z(z_j + \epsilon\tau_3, t)(x_j - iy_j + \epsilon(\tau_1 - i\tau_2)) \\ \times (P_j^a + \epsilon(\tau_1 + i\tau_2))^n d\boldsymbol{\tau}\, dt + O(\epsilon^\kappa), \end{aligned}$$

where $\gamma_j(\boldsymbol{\tau}, t)$ is defined in (3.15).

Thus,

$$R(f,h_n^a) = 2n\sum_{j=1}^{m}\epsilon^3\int_0^T\int_{B_j}\gamma_j(\boldsymbol{\tau},t)\rho(z_j+\epsilon\tau_3,t)z_j(P_j^a)^{n-1}d\boldsymbol{\tau}\ dt$$
$$-\sum_{j=1}^{m}\epsilon^3\int_0^T\int_{B_j}\gamma_j(\boldsymbol{\tau},t)\rho_z(z_j+\epsilon\tau_3,t)(x_j-iy_j)(P_j^a)^n d\boldsymbol{\tau}\ dt + O(\epsilon^4),$$

Therefore, one has

$$R(f,h_n^a) = 2n\sum_{j=1}^{m}(P_j^a)^{n-1}\nu_j^{0,a}z_j - \sum_{j=1}^{m}(x_j-iy_j)(P_j^a)^n\tilde{\nu_j}^{0,a} + O(\epsilon^4).$$

Hence,

$$\frac{1}{2n}\left(R(f,h_n^a) + \sum_{j=1}^{m}(x_j-iy_j)(P_j^a)^n\tilde{\nu_j}^{0,a}\right) = \sum_{j=1}^{m}(P_j^a)^{n-1}\nu_j^{0,a}z_j + O(\epsilon^4) \quad \forall n\in\mathbb{N}.$$

Now, if we define for $n\in\mathbb{N}$

$$\widetilde{R}_n = \frac{1}{2n}\left(R(f,h_n^a) + \sum_{j=1}^{m}(x_j-iy_j)(P_j^a)^n\tilde{\nu_j}^{0,a}\right), \tag{3.43}$$

and we take

$$\widetilde{R} = \left(\widetilde{R}_1,\cdots,\widetilde{R}_m\right)^t$$

and

$$\widetilde{\Lambda}_z = \left(\nu_1^{0,a}z_1,\cdots,\nu_m^{0,a}z_m\right)^t,$$

we get, modulo $O(\epsilon^4)$, the following system

$$P_m\widetilde{\Lambda}_z = \widetilde{R}, \tag{3.44}$$

where P_m is the $m\times m$ Vandermonde matrix defined by

$$P_m = \begin{pmatrix} 1 & 1 & \dots & 1 \\ P_1^a & P_2^a & \dots & P_m^a \\ \vdots & & & \vdots \\ (P_1^a)^{m-1} & (P_2^a)^{m-1} & \dots & (P_m^a)^{m-1} \end{pmatrix}.$$

Since the projections P_j^a are assumed to be mutually distinct, thus P_m is invertible and equation (3.44) admits a unique solution. By solving this equation we can reconstruct $\nu_j^{0,a}z_j$ up to $O(\epsilon^4)$, and since the coefficients $\nu_j^{0,a}$ are of order ϵ^3, and are previously calculated and chosen to be

different from zero, thus we can calculate the values of z_j up to $O(\epsilon)$. Finally, combining this result with that of step 2, we get the locations of the centers $\mathbf{S}_j$.

Remark 3.3. *The projections on the xy-, yz-, and xz-planes do not uniquely determine the centers* $\mathbf{S}_j$. *For example, the two sets of points*

$$\mathcal{F}_1 = \{(1,0,2),(1,-1,3),(2,0,3),(2,-1,2)\},$$

and

$$\mathcal{F}_2 = \{(1,0,3),(1,-1,2),(2,0,2),(2,-1,3)\}$$

have the same projections

$$P^a = \{(1,0),(1,-1),(2,0),(2,-1)\},$$

$$P^b = \{(0,2),(-1,3),(0,3),(-1,2)\},$$

and

$$P^c = \{(1,2),(1,3),(2,3),(2,2)\}$$

on the xy-, yz- and xz-planes respectively. Thus, knowing the projections P^a, P^b *and* P^c *is not enough to uniquely determine the corresponding locations* $\mathbf{S}_j$.

The last step allows us to uniquely determine the centers $\mathbf{S}_j$. *However, we lose some accuracy as the obtained values of* z_j *are given modulo* ϵ.

Summary: identification algorithm

To sum up, our identification algorithm can be summarized as follows. First, we choose a fixed integer $K > 0$ such that ϵ^{K+4} is small enough and we suppose that we know an upper bound $\bar{J}$ of the number $J = m(K+1)$. Then, we proceed in the following steps:

- **Step 1.** We fix $r = a, b$ or c, and we estimate for $n = 0, \cdots, 2\bar{J} - 2$ the coefficients α_n^r by $R(f, v_n^r)$ defined in (3.8), which introduces an accuracy error $O(\epsilon^{K+4})$ in our identification algorithm. Then we construct the Hankel matrix $H_{\bar{J}}^r$ defined in (3.25).

- **Step 2.** We calculate J as the rank of the Hankel matrix $H_{\bar{J}}^r$, which can be numerically estimated using, for example, the Singular Value Decomposition (SVD) method, and we deduce the number of absorbers m using the relation $J = m(K+1)$.

- **Step 3.** We construct $C^r = (c_0^r, \cdots, c_{J-1}^r)^t$ by solving the system $H_J^r C^r = \xi_J^r$, where $\xi_J^r = (\alpha_J^r, \cdots, \alpha_{2J-1}^r)^t$. The projections P_j^r of the centers S_j then can be determined as the eigenvalues of the matrix B^r defined in (3.32), which can be constructed using the previously calculated coefficients $\{c_j^r\}_{0 \le j \le J-1}$.

- **Step 4.** The coefficients $\nu_j^{k,a}$ can be obtained by solving the system (3.34).

- **Step 5.** We fix $r = a$ and we estimate for $n = 0, 1, \cdots, J-1$ the coefficients $\widetilde{\alpha}_n^a$ by $R(f, g_n^a)$ defined in (3.8), where g_n^a is given by (3.36), then we calculate the coefficients $\widetilde{\nu}_j^{k,a}$ defined in (3.38) by solving system (3.42).

- **Step 6.** We calculate $R(f, h_n^a)$ for $n = 1, \cdots, m$, where h_n^a is defined by (3.37). Then using these values and the previously calculated coefficients $\widetilde{\nu}_j^{k,a}$, we may calculate the coefficients $\widetilde{R}_n$ defined in (3.43).

- **Step 7.** Finally, by solving (3.44) we get the values of $\nu_j^{0,a} z_j$ for $j = 1, \cdots, m$. Then under the assumption that the coefficients $\nu_j^{0,a}$ calculated in step 4 are different from zero, we may calculate the values of z_j that correspond to the projections P_j^a, and thus we deduce the complete location of the centers S_j.

Remark 3.4. *From the previous calculations, one can see that the resolution of the problem depends on the conductivity of the background medium σ_0. More precisely, on how much σ_0 is small. In other words, from equations (3.16)-(3.19), we notice that to solve the problem, it is necessary to have $\kappa > 4 + K$, for some positive integer K, where κ is given by the relation $\sigma_0 = O(\epsilon^\kappa)$. On the other hand, the conductivity coefficient σ_0 plays an important role in the resolution of the problem in higher dimensions, on which we notice that our reconstruction algorithm can be generalized to higher dimensions $\mathbb{R}^N$, if we can find a positive integer K such that*

$$N + 1 + K < \kappa.$$

We give in the following section a detailed explanation of this generalization.

3 Generalization to higher dimensions

In this section, we give a generalization of our algebraic algorithm to higher dimensions $\mathbb{R}^N$, under some conditions related to the physical properties of the medium, more precisely, to the conductivity of the background medium σ_0.

Let $\gamma_i^k \in \mathbb{R}$, for $i = 1, 2$ and $k = 1, \cdots, N$, such that

$$\Omega \subset [\gamma_1^1, \gamma_2^1] \times [\gamma_1^2, \gamma_2^2] \times \cdots \times [\gamma_1^N, \gamma_2^N].$$

We denote by $\mathbf{S}_j = \left(x_j^1, x_j^2, \cdots, x_j^N\right)$ the centers of the absorbers $\omega_j = \mathbf{S}_j + \epsilon B_j$, for $j = 1, \cdots, m$.

Now, let $\mathbf{x} = (x^1, x^2, \cdots, x^N)$ be a vector of Ω. First, we consider the one-dimensional wave

equation

$$\begin{cases} \frac{1}{c_s^2}\rho_{tt}(x^3,t) - \rho_{x^3x^3}(x^3,t) = 0 & \text{in} \quad (\gamma_1^3,\gamma_2^3)\times(0,T) \\ \\ \rho(x^3,T) = \rho_t(x^3,T) = 0 & \text{in} \quad (\gamma_1^3,\gamma_2^3). \end{cases}$$

Then, we define, for $n \in \mathbb{N}$, the test functions

$$v_n^3(\mathbf{x},t) = \rho(x^3,t)(x^1+ix^2)^n,$$

that are solutions of the adjoint problem (3.6), (3.10). Following the same procedure as in subsection 2.2 , we get

$$R(f,v_n^3) = \sum_{j=1}^{m}\int_0^T\int_{\omega_j}\sigma_j(\mathbf{x})g(\mathbf{x},t)\rho(x^3,t)(x^1+ix^2)^n d\mathbf{x}\ dt + O(\epsilon^\kappa),$$

where $R(f,v)$ is defined in (3.8). Applying the change of variable $\mathbf{x} = \mathbf{S}_j + \epsilon\boldsymbol{\tau}$, where $\boldsymbol{\tau} = (\tau_1,\cdots,\tau_N)$, one obtains

$$\mathcal{R}(f,v_n^3) = \sum_{j=1}^{m}\int_0^T\int_{B_j}\epsilon^N\gamma_j(\boldsymbol{\tau},t)\rho(x_j^3+\epsilon\tau_3,t)[P_j^1+\epsilon(\tau_1+i\tau_2)]^n d\tau\ dt + O(\epsilon^\kappa), \tag{3.45}$$

where

$$\gamma_j(\boldsymbol{\tau},t) = \sigma_j(\mathbf{S}_j+\epsilon\boldsymbol{\tau})g(\mathbf{S}_j+\epsilon\boldsymbol{\tau},t),$$

and

$$P_j^1 = x_j^1 + ix_j^2.$$

Therefore, we have for every $n \in \mathbb{N}$,

$$R(f,v_n^3) = \sum_{j=1}^{m}\sum_{k=0}^{n}\nu_j^{k,3}\binom{n}{k}(P_j^1)^{n-k} + O(\epsilon^\kappa), \tag{3.46}$$

where

$$\nu_j^{k,3} = \epsilon^{N+k}\int_0^T\int_{B_j}\gamma_j(\boldsymbol{\tau},t)\rho(x_j^3+\epsilon\tau_3,t)[\tau_1+i\tau_2]^k d\boldsymbol{\tau}\ dt. \tag{3.47}$$

Our goal now is to solve the equations (3.46) to reconstruct the number of absorbers m, the projections P_j^1 of the centers $\mathbf{S}_j$ on the x^1x^2-plane, and the coefficients $\nu_j^{k,3}$. Again, the equations (3.46) don't allow us to uniquely solve the problem, as the number of unknowns is greater than that of equations. For this purpose, we define for a positive integer K,

$$\alpha_n^3 = \sum_{j=1}^{m}\sum_{k=0}^{K}\nu_j^{k,3}\binom{n}{k}(P_j^1)^{n-k},$$

on which we need, as in case of $\mathbb{R}^3$, the condition

$$N + K + 1 < \kappa,$$

to be satisfied in order to get the relations

$$R(f, v_n^3) = \alpha_n^3 + O(\epsilon^\kappa) \quad \text{for } n \leq K$$

and

$$R(f, v_n^3) = \alpha_n^3 + O(\epsilon^{N+K+1}) \quad \text{for } n > K,$$

where

$$O(\epsilon^{N+K+1}) = \sum_{j=1}^{m} \sum_{k=K+1}^{n} \nu_j^{k,3} \binom{n}{k} (P_j^1)^{n-k}.$$

Now, assuming that the projections are mutually distinct, one can apply the algebraic algorithm (steps 1-4), as in the case of $\mathbb{R}^3$, to reconstruct, modulo $O(\epsilon^{N+K+1})$, the number of absorbers m, the projections P_j^1 and the coefficients $\nu_j^{k,3}$. Similarly, we can reconstruct all the projections of the centers $\mathbf{S}_j$ on the $x^i x^k$-planes, for $1 \leq i, k \leq N$.

As in the case of $\mathbb{R}^3$, we can uniquely determine the complete locations of the centers $\mathbf{S}_j$ modulo $O(\epsilon)$. For this purpose, we consider for $k = 3, ..., N$, the one-dimensional wave equations

$$\begin{cases} \frac{1}{c_s^2}\rho_{tt}(x^k, t) - \rho_{x^k x^k}(x^k, t) &= 0 \quad \text{in} \quad (\gamma_1^k, \gamma_2^k) \times (0, T) \\ \rho(x^k, T) = \rho_t(x^k, T) &= 0 \quad \text{in} \quad (\gamma_1^k, \gamma_2^k), \end{cases} \tag{3.48}$$

and we define, for $n \in \mathbb{N}$, the test functions

$$g_n^k(\mathbf{x}, t) = -\rho_{x^k}(x^k, t)(x^1 + ix^2)^n \tag{3.49}$$

and

$$h_n^k(\mathbf{x}, t) = 2nx^k \rho(x^k, t)(x^1 + ix^2)^{n-1} - \rho_{x^k}(x^k, t)(x^1 - ix^2)(x^1 + ix^2)^n. \tag{3.50}$$

First, taking $k = 3$, and since the projections $P_j^1 = x_j^1 + ix_j^2$ are previously calculated up to $O(\epsilon^{N+K+1})$, then following the steps 5, 6 and 7 of the algebraic algorithm, one can determine the components x_j^3 up to $O(\epsilon)$, and then, by recurrence, we obtain, modulo $O(\epsilon)$, the locations $\mathbf{S_j}$ for all $k = 4, ...N$, and $j = 1, ..., m$.

In fact, for every $i = 4, \cdots, N$ we define

$$w_n^i(\mathbf{x}, t) = \rho(x^i, t)(x^1 + ix^2)^n,$$

which is a solution of (3.6) satisfying (3.10). Then, substituting w_n^i in (3.9) we get

$$R(f, w_n^i) = \sum_{j=1}^{m} \sum_{k=1}^{n} \binom{n}{k} \nu_j^{k,i} (P_j^1)^{n-k} + O(\epsilon^\kappa),$$

where for every $j = 1, \cdots, m$ and $k = 1, \cdots, K$,

$$\nu_j{}^{k,i} = \epsilon^{N+k} \int_0^T \int_{B_j} \sigma_j(\mathbf{S}_j + \epsilon\boldsymbol{\tau}) g(\mathbf{S}_j + \epsilon\boldsymbol{\tau}, t) \rho(x^i + \epsilon\tau_i, t)(\tau_1 + i\tau_2)^k d\boldsymbol{\tau}\, dt.$$

Now, if we choose K such that $N + K + 1 < \kappa$, and we take for $n \in \mathbb{N}$

$$\alpha_n^i = \sum_{j=1}^{m} \sum_{k=0}^{K} \binom{n}{k} \nu_j^{k,i} (P_j^1)^{n-k}, \tag{3.51}$$

then, similar to the previous section, we have for $n \leq K$

$$R(f, w_n^i) = \alpha_n^i + O(\epsilon^\kappa), \tag{3.52}$$

and for $n > K$

$$R(f, w_n^i) = \alpha_n^i + O(\epsilon^{N+K+1}). \tag{3.53}$$

We define the following quantities

$$\xi_n^i = (\alpha_n^i, \cdots, \alpha_{J+n-1}^i)^t,$$

$$\Lambda_k^i = \left(\nu_1^{k,i}, \cdots, \nu_m^{k,i}\right)^t \quad \text{for } k = 0, \ldots, K$$

and

$$\Lambda = \left((\Lambda_0^i)^t, \cdots, (\Lambda_K^i)^t\right)^t,$$

where $J = m(K+1)$, we get using the formula (3.51) the following system of equations

$$A_0^a \Lambda^i = \xi_0^i, \tag{3.54}$$

where A_0^a is defined as in (3.24), and ξ_0^i can be approximated using the equations (3.52) and (3.53). Under the assumption that the projections P_j^1 are mutually distinct, then A_0^a is invertible, and system (3.54) admits a unique solution. By solving this system, we can reconstruct the quantities $\nu_j^{k,i}$.

Again, following steps 5, 6 and 7 of the algebraic algorithm we can reconstruct the components x^i up to $O(\epsilon)$.

We remark that this generalization technique in fact holds for the algebraic algorithm in general, with its application in different inverse problems, not just the TAT problem. As we can see in the next chapter, this algorithm, as well as its generalization to higher dimensions is also applicable for the inverse PAT problem. Also, one can apply a similar generalization of this algorithm for the resolution of the inverse source problem given in [35] in higher dimensions.

4 Stability

The main goal in this section is to study the stability of reconstruction of the centers of the absorbers based on the method proposed in [33], on which the authors have used specific wave functions, then, using the reciprocity gap functional and suitable inequalities estimates, one gets the desired result.

4.1 Definitions and Notations

Before giving our stability results, we first introduce several notations and definitions needed throughout the rest of the section.

First, let $S = (x, y, z) \in \Omega$ and $d(\Gamma, S)$ be the Euclidean distance between the boundary Γ and S. Let $\omega_j,\ j = 1..., m$, be m absorbers with centers

$$\mathbf{S}_j = (x_j, y_j, z_j), \quad \text{for} \quad j = 1, \ldots, m.$$

We set

$$\alpha = \min_{1 \leq j \leq m} d(\Gamma, \mathbf{S}_j),$$

which is strictly positive, since $\mathbf{S}_j \in \Omega$. Then, we define the set

$$\Omega_\alpha = \{S \in \Omega : d(\Gamma, S) \geq \alpha\},$$

and let

$$d = \text{diam } (\Omega) - \alpha.$$

As denoted before, we take

$$P_j^a = x_j + iy_j \quad \text{and} \quad P_j^b = y_j + iz_j$$

to be the projections of the centers S_j onto the xy and yz- planes respectively, and set

$$P^a = (P_j^a)_{1\leq j\leq m} \quad \text{and} \quad P^b = (P_j^b)_{1\leq j\leq m}.$$

Then, we introduce the following real coefficients

$$\delta_r = \min_{\substack{1\leq j\leq m,\ 1\leq n\leq m \\ j\neq n}} \left\| P_j^r - P_n^r \right\|, \quad r = a, b,$$

and take

$$\delta = \min(\delta_a, \delta_b). \tag{3.55}$$

Thus, δ is strictly positive according to hypothesis **(H)**. Finally, for two points configurations $R^\ell = (R_j^\ell)_{1\leq j\leq N_\ell}$ for $\ell = 1, 2$, we recall the Hausdorff distance between R^1 and R^2, defined as follows

$$d_H(R^1, R^2) = \max\left\{ \max_{1\leq n\leq N_2; 1\leq j\leq N_1} \min \left\| R_n^2 - R_j^1 \right\|, \max_{1\leq n\leq N_1; 1\leq j\leq N_2} \min \left\| R_n^1 - R_j^2 \right\| \right\}.$$

4.2 Stability estimate for the locations of the absorbers

Let

$$(\gamma_j^\ell, \mathbf{S}_j^\ell)_{1\leq j\leq m_\ell} \quad \text{for} \quad \ell = 1, 2,$$

be two absorber configurations with γ_j^ℓ defined in (3.15), and consider the following constants

$$c_0 = \min_{\substack{1\leq i\leq m_1 \\ 1\leq j\leq m_2}} \left(\left| \nu_{i,1}^{0,a} \right|, \left| \nu_{j,2}^{0,a} \right| \right) \tag{3.56}$$

and

$$c_1 = \left(2\frac{(m_1 + m_2 - 1)^2}{d^2} + 1 \right)^{\frac{1}{2}}, \tag{3.57}$$

where $\nu_{i,1}^{0,a}$ and $\nu_{j,2}^{0,a}$ are as defined in (3.17):

$$\nu_{i,1}^{0,a} = \epsilon^3 \int_0^T \int_{B_i^1} \gamma_i^1(\boldsymbol{\tau}, t)\rho(z_i^1 + \epsilon\tau_3, t)d\boldsymbol{\tau}dt$$

and

$$\nu_{j,2}^{0,a} = \epsilon^3 \int_0^T \int_{B_j^2} \gamma_j^2(\boldsymbol{\tau}, t)\rho(z_j^2 + \epsilon\tau_3, t)d\boldsymbol{\tau}dt,$$

and the function ρ is the solution of (3.11). Then take $\varrho > 0$ such that

$$\sup_{t\in[0,T]} \|\rho(.,t)\|_{H^1(\gamma_1,\gamma_2)} \leq \varrho, \tag{3.58}$$

where $\|\cdot\|_{H^1(\gamma_1,\gamma_2)}$ is the classical H^1 norm defined by

$$\|\rho(.,t)\|_{H^1(\gamma_1,\gamma_2)} = \left(|\rho(.,t)|^2_{L^2(\gamma_1,\gamma_2)} + |\rho_z(.,t)|^2_{L^2(\gamma_1,\gamma_2)}\right)^{\frac{1}{2}}.$$

Now we are able to state our stability result for the absorbers' centers.

Theorem 3.13. *Let p^k, for $k = 1, 2$, be the solutions of (3.3) corresponding to two different sets of absorption domains, $\omega_j^k = \mathbf{S}_j^k + \epsilon B_j^k, 1 \leq j \leq m_k$, and characterized by the configurations $(\gamma_j^k, \mathbf{S}_j^k)_{1\leq j\leq m_k}$ with $\nu_{j,k}^{0,a} \neq 0$. For $k = 1, 2$, we take $f^k := p^k_{\Gamma\times(0,T)}$ to be the corresponding measurements on the boundary $\Sigma = \Gamma \times (0, T)$, and $\mathbf{S}^k = \left\{\mathbf{S}_j^k\right\}_{1\leq j\leq m_k}$. Assuming that $\mathbf{S}_j^k \in \Omega_\alpha$, then the following estimate holds,*

$$d_H(\mathbf{S}^1, \mathbf{S}^2) \leq 2\max_{k=1,2}\left[\frac{c_1\varrho\sqrt{T|\Gamma|}}{c_0\delta^{m_{3-k}-1}} d^{m_1+m_2-1} \left\| f^2 - f^1\right\|_{L^2(\Sigma)} + O(\epsilon)\right]^{\frac{1}{m_k}}.$$

The proof of Theorem 3.13 is based on the following lemma.

Lemma 3.2. *Let $P^{r,k} = \left\{P_j^{r,k}\right\}_{1\leq j\leq m_k}$, for $r = a, b$, be respectively the corresponding projections on the xy- and yz-planes of $\mathbf{S}^k$. Under the assumptions of Theorem 3.13, we have, for $r = a, b$ and $k = 1, 2$,*

$$d_H(P^{r,1}, P^{r,2}) \leq \max_{k=1,2}\left[\frac{c_1\varrho\sqrt{T|\Gamma|}}{c_0\delta^{m_{3-k}-1}} d^{m_1+m_2-1} \left\|f^2 - f^1\right\|_{L^2(\Sigma)} + O(\epsilon)\right]^{\frac{1}{m_k}}. \tag{3.59}$$

Proof.

The proof is based on the idea of choosing specific wave functions. In fact, if we take for $1 \leq \ell \leq m_2$,

$$\Phi_\ell(x, y) = \prod_{m=1}^{m_1}\left(x + iy - P_m^{a,1}\right)\prod_{m\neq\ell}^{m_2}\left(x + iy - P_m^{a,2}\right)$$

and

$$\Psi_\ell(\mathbf{x}, t) = \rho(z, t)\Phi_\ell(x, y),$$

where ρ is a non trivial solution of (3.11). Then, we observe that Ψ_ℓ is a solution of (3.6) satisfying (3.10). Thus,

$$\mathcal{R}(f, \Psi_\ell) = \int_0^T\int_\Gamma f(\xi, t)\frac{\partial\Psi_\ell}{\partial\nu}(\xi, t)\, d\xi\, dt, \tag{3.60}$$

where $\mathcal{R}(f,\Psi_\ell)$ is defined in (3.8). Also, substituting Ψ_ℓ in (3.9) we get

$$\mathcal{R}(f^2,\Psi_\ell) = \sum_{j=1}^{m_2}\int_0^T\int_{\omega_j^2}\sigma_j^2(\mathbf{x})g^2(\mathbf{x},t)\rho(z,t)\prod_{m=1}^{m_1}\left(x+iy-P_m^{a,1}\right)\prod_{m\neq\ell}^{m_2}\left(x+iy-P_m^{a,2}\right)d\mathbf{x}\;dt + O(\epsilon^\kappa).$$

Applying the change of variable $\omega_j^2 = \mathbf{S}_j^2 + \epsilon B_j^2$, we obtain

$$\begin{aligned}\mathcal{R}(f^2,\Psi_\ell) =& \epsilon^3\sum_{j=1}^{m_2}\int_0^T\int_{B_j^2}\sigma_j^2(\mathbf{S}_j^2+\epsilon\boldsymbol{\tau})g^2(\mathbf{S}_j^2+\epsilon\boldsymbol{\tau},t)\rho(z_j^2+\epsilon\tau_3,t)\\ &\times\prod_{m=1}^{m_1}\left(P_j^{a,2}-P_m^{a,1}+\epsilon(\tau_1+i\tau_2)\right)\prod_{m\neq\ell}^{m_2}\left(P_j^{a,2}-P_m^{a,2}+\epsilon(\tau_1+i\tau_2)\right)d\boldsymbol{\tau}\;dt\\ &+O(\epsilon^\kappa).\end{aligned}$$

Since $\kappa > 4$, we have

$$\begin{aligned}\mathcal{R}(f^2,\Psi_\ell) &= \epsilon^3\sum_{j=1}^{m_2}\int_0^T\int_{B_j^2}\sigma_j^2(\mathbf{S}_j^2+\epsilon\boldsymbol{\tau})g^2(\mathbf{S}_j^2+\epsilon\boldsymbol{\tau},t)\rho(z_j^2+\epsilon\tau_3,t)\\ &\quad\times\prod_{m=1}^{m_1}\left(P_j^{a,2}-P_m^{a,1}\right)\prod_{m\neq\ell}^{m_2}\left(P_j^{a,2}-P_m^{a,2}\right)d\boldsymbol{\tau}\;dt+O(\epsilon^4)\\ &= \prod_{m=1}^{m_1}\left(P_\ell^{a,2}-P_m^{a,1}\right)\prod_{m\neq\ell}^{m_2}\left(P_\ell^{a,2}-P_m^{a,2}\right)\nu_{\ell,2}^{0,a}+O(\epsilon^4).\end{aligned}$$

Similarly, one has

$$\begin{aligned}\mathcal{R}(f^1,\Psi_\ell) =& \sum_{j=1}^{m_1}\epsilon^3\int_0^T\int_{B_j^1}\sigma_j^1(\mathbf{S}_j^1+\epsilon\boldsymbol{\tau})g^1(\mathbf{S}_j^1+\epsilon\boldsymbol{\tau},t)\rho(z_j^1+\epsilon\tau_3,t)\prod_{m=1}^{m_1}\left(P_j^{a,1}-P_m^{a,1}\right)\\ &\times\prod_{m\neq\ell}^{m_2}\left(P_j^{a,1}-P_m^{a,2}\right)d\boldsymbol{\tau}\;dt+O(\epsilon^4)=O(\epsilon^4).\end{aligned}$$

Subtracting the two previous sums, we get

$$\mathcal{R}(f^2-f^1,\Psi_\ell) = \prod_{m=1}^{m_1}\left(P_\ell^{a,2}-P_m^{a,1}\right)\prod_{m\neq\ell}^{m_2}\left(P_\ell^{a,2}-P_m^{a,2}\right)\nu_{\ell,2}^{0,a}+O(\epsilon^4).$$

Therefore, from (3.55), (3.56) and (3.60), we obtain

$$c_0\min_{1\le m\le m_1}\left\|P_\ell^{a,2}-P_m^{a,1}\right\|^{m_1} \le \frac{1}{\delta^{m_2-1}}\left\|f^2-f^1\right\|_{L^2(\Sigma)}\left\|\frac{\partial\Psi_\ell}{\partial\nu}\right\|_{L^2(\Sigma)}+O(\epsilon^4).$$

Moreover, from (3.57) and (3.58), one can easily check that

$$\left\| \frac{\partial \Psi_\ell}{\partial \nu} \right\|_{L^2(\Sigma)} \leq c_1 \varrho \sqrt{T|\Gamma|} d^{m_1+m_2-1}.$$

Finally, we note from (3.56) that $c_0 = O(\epsilon^3)$, therefore we have

$$\max_{1\leq \ell \leq m_2; 1\leq m\leq m_1} \min \left\| P_\ell^{a,2} - P_m^{a,1} \right\| \leq \left[\frac{c_1 \varrho \sqrt{T|\Gamma|}}{c_0 \delta^{m_2-1}} d^{m_1+m_2-1} \left\| f^2 - f^1 \right\|_{L^2(\Sigma)} + O(\epsilon) \right]^{\frac{1}{m_1}}. \tag{3.61}$$

Similarly, by considering, first,

$$\widetilde{\Phi}_\ell(x,y) = \prod_{m\neq \ell}^{m_1} \left(x + iy - P_m^{a,1} \right) \prod_{m=1}^{m_2} \left(x + iy - P_m^{a,2} \right),$$

and then,

$$\widetilde{\Psi}_\ell(\mathbf{x},t) = \rho(z,t) \widetilde{\Phi}_\ell(x,y),$$

we get

$$\max_{1\leq \ell \leq m_1; 1\leq m\leq m_2} \min \left\| P_\ell^{a,1} - P_m^{a,2} \right\| \leq \left[\frac{c_1 \varrho \sqrt{T|\Gamma|}}{c_0 \delta^{m_1-1}} d^{m_1+m_2-1} \left\| f^2 - f^1 \right\|_{L^2(\Sigma)} + O(\epsilon) \right]^{\frac{1}{m_2}}. \tag{3.62}$$

Taking the maximum between (3.61) and (3.62), we get (3.59) for $r = a$. To prove the inequality (3.59) for $r = b$, we consider the following functions

$$\Psi_\ell(\mathbf{x},t) = \rho_1(x,t)\Phi_\ell(y,z), \quad \widetilde{\Psi}_\ell(\mathbf{x},t) = \rho_1(x,t)\widetilde{\Phi}_\ell(y,z),$$

where ρ_1 is the solution of (3.11) with the space variable z replaced by x. ■

Now we are able to give the proof of Theorem 3.13.

Proof.

Using the fact that

$$\max_{1\leq n\leq m_1; 1\leq j\leq m_2} \min \left\| \mathbf{S}_n^1 - \mathbf{S}_j^2 \right\| \leq \max_{1\leq n\leq m_1; 1\leq j\leq m_2} \min \left\| P_n^{a,1} - P_j^{a,2} \right\| + \max_{1\leq n\leq m_1; 1\leq j\leq m_2} \min \left\| P_n^{b,1} - P_j^{b,2} \right\|$$

and

$$\max_{1\leq n\leq m_2; 1\leq j\leq m_1} \min \left\| \mathbf{S}_n^2 - \mathbf{S}_j^1 \right\| \leq \max_{1\leq n\leq m_2; 1\leq j\leq m_1} \min \left\| P_n^{a,2} - P_j^{a,1} \right\| + \max_{1\leq n\leq m_2; 1\leq j\leq m_1} \min \left\| P_n^{b,2} - P_j^{b,1} \right\|,$$

we have

$$d_H(\mathbf{S}^1, \mathbf{S}^2) \leq d_H(P_1^a, P_2^a) + d_H(P_1^b, P_2^b).$$

Using the previous lemma, we get the desired result. ■

Remark 3.5 (Numerical simulations)**.** *The numerical implementation of our algorithm and some extensions of this work, in particular, the investigation of stability in case of variable sound speed, will be considered in some future work. For this reason, we leave the numerical analysis of this inverse problem for some future investigations. Moreover, we would like to compare our results to those obtained in [6] even if they were in the context of photoacoustics.*

5 Conclusion

In this chapter, we consider the inverse TAT problem, an effective imaging technique for detecting tumors based on the photo-acoustic effect. In TAT the biological tissue is subjected to a low frequency radiation, which results in a remarkable difference in conductivity between healthy tissues and cancerous ones. In our work, we take advantage of this difference to detect tumors, represented by small absorbers $\{\omega_j\}_{1\leq j\leq m}$. More precisely, we consider the inverse source problem for the wave equation (3.3), on which we reconstruct these absorbers from the boundary measurements. Unlike prior methods, our method doesn't follow the quantitative thermo-acoustic tomography approach. Instead, we develop a direct reconstruction process based on the algebraic algorithm proposed in [35]. This method allows us, directly from the wave equation, and using only one Cauchy data, to reconstruct modulo ϵ^{K+4} the number of absorbers m, their centers $\mathbf{S}_j$, and some information on the conductivity coefficient σ_j. Moreover, our algorithm doesn't require the knowledge of the *Grüneisen* coefficient $\beta(\mathbf{x})$, which is supposed throughout this chapter to be variable and unknown with $\beta(\mathbf{x}) \in L^\infty(\Omega)$. Also, we provide a Hölder stability estimate.

4

Inverse PAT problem

Life is good for only two things, discovering mathematics and teaching mathematics.

– Siméon Denis Poisson

This chapter is devoted to study the inverse PAT problem. As stated in Chapter 1, PAT is an imaging technique similar to TAT, however, in this case a high frequency radiation is delivered into the biological tissue to be imaged, such as visible or near infra red light that are characterized by their high speed compared to that of radio waves that are used in TAT. As in the case of TAT, the inverse problem we are concerned in is the reconstruction of small absorbers in a bounded domain $\Omega \subset \mathbb{R}^3$. Again, we follow the algebraic algorithm that allows us to resolve the problem from a single Cauchy data and without the knowledge of the *Grüneisen's* coefficient. However, the high frequency radiation used in this case makes some changes in the context of the problem and allows us to give our results using partial boundary observations and in both cases of constant and variable acoustic speed.

This chapter is organized as follows:

- **Section 1** introduces the main problem studied in this chapter and states the mathematical inverse problem that shall be resolved. Moreover, we discuss the methods used in literature and the difficulties behind them.

- **Section 2** provides a study of the inverse problem in case of constant acoustic speed. We give a reconstruction algorithm based on the algebraic method used in the previous chapter that uniquely determines the number of absorbers, their locations and the absorbed energy by each absorber. Moreover, we give a Hölder stability result for the reconstruction of the centers of the absorbers in this case.

- **Section 3** is intended to the study of the PAT problem in case of variable speed. We view the difference in the mathematical context between this case and that of constant speed and we provide a reconstruction algorithm as well as the stability results in this case.

1 Introduction and statement of the problem

The objective of this chapter is to study the inverse PAT problem, whose aim is to reconstruct the absorption properties of the biological tissues, which vary significantly between healthy tissues and cancerous ones. This rises from the fact that the absorption in biological tissues is enhanced by specific molecules such as hemoglobin and melanin, and tumors are known to contain more blood vessels than healthy cells, which increases the hemoglobin concentration in such tissues, and enhances light absorption. Thus, knowing the absorption coefficient highly contributes in detecting tumors. Moreover, the wavelength of the high frequency radiations used in PAT corresponds to the absorption spectrum of hemoglobin which enhances energy absorption in the biological tissues and makes PAT an effective method in detecting tumors.

When light propagates in the biological tissues, it interacts with it, and some of the delivered energy is absorbed by the underlying medium and converted into heat which leads to the generation of acoustic waves that propagate inside the medium. The stress confinement condition satisfied by the high frequency radiations used in this problem (see Chapter 1) allows us to assume that the acoustic pressure is generated initially in the biological tissue, which is thus known to satisfy the following wave equation

$$\begin{cases} \frac{1}{c_s^2} p_{tt}(\mathbf{x},t) - \Delta p(\mathbf{x},t) = 0 & \text{in } \Omega\times]0,T[, \\ p(\mathbf{x},0) = p_0(\mathbf{x}) & \text{in } \Omega, \\ p_t(\mathbf{x},0) = 0 & \text{in } \Omega, \\ p(\xi,t) = 0 & \text{on } \Gamma\times]0,T[, \end{cases} \tag{4.1}$$

where, $\Omega \subset \mathbb{R}^3$ is an open and bounded domain representing the imaged object, with a smooth boundary Γ, p denotes the acoustic pressure, c_s is the acoustic speed assumed to be known, $\mathbf{x} = (x,y,z) \in \Omega$, $p_t(x,t) = \frac{\partial p}{\partial t}(x,t)$, and $p_{tt}(x,t) = \frac{\partial^2 p}{\partial t^2}(x,t)$.

The initial pressure is given by

$$p_0(\mathbf{x}) = \beta(\mathbf{x})\mu_a(\mathbf{x})u(\mathbf{x}), \tag{4.2}$$

where β is the *Grüneisen*'s coefficient, μ_a is the absorption coefficient, and u is the light fluence satisfying the diffusion equation

$$\begin{aligned} -div(D(\mathbf{x})\nabla u) + \mu_a u &= 0 \text{ in } \Omega \\ u &= f \text{ on } \Gamma, \end{aligned} \tag{4.3}$$

where D denotes the diffusion coefficient. The main objective of this problem is to reconstruct the absorption coefficient from the measurement of the normal derivative of the pressure p at the boundary.

1.1 Methods used in literature

The PAT problem is highly considered in literature and different methods are used to solve this problem. As in the TAT problem, one of the main approaches used is the quantitative photo-acoustic tomography (qPAT) approach, see [6, 29–32, 64, 75, 84] and references therein. It is divided into two steps: the acoustic inversion and the optical inversion. The first step, which is the acoustic inversion, is to invert the wave equation (4.1) in order to reconstruct the initial pressure p_0 from the boundary measurements (4.4), and then the second step, or the optical inversion, is to reconstruct the optical parameters (β, μ_a, D) using the relation (4.2) and the diffusion equation (4.3). In [6], the authors proposed an algorithm for solving the acoustic inversion problem for small absorbers. In fact, they gave a method for reconstructing the location of the absorbers and the quantity $\epsilon^2 A$, where A represents the absorbed electromagnetic energy, and ϵ the diameter of the absorber. However, they considered a particular case when there is only one absorber and the acoustic speed is constant. Then in 2011, they proposed an algorithm to recover the absorption coefficient μ_a from the reconstructed quantity $\epsilon^2 A$ using asymptotic expansion of the light fluence and multiple optical wavelength data [7]. However, as in the TAT problem, the qPAT approach involves many difficulties leading to the ill-posedness of the inverse map, (for more details on the drawbacks of the qPAT approach we refer the reader to Section 1.8 in Chapter 1). Furthermore, different studies in literature have proposed numerical algorithms to solve the problem. In [15], for example, the authors have considered the problem in $\mathbb{R}^n$ with variable sound speed, and proposed a numerical reconstruction method based on the back projection algorithms. For more work on PAT we refer the reader to Section 1.7 in Chapter 1 and to [31, 45, 46, 67, 77, 78] and references therein.

In our work, we don't follow the qPAT approach. However, we develop a reconstruction method based on the algebraic algorithm, which enables us to uniquely solve the problem using only one partial observation on part of the boundary, chosen to satisfy certain geometric conditions, and the exact controllability problem for wave equations. Moreover, we give our results in both cases of constant and variable acoustic speed.

1.2 Statement of the problem

In this chapter, we consider the problem of reconstructing small absorbers in the wave equation (4.1) from partial boundary measurements. In other words, let Γ_0 be an open subset of Γ with non-void interior (with respect to the boundary topology).

We denote by Σ_T the lateral boundary $\Gamma \times (0,T)$ of the cylinder $\Omega \times (0,T)$, $\Sigma_T^0 = \Gamma_0 \times (0,T)$ the space-time observation domain, and Σ_T^1 the complementary part of Σ_T^0. Our goal now is to

reconstruct the absorption domains from the boundary measurement

$$\frac{\partial p}{\partial \nu}(\xi, t) := h(\xi, t) \quad \text{on} \quad \Sigma_T^0, \tag{4.4}$$

For this purpose, the observation boundary Γ_0 is assumed to satisfy some geometric conditions. Assuming that the acoustic speed is constant, and by referring to the work of Jacques Louis Lions [60] stated in Chapter 2, one can specify the following space-time observability domain:

We assume that there exists $\mathbf{x}_0 \in \mathbb{R}^n$, such that

$$\Gamma_0 = \Gamma(\mathbf{x}_0) = \{\mathbf{x} \in \Gamma \text{ such that } (\mathbf{x} - \mathbf{x}_0).\nu > 0\}, \tag{4.5}$$

where ν denotes the unit outward normal vector to Γ, and we take

$$T > T_0 = \frac{2R(\mathbf{x}_0)}{c_s}, \tag{4.6}$$

where

$$R(\mathbf{x}_0) = \sup_{\mathbf{x} \in \bar{\Omega}} |\mathbf{x} - \mathbf{x}_0|. \tag{4.7}$$

Now, we consider the problem of recovering the absorption coefficient μ_a, defined piece-wisely. That is

$$\mu_a = \begin{cases} \mu_0 & \text{in } \Omega \setminus \overline{\bigcup_{j=1}^{N} w_j} \\ \mu_j & \text{in } w_j, \end{cases} \tag{4.8}$$

where $w_j \subset \Omega$ are the small absorption domains defined as follows,

$$w_j = \mathbf{S}_j + \epsilon B_j \quad \text{and} \quad j \in \{1, .., N\}, \tag{4.9}$$

with $\mathbf{S}_j \in \Omega$ being the locations of the sub-domains w_j, and $B_j \subset \mathbb{R}^3$ are bounded domains containing the origin. The constant ϵ is the common order of magnitude of the diameters of w_j, supposed to be a sufficiently small positive real number, taken without loss of generality, smaller than 1. Moreover, the domains w_j are assumed to be far from the boundary Γ and their centers are supposed to be mutually distinct. Therefore, the problem we are interested in consists in determining the absorbers' number N, their centers $\mathbf{S}_j$ and some characteristics related to ω_j, using only one acoustic boundary measurement $h(\xi, t)$ on Σ_T^0. In particular, we reconstruct the *absorbed energy* by each sub-domain ω_j given by:

$$\int_{\omega_j} \beta(\mathbf{x}) \mu_j(\mathbf{x}) u(\mathbf{x}) d\mathbf{x}, \quad \text{for} \quad j = 1, ..., N. \tag{4.10}$$

Furthermore, we give an extension of our method to the case of variable speed, on which we prove that the same algorithm can be applied in case of variable acoustic speed, $c_s = c_s(\mathbf{x})$, and we give the corresponding stability result in each case.

We notice that the high frequency radiation used in this case facilitates the inverse problem and enables us to obtain our results with partial boundary measurements on a non-empty subset Γ_0 of the boundary Γ. Unlike the TAT problem studied in the previous chapter, the assumption that the acoustic pressure is generated initially due to the stress confinement condition (see Chapter 1 section 1.4.3), allows us to solve the inverse problem with partial boundary observations and in both cases of constant and variable acoustic speed.

Reconstruction of the diffusion coefficient D was also considered in literature, see [2, 12] and references therein. However, this requires an optical inversion of the diffusion equation (4.3) following the qPAT approach, at which multiple optical data may be required to uniquely resolve the problem [9, 10]. In our work, we restrict our self to the problem of reconstruction of the absorption coefficient μ_a, and we develop a direct identification process for solving the inverse problem that we are concerned with directly from the wave equation (4.1).

Remark 4.1. *Note that one can consider the inverse photoacoustic problem (4.1), (4.4) with Neumann boundary condition, $\frac{\partial p}{\partial \nu}(\xi, t) := 0$ on Σ_T, and boundary measurement $p(\xi, t) = h(\xi, t)$ on Σ_T^0. The both mathematical models are considered in practice, see, for example [6] and references therein.*

2 Case of constant acoustic speed

This section is intended to study the PAT inverse problem in case of constant acoustic speed c_s. We give a reconstruction method following the algebraic algorithm, and then we establish the corresponding stability result.

2.1 A reconstruction method

We present in this section a direct algorithm, without any optimization procedure, to construct the number N of the absorbers ω_j, their locations $\mathbf{S}_j$ and the *absorbed energy* (4.10) by each sub-domain ω_j. Our method, however, requires the knowledge of the normal derivative $\frac{\partial p}{\partial \nu}$ on the whole boundary Σ_T. For this purpose, we reconstruct first the initial pressure p_0 from the boundary measurement (4.4), then the data completion of $\frac{\partial p}{\partial \nu}$ on Σ_T^1 can be obtained by solving the initial-boundary value problem (4.1).

First, we give the following remark on the regularity of the forward problem (4.1).

Remark 4.2. *We assume throughout this chapter that the coefficients $\beta, \mu_a \in L^\infty(\Omega)$, and the initial pressure p_0 is in $L^2(\Omega)$. It is well known, from the regularity of wave equation [57] that*

for $p_0 \in L^2(\Omega)$, (4.1) admits a unique solution p with

$$p \in C((0,T), L^2(\Omega)) \cap C^1((0,T), H^{-1}(\Omega)).$$

Moreover, as proved in [60], the solution p of (4.1) satisfies

$$\frac{\partial p}{\partial \nu} \in H^{-1}((0,T), L^2(\Gamma)).$$

2.1.1 Data completion

We start by considering the inverse problem for the wave equation (4.1) in order to determine the initial pressure p_0 by means of the exact controllability theory, provided that Σ_T^0 satisfies the space-time observability conditions (4.5),(4.6). This problem was highly considered in literature, and for more details about the methods used for solving it, we refer the reader, for example, to [14, 60, 90] and references therein. Moreover, one can observe that determining the initial pressure requires the knowledge of the acoustic speed c_s over Ω. The computation of p_0 is given by the following lemma.

Lemma 4.1. *Let p be the solution of (4.1), with $p_0 \in L^2(\Omega)$. Then, for all $\varphi \in L^2(\Omega)$, there exists $\omega \in H_0^1((0,T), L^2(\Gamma_0))$ such that*

$$\int_\Omega p_0(\mathbf{x})\varphi(\mathbf{x})d\mathbf{x} = c_s^2 \int_{\Sigma_T^0} h(\xi,t)\omega(\xi,t)d\xi dt, \tag{4.11}$$

where $h(\xi,t)$ is given by (4.4).

Sketch of the proof

The proof of this lemma is related to the exact controllability for wave equation explained in Chapter 2. Indeed, under the conditions (4.5),(4.6), it is well known, from [60], that for all $\varphi \in L^2(\Omega)$, there exists $\omega \in H_0^1((0,T), L^2(\Gamma_0))$ such that the solution ψ of

$$\begin{cases} \frac{1}{c_s^2}\psi_{tt}(\mathbf{x},t) - \Delta\psi(\mathbf{x},t) = 0 & \text{in } \Omega\times]0,T[, \\ \psi(\mathbf{x},0) = 0 & \text{in } \Omega, \\ \psi_t(\mathbf{x},0) = \varphi(\mathbf{x}) & \text{in } \Omega, \\ \psi(\xi,t) = \omega(\xi,t) & \text{on } \Sigma_T^0, \\ \psi(\xi,t) = 0 & \text{on } \Sigma_T^1, \end{cases} \tag{4.12}$$

satisfies $\psi(\mathbf{x},T) = \psi_t(\mathbf{x},T) = 0$ in Ω. A numerical method to compute the control ω is given in [41]. Now, multiplying (4.1) by ψ, and using Green's formula, one obtains (4.11).

■.

Using the relation (4.11), one can now approximate p_0 by taking φ in a basis of $L^2(\Omega)$. After computing p_0, the data completion, $\frac{\partial p}{\partial \nu}$ on Σ_T^1, can be obtained by solving (4.1).

For simplicity, we denote by h in the rest of this section the value of $\frac{\partial p}{\partial \nu}$ on the whole boundary Γ.

2.1.2 Algebraic relations

We return to our inverse problem of determining the small absorbers from the knowledge of $\frac{\partial p}{\partial \nu}$ on Σ_T, obtained in subsection 2.1.1. We follow an algebraic reconstruction algorithm similar to that used in the previous chapter, whose main tool is the concept of the so-called *reciprocity gap functional* and special solutions of the wave equation

$$\frac{1}{c_s^2} v_{tt}(\mathbf{x},t) - \Delta v(\mathbf{x},t) = 0 \quad \text{in } \Omega\times]0,T[, \tag{4.13}$$

Indeed, multiplying (4.1) by v and integrating over $\Omega\times]0,T[$, we get

$$\int_\Omega \frac{1}{c_s^2}(p(\mathbf{x},T)v_t(\mathbf{x},T) - p_t(\mathbf{x},T)v(\mathbf{x},T))d\mathbf{x} + \int_{\Sigma_T} v(\xi,t)h(\xi,t)\, d\xi dt = \int_\Omega \frac{1}{c_s^2} p_0(\mathbf{x})v_t(\mathbf{x},0)\, d\mathbf{x}.$$

Let $\mathcal{R}$ be the *reciprocity gap operator* defined by

$$\mathcal{R}(h,v) := \int_\Omega \frac{1}{c_s^2}(p(\mathbf{x},T)v_t(\mathbf{x},T) - p_t(\mathbf{x},T)v(\mathbf{x},T))d\mathbf{x} + \int_{\Sigma_T} v(\xi,t)h(\xi,t)d\xi dt.$$

Thus, for all solutions v of (4.13) we have

$$\mathcal{R}(h,v) = \int_\Omega \frac{1}{c_s^2} p_0(\mathbf{x})v_t(\mathbf{x},0)d\mathbf{x}. \tag{4.14}$$

We notice from the previous equation that in order to solve the inverse problem we need to ensure that $v_t(\mathbf{x},0) \not\equiv 0$. Moreover, the resolution of the problem requires the knowledge of $p(.,T)$ and $p_t(.,T)$, or otherwise we impose the following condition,

$$v(\mathbf{x},T) = v_t(\mathbf{x},T) = 0, \tag{4.15}$$

which can be obtained by solving certain controllability problem. In this case we get

$$\mathcal{R}(h,v) := \int_{\Sigma_T} v(\xi,t)h(\xi,t)d\xi dt. \tag{4.16}$$

Moreover, from (4.2), (4.8) and (4.14), we obtain

$$\mathcal{R}(h,v)=\sum_{j=0}^{N}\int_{w_j}\frac{1}{c_s^2}\beta(\mathbf{x})\mu_j(\mathbf{x})u(\mathbf{x})v_t(\mathbf{x},0)d\mathbf{x}$$

where

$$w_0=\Omega\setminus\overline{\bigcup_{j=1}^{N}w_j}.$$

Furthermore, absorption in biological tissues is done by specific molecules such as hemoglobin and melanin. From a medical point of view, tumors are highly concentrated in such absorbing molecules, which results in a large difference in absorption between healthy tissues and cancerous ones [31, 75]. This permits us to assume that $\mu_0=O(\epsilon^\kappa)$, for some $\kappa>0$, assumed in our work to be $\kappa>4$. Consequently, we have

$$\mathcal{R}(h,v)=\sum_{j=1}^{N}\int_{w_j}\frac{1}{c_s^2}\lambda_j(\mathbf{x})v_t(\mathbf{x},0)d\mathbf{x}+O(\epsilon^\kappa),\tag{4.17}$$

where

$$\lambda_j(\mathbf{x})=\beta(\mathbf{x})\mu_j(\mathbf{x})u(\mathbf{x}).\tag{4.18}$$

The idea behind our identification method, as developed in [35], consists in choosing particular functions v, solutions of (4.13)-(4.15), with $v_t(\mathbf{x},0)\not\equiv 0$. For this purpose, we use the idea of exact controllability for wave equation. Let $\alpha_i,\beta_i,\gamma_i\in\mathbb{R}$, for $i=1,2$, such that

$$\Omega\subset[\alpha_1,\alpha_2]\times[\beta_1,\beta_2]\times[\gamma_1,\gamma_2].$$

We assume in this section that

$$T>\max\left\{T_0,\frac{2\text{diam }(\Omega)}{c_s}\right\},\tag{4.19}$$

where T_0 is defined in (4.6). We define for $n\in\mathbb{N}$,

$$v_n^a(\mathbf{x},t)=\rho(z,t)(x+iy)^n,\ \mathbf{x}=(x,y,z)\in\Omega,\tag{4.20}$$

where ρ is a solution of the one dimensional wave equation

$$\begin{cases}\dfrac{1}{c_s^2}\rho_{tt}(z,t)-\rho_{zz}(z,t)=0 & \text{in } (\gamma_1,\gamma_2)\times(0,T)\\ \rho(z,0)=0\quad \rho_t(z,0)=1 & \text{in } (\gamma_1,\gamma_2)\\ \rho(\gamma_1,t)=0\ \rho(\gamma_2,t)=w(t) & \text{for } t\in(0,T).\end{cases}\tag{4.21}$$

From the regularity of wave equation [57], we know that for every $w \in H^1(0,T)$, with the compatibility condition $w(0) = 0$, equation (4.21) admits a unique solution $\rho \in C((0,T), H^1(\gamma_1,\gamma_2)) \cap C^1((0,T), L^2(\gamma_1,\gamma_2))$.

Moreover, since $T > 2\frac{\text{diam }(\Omega)}{c_s}$, then by exact controllability [60], we can find $w \in H_0^1(0,T)$, such that the solution ρ of (4.21) satisfies

$$\rho(.,T) = \rho_t(.,T) = 0. \tag{4.22}$$

Therefore v_n^a is a solution of (4.13),(4.15) with

$$\frac{\partial v_n^a}{\partial t}(\mathbf{x},0) = (x+iy)^n, \ n \in \mathbb{N}.$$

Remark 4.3. *We note that the time condition given in (4.19) ensures that the data completion problem and the reconstruction of p_0 given in section 2.1.1 are applicable (since $T > T_0$). Moreover, the exact controllability problem for the one-dimensional wave equation (4.21) can also be applied (since $T > \frac{2\text{diam }(\Omega)}{c_s}$).*

We note from (4.17) that unlike the TAT problem, in this case the condition $v_t(.,0) \not\equiv 0$ is essential for the resolution of the problem. For this purpose, mollifier functions given in Remark 3.1 in the previous chapter are not applicable in this case, otherwise one shall take ρ a solution of (4.21) satisfying the controllability condition (4.22). Moreover, in case of variable speed, $c_s = c_s(\mathbf{x})$, one cannot take $\rho(z,t)$, a function of one space variable, to be a solution of (4.21), thus it is impossible to take v of the form (4.20). For this purpose we move in this case, as we will see in the next section, to the reconstruction of the final pressure $p(.,T)$, which describes why we consider the two cases separately.

Now, replacing v_n^a in (4.17), we have

$$R(h, v_n^a) = \sum_{j=1}^{N} \int_{w_j} \frac{1}{c_s^2} \lambda_j(\mathbf{x})(x+iy)^n d\mathbf{x} + O(\epsilon^\kappa).$$

Applying the change of variable

$$\mathbf{x} = \mathbf{S}_j + \epsilon\boldsymbol{\tau}, \quad \text{where } \mathbf{S}_j = (x_j, y_j, z_j) \text{ and } \boldsymbol{\tau} = (\tau_1, \tau_2, \tau_3) \in B_j$$

we get

$$R(h, v_n^a) = \epsilon^3 \sum_{j=1}^{N} \int_{B_j} \frac{1}{c_s^2} \lambda_j(\mathbf{S}_j + \epsilon\boldsymbol{\tau})[x_j + iy_j + \epsilon(\tau_1 + i\tau_2)]^n d\boldsymbol{\tau} + O(\epsilon^\kappa).$$

Therefore, $\forall\, n \in \mathbb{N}$ we have

$$\mathcal{R}(h, v_n^a) = \sum_{j=1}^{N} \sum_{k=0}^{n} \nu_j^{k,a} \binom{n}{k} (P_j^a)^{n-k} + O(\epsilon^\kappa), \tag{4.23}$$

where

$$\nu_j^{k,a} = \epsilon^{3+k} \int_{B_j} \frac{1}{c_s^2} \lambda_j(\mathbf{S}_j + \epsilon\boldsymbol{\tau})(\tau_1 + i\tau_2)^k d\boldsymbol{\tau}, \tag{4.24}$$

$$P_j^a = x_j + iy_j$$

and

$$\binom{n}{k} = \begin{cases} \dfrac{n!}{k!(n-k)!} & \text{if } n \geq k \\ 0 & \text{if } n < k. \end{cases} \tag{4.25}$$

We observe that for every $n_0 \in \mathbb{N}$, the system (4.23), with $n = 0, \cdots, n_0$, has $n_0 + 1$ equations and $N(n_0 + 2)$ unknowns. Then, the number of unknowns is variable with n_0, and it increases with the increase of the number of equations. Thus, it is impossible to uniquely reconstruct the unknowns, no matter how many equations are taken. To overcome this difficulty, we truncate these equations up to a small error. First, for a given positive $\epsilon < 1$, we choose a fixed positive integer $K < \kappa - 4$ such that ϵ^{K+4} is small enough and we set

$$\alpha_n^a := \sum_{j=1}^{N} \sum_{k=0}^{K} \nu_j^{k,a} \binom{n}{k} (P_j^a)^{n-k}, \quad \text{for all} \quad n \in \mathbb{N} \tag{4.26}$$

Then, using (4.23), we have for $n \leq K$,

$$R(h, v_n^a) = \alpha_n^a + O(\epsilon^\kappa),$$

and for $n > K$ we have

$$R(h, v_n^a) = \alpha_n^a + O(\epsilon^{K+4}),$$

where, one can see form (4.23) and (4.24) that

$$O(\epsilon^{K+4}) = \sum_{j=1}^{N} \sum_{k=K+1}^{n} \nu_j^{k,a} \binom{n}{k} (P_j^a)^{n-k} + O(\epsilon^\kappa).$$

Before presenting our identification algorithm, we introduce some notations and definitions that are used throughout this subsection. First, we denote by P_j^b and P_j^c the projections of $\mathbf{S}_j$ on the yz and xz planes respectively. Then, we define the following test functions

$$v_n^b(x, y, z) = \rho_1(x, t)(y + iz)^n \quad \text{and} \quad v_n^c(x, y, z) = \rho_2(y, t)(x + iz)^n,$$

where ρ_1 and ρ_2 are the solutions of (4.21)-(4.22), with the space variable z being replaced by x and y respectively, and the algebraic quantities

$$\alpha_n^b := \sum_{j=1}^{N}\sum_{k=0}^{K} \nu_j^{k,b} \binom{n}{k} (P_j^b)^{n-k}, \quad \text{for all} \quad n \in \mathbb{N}, \tag{4.27}$$

and

$$\alpha_n^c := \sum_{j=1}^{N}\sum_{k=0}^{K} \nu_j^{k,c} \binom{n}{k} (P_j^c)^{n-k}, \quad \text{for all} \quad n \in \mathbb{N}, \tag{4.28}$$

where

$$\nu_j^{k,b} = \epsilon^{3+k} \int_{B_j} \frac{1}{c_s^2} \lambda_j(\mathbf{S}_j + \epsilon\boldsymbol{\tau})(\tau_2 + i\tau_3)^k d\boldsymbol{\tau}$$

and

$$\nu_j^{k,c} = \epsilon^{3+k} \int_{B_j} \frac{1}{c_s^2} \lambda_j(\mathbf{S}_j + \epsilon\boldsymbol{\tau})(\tau_1 + i\tau_3)^k d\boldsymbol{\tau}.$$

Then, the algebraic relations (4.26, 4.27, 4.28) can be rewritten as

$$\alpha_n^r := \sum_{j=1}^{N}\sum_{k=0}^{K} \nu_j^{k,r} \binom{n}{k} (P_j^r)^{n-k} \qquad r = a, b, c. \tag{4.29}$$

Finally, we approximate the coefficients α_n^r by $\mathcal{R}(h, v_n^r)$, and then, we determine the quantities $(N, P_j^r, \nu_j^{k,r})$ by solving the equations (4.29), by means of the algebraic algorithm. To do this, we need to know if the projections P_j^r are mutually distinct. Indeed, one can remark that there is only a finite number of planes containing the origin such that at least two points among $\mathbf{S}_j$ are projected onto the same point on this plane. So, if a basis is chosen randomly, one is almost sure that the positions $\mathbf{S}_j$ are projected onto distinct points. Therefore, without loss of generality, we suppose that:

(H) The projections onto the xy, yz and xz-planes of the points $\mathbf{S}_j$ are mutually distinct.

2.1.3 Identification algorithm

First, we suppose that we know an upper bound $\bar{N}$ of the number of sources N, which implies that $\bar{J} = \bar{N}(K+1)$ is an upper bound of the number $J = N(K+1)$. Then, we define for $r = a, b, c$, and $k = 0, \ldots, K$, the complex vectors

$$\xi_n^r = (\alpha_n^r, \ldots, \alpha_{\bar{J}+n-1}^r)^t, \ \Lambda_k^r = (\nu_1^{k,r}, \ldots, \nu_N^{k,r})^t, \text{ and } \Lambda^r = \begin{pmatrix} (\Lambda_0^r)^t & (\Lambda_1^r)^t & \ldots & (\Lambda_K^r)^t \end{pmatrix}^t, \tag{4.30}$$

and consider, for all $n \in \mathbb{N}$, the complex $\bar{J} \times J$ matrices

$$A_n^r = \begin{pmatrix} V_n^{0,r} & V_n^{1,r} & \ldots & V_n^{K,r} \end{pmatrix}, \tag{4.31}$$

where for $k = 0, \dots, K$ and $r = a, b, c$, $V_n^{k,r}$ are the $\bar{J} \times N$ Vandermonde matrices

$$V_n^{k,r} = \begin{pmatrix} \binom{n}{k} (P_1^r)^{n-k} & \dots & \binom{n}{k} (P_N^r)^{n-k} \\ \binom{n+1}{k} (P_1^r)^{n-k+1} & \dots & \binom{n+1}{k} (P_N^r)^{n-k+1} \\ \vdots & \ddots & \vdots \\ \binom{\bar{J}+n-1}{k} (P_1^r)^{n-k+\bar{J}-1} & \dots & \binom{\bar{J}+n-1}{k} (P_N^r)^{n-k+\bar{J}-1} \end{pmatrix}.$$

Let us now introduce the Hankel matrix

$$H_{\bar{J}}^r = \begin{pmatrix} \alpha_0^r & \alpha_1^r & \dots & \alpha_{\bar{J}-1}^r \\ \alpha_1^r & \alpha_2^r & \dots & \alpha_{\bar{J}}^r \\ \vdots & \vdots & & \vdots \\ \alpha_{\bar{J}-1}^r & \alpha_{\bar{J}}^r & \dots & \alpha_{2\bar{J}-2}^r \end{pmatrix}, \tag{4.32}$$

and the following multi-diagonal matrices

$$L^r = \begin{pmatrix} \nu^{0,r} & \nu^{1,r} & \dots & \nu^{K,r} \\ \nu^{1,r} & \dots & \nu^{K,r} & 0 \\ \vdots & \iddots & & \vdots \\ \nu^{K,r} & 0 & \dots & 0 \end{pmatrix}, \tag{4.33}$$

where

$$\nu^{k,r} = diag(\nu_1^{k,r}, \dots, \nu_N^{k,r}).$$

Now, we propose an identification method in four steps.

Step 1: Determination of the number of absorbers.

The number N of absorbers is given by the following theorem

Theorem 4.14. *Let $H_{\bar{J}}^r$ be the Hankel matrix defined in (4.32), then under the hypothesis **(H)**, the number of absorbers is obtained as:*

$$N = \frac{1}{K+1} rank(H_{\bar{J}}^r) \quad \text{if and only if} \quad \nu_j^{K,r} \neq 0, \forall j = 1, \dots, N;\ r = a, b, c.$$

The proof of this theorem is similar to that of Theorem 3.11 in Chapter 3. It is based on the decomposition of the Hankel matrix $H_{\bar{J}}^r$ provided in the following lemma

Lemma 4.2. *Let $H^r_{\bar{J}}$ be the Hankel matrix defined in (4.32), L^r the multi-diagonal matrix defined in (4.33), A^r_0 the Vandermonde matrix defined in (4.31) and $(A^r_0)^t$ its transpose. Then,*

$$H^r_{\bar{J}} = A^r_0 L^r (A^r_0)^t \tag{4.34}$$

The proof of this lemma is similar to that of lemma 3.1 in the previous chapter.

Step 2: Reconstruction of the projections P^r_j.

The second step consists in determining the projections onto the xy, yz, and xz complex planes of the centers $\mathbf{S}_j$. In fact, if we replace $\bar{J}$ by J in the quantities defined above we get

$$H^r_J = \begin{pmatrix} \xi^r_0 & \xi^r_1 & \dots & \xi^r_{J-1} \end{pmatrix} \quad \text{and} \quad rank(H^r_J) = J.$$

Hence, the family $(\xi^r_0, \dots, \xi^r_{J-1})$ forms a basis for $\mathbb{C}^J$. Therefore, we consider the unique vector $C = (c^r_0, c^r_1, \dots, c^r_{J-1})^t$, solution of

$$H^r_J C = \xi^r_J,$$

that can be rewritten as follows,

$$\xi^r_J = c^r_0 \xi^r_0 + c^r_1 \xi^r_1 + \dots + c^r_{J-1} \xi^r_{J-1}.$$

Now, we define for $r = a, b, c$ the following matrices

$$B^r = \begin{pmatrix} 0 & 1 & \dots & 0 & 0 \\ 0 & 0 & 1 & \dots & 0 \\ \vdots & \vdots & \ddots & \ddots & 0 \\ \vdots & \vdots & \ddots & \ddots & 1 \\ c^r_0 & c^r_1 & \dots & \dots & c^r_{J-1} \end{pmatrix}. \tag{4.35}$$

Then, the projections P^r_j can be determined by the following theorem.

Theorem 4.15. *Let B^r, for $r = a, b, c$ be the companion matrices defined in (4.35). Under the hypothesis **(H)**, and assuming that $\nu^{K,r}_j \neq 0$ for $j = 1, \dots, N$, then*

1. *B^r admits N distinct eigenvalues, each of multiplicity $K + 1$;*
2. *The N eigenvalues of B^r are the projections P^r_j of the centers $\mathbf{S}_j$.*

The proof of this theorem is similar to that of Theorem 3.12 in the previous chapter.

Remark 4.4 (Numerical Simulations)**.** *We note that the rank of $H^r_{\bar{J}}$ can be obtained numerically as the number of its non-zero singular values. Moreover, as shown in Theorem 4.14 and*

(4.34), *the rank of* $H_{\tilde{J}}^r$ *depends on the separability of the projections* P_j^r, *for* $r = a, b, c$. *In fact, numerically, if the distance between the projections is relatively small, then, these point cannot be well approximated as separated sources, and thus their number is not accurately reconstructed. Thus, numerically one might obtain three distinct approximations* N_a, N_b *and* N_c *of the number of sources* N. *Consequently, the number of sources is taken as the maximum between these three, see [3]. More precisely, we choose* r *such that* $N_r = \max\{N_a, N_b, N_c\}$. *Without loss of generality, if we assume that* $N_r = N_a$, *then one can reconstruct the projections* P_j^a, $j = 1, \cdots, N_a$, *and then the third components* z_j *folllowing steps 2-4.*

We leave the numerical analysis of this inverse problem for some future investigations.

Step 3: Determination of the vectors Λ^r.

Following the same work done in the previous chapter, one can obtain the same relation (3.28). In order to determine the quantities $\nu_j^{k,r}$ it is sufficient to solve the linear systems

$$A_0^r \Lambda^r = \xi_0^r. \tag{4.36}$$

Remark 4.5. *If we assume that the Grüneisen's coefficient is constant* $\beta(\mathbf{x}) = \beta$, *then the knowledge of the coefficients* $\nu_j^{0,a}$ *obtained by solving equations (4.36) allows us to reconstruct the product of* β *by the average absorbed electromagnetic energy in each absorber* w_j *given by*

$$A_j = \beta \int_{w_j} \mu_j(\mathbf{x}) u(\mathbf{x}) \, d\mathbf{x}.$$

In fact, by definition we have

$$\nu_j^{0,a} = \epsilon^3 \int_{B_j} \frac{1}{c_s^2} \lambda_j(\mathbf{S}_j + \epsilon \boldsymbol{\tau}) \, d\boldsymbol{\tau}.$$

Applying the change of variable $\mathbf{x} = \mathbf{S}_j + \epsilon\boldsymbol{\tau}$, *and from (4.18) we get*

$$\nu_j^{0,a} = \int_{w_j} \frac{1}{c_s^2} \beta \mu_j(\mathbf{x}) u(\mathbf{x}) d\mathbf{x}.$$

Since the acoustic speed c_s *is constant, we obtain*

$$A_j = \beta \int_{w_j} \mu_j(\mathbf{x}) u(\mathbf{x}) d\mathbf{x} = c_s^2 \nu_j^{0,a}.$$

Step 4: Reconstruction of the third component z_j.

In step 2, we were able to reconstruct, modulo ϵ^{K+4}, the projections P_j^r of the centers $\mathbf{S}_j$ on the xy-, yz- and xz- planes. However, this is not enough to uniquely determine $\mathbf{S}_j$. In fact, the

combination of different projections does not uniquely determine the centers $\mathbf{S}_j$ (see remark 3.3 in the previous chapter). For this purpose, in this step we fix $r = a$ and we propose a direct method to determine the third component z_j of the previously calculated projections P_j^a using a specific wave function. However, we assume that the previously calculated coefficients $\nu_j^{0,a}$ satisfy

$$\nu_j^{0,a} \neq 0 \ \forall j = 1, \cdots, N.$$

Also, we take

$$T > 2\frac{\text{diam } \Omega}{c_s}.$$

Now, for every $n \in \mathbb{N}$ we consider the following wave function

$$g_n^a(\mathbf{x}, t) = 2nz\rho(z, t)(x + iy)^{n-1} - \rho_z(z, t)(x - iy)(x + iy)^n, \tag{4.37}$$

where ρ is a solution of (4.21), satisfying the controllability condition

$$\rho(., T) = \rho_t(., T) = 0.$$

Then, g_n^a is a solution of (4.13)-(4.15), with

$$(g_n^a)'(z, 0) = 2nz(x + iy)^{n-1}.$$

Substituting g_n^a in (4.17) we get

$$\begin{aligned} R(h, g_n^a) &= \sum_{j=1}^{N} 2n \int_{w_j} \frac{1}{c_s^2} \lambda_j(\mathbf{x}) z (x + iy)^{n-1} d\mathbf{x} + O(\epsilon^\kappa) \\ &= \sum_{j=1}^{N} 2n\epsilon^3 \int_{B_j} \frac{1}{c_s^2} \lambda_j(\mathbf{S}_j + \epsilon\boldsymbol{\tau})(z_j + \epsilon\tau_3) \left(P_j^a + \epsilon(\tau_1 + i\tau_2)\right)^{n-1} d\boldsymbol{\tau} + O(\epsilon^\kappa) \\ &= \sum_{j=1}^{N} 2n(P_j^a)^{n-1} \nu_j^{0,a} z_j + O(\epsilon^4). \end{aligned}$$

Taking $\widetilde{R}_n = \frac{1}{2n} R(h, g_n^a)$, we get

$$\widetilde{R}_n = \sum_{j=1}^{N} (P_j^a)^{n-1} \nu_j^{0,a} z_j + O(\epsilon^4) \ \forall n \in \mathbb{N}. \tag{4.38}$$

Now, we define the following complex vectors,

$$\widetilde{R} = (\ \widetilde{R}_1 \quad \widetilde{R}_2 \quad \dots \quad \widetilde{R}_N\ )^t \quad \text{and} \quad \widetilde{\Lambda}_z = (\ \nu_1^{0,a} z_1 \quad \nu_2^{0,a} z_2 \quad \dots \quad \nu_N^{0,a} z_N\ )^t,$$

and the $N \times N$ complex matrix

$$P_N = \begin{pmatrix} 1 & 1 & \dots & 1 \\ P_1^a & P_2^a & \dots & P_N^a \\ \vdots & \vdots & & \vdots \\ (P_1^a)^{N-1} & (P_2^a)^{N-1} & \dots & (P_N^a)^{N-1} \end{pmatrix}.$$

Then, the algebraic relation (4.38) can be rewritten, modulo $O(\epsilon^4)$, as

$$\widetilde{R} = P_N \widetilde{\Lambda}_z. \tag{4.39}$$

As the projections P_j^a are assumed to be mutually distinct, then P_N is invertible, and the equation (4.39) admits a unique solution. By solving this equation, we can reconstruct $\nu_j^{0,a} z_j$ up to $O(\epsilon^4)$. Moreover, since $\nu_j^{0,a}$ are of order ϵ^3 and are previously calculated and assumed to be different from zero for every $j = 1, \cdots, N$, then we can calculate the values of z_j up to $O(\epsilon)$. Finally, combining this result with that of step 2, we get the locations of the centers $\mathbf{S}_j$.

To sum up, the previous steps allow us, if we have a priori information on the number of sources, to reconstruct modulo ϵ^{K+4} the number of sources N, the centers $\mathbf{S}_j$ and the absorbed electromagnetic energy by each absorber in case of constant acoustic speed.

Remark 4.6. *We note that the algebraic algorithm presented in this section allows us to resolve the inverse PAT problem, and to reconstruct the number of the absorbers as well as their locations modulo $O(\epsilon^{K+4})$ for some $K > 0$. However, the resolution of the problem depends on the energy absorption in the background medium, more precisely, on how much the coefficient μ_0 is small, on which we require to have $\mu_0 = O(\epsilon^\kappa)$ for some $\kappa > 4$. Moreover, we remark that as in the TAT problem, the algorithm can be generalized to higher dimensions $\mathbb{R}^n$, under the assumption that $n + K + 1 < \kappa$ for some $K > 0$.*

2.2 Stability result for the reconstruction of the centers $\mathbf{S}_j$

Our aim in this section is to study the stability of reconstruction of the centers of the absorbers in case of constant sound speed based on the method proposed in [33]. Their method that we employ here is based on the choice of a suitable wave function. Then using the reciprocity gap functional and suitable inequalities estimates, we obtain the needed results.

First we give the stability results in case of total boundary observations ($\Gamma_0 = \Gamma$), next we move to the problem with partial boundary measurements.

2.2.1 Definitions and Notations.

Before giving our stability results, we first introduce several notations and definitions needed throughout the rest of the section.

First, let $S = (x, y, z) \in \Omega$ and $d(\Gamma, S)$ be the Euclidean distance between the boundary Γ and S. Let $\{\omega_j\}_{j=1...,N}$ be N absorbers with centers

$$\mathbf{S}_j = (x_j, y_j, z_j), \quad \text{for} \quad j = 1, \dots, N.$$

We set

$$\alpha = \min_{1\leq j\leq N} d(\Gamma, \mathbf{S}_j), \tag{4.40}$$

which is strictly positive, since $\mathbf{S}_j \in \Omega$. Then, we define the set

$$\Omega_\alpha = \{S \in \Omega : d(\Gamma, S) \geq \alpha\},$$

and let

$$d = \text{diam } (\Omega) - \alpha. \tag{4.41}$$

As denoted before, we take

$$P_j^a = x_j + iy_j \quad \text{and} \quad P_j^b = y_j + iz_j$$

to be the projections of the centers $\mathbf{S}_j$ onto the xy and yz- planes respectively, and set

$$P^a = (P_j^a)_{1\leq j\leq N} \quad \text{and} \quad P^b = (P_j^b)_{1\leq j\leq N}.$$

Then, we introduce the following real coefficients

$$\delta_r = \min_{\substack{1\leq j\leq N,\ 1\leq n\leq N \\ j\neq n}} \left\| P_j^r - P_n^r \right\|, \quad r = a, b$$

and take

$$\delta = \min(\delta_a, \delta_b). \tag{4.42}$$

Thus, δ is strictly positive according to hypothesis **(H)**. Finally, for two points configurations $R^\ell = (R_j^\ell)_{1\leq j\leq N_\ell}$ for $\ell = 1, 2$, we recall the Hausdorff distance between R^1 and R^2, defined as follows

$$d_H(R^1, R^2) = \max\left\{ \max_{1\leq n\leq N_2; 1\leq j\leq N_1} \min \left\| R_n^2 - R_j^1 \right\|, \max_{1\leq n\leq N_1; 1\leq j\leq N_2} \min \left\| R_n^1 - R_j^2 \right\| \right\}. \tag{4.43}$$

2.2.2 Stability estimate for total boundary observations

In this section, we assume that we have observation on the whole boundary Γ. That is, we assume that $\Gamma_0 = \Gamma$ in (4.4), and we take

$$T > 2\frac{\text{diam }(\Omega)}{c_s}. \tag{4.44}$$

Let

$$(\lambda_j^\ell, \mathbf{S}_j^\ell)_{1\leq j\leq N_\ell} \quad \text{for} \quad \ell = 1, 2$$

be two absorber configurations with λ_j^ℓ defined in (4.18), and consider the following constant

$$c_0 = \min_{\substack{1\leq i\leq N_1\\ 1\leq j\leq N_2}} (\left|\nu_{i,1}^{0,a}\right|, \left|\nu_{j,2}^{0,a}\right|), \tag{4.45}$$

where $\nu_{i,1}^{0,a}$ and $\nu_{j,2}^{0,a}$ are as defined in (4.24):

$$\nu_{i,1}^{0,a} = \epsilon^3 \int_{B_i^1} \frac{1}{c_s^2}\lambda_i(\mathbf{S}_i^1 + \epsilon\boldsymbol{\tau})d\boldsymbol{\tau}$$

and

$$\nu_{j,2}^{0,a} = \epsilon^3 \int_{B_j^2} \frac{1}{c_s^2}\lambda_j^2(\mathbf{S}_j^2 + \epsilon\boldsymbol{\tau})d\boldsymbol{\tau}.$$

Let ρ_a be a solution of the one-dimensional wave equation (4.21), then, as proved in [57], for every $w \in H^1(0,T)$, with the compatibility condition $w(0) = 0$, (4.21) admits a unique solution ρ_a satisfying,

$$\rho_a \in C\left((0,T), H^1(\gamma_1,\gamma_2)\right) \cap C^1\left((0,T), L^2(\gamma_1,\gamma_2)\right). \tag{4.46}$$

Moreover, as T satisfies (4.44), then using exact controllability [60], one can find $\omega \in H_0^1(0,T)$ such that the solution ρ_a of (4.21) satisfies

$$\rho_a(.,T) = \frac{\partial\rho_a}{\partial t}(.,T) = 0. \tag{4.47}$$

Take $\varrho^a, \varrho_1^a > 0$ such that

$$\sup_{t\in[0,T]} |\rho_a(.,t)|_{L^2(\gamma_1,\gamma_2)} \leq \varrho^a, \qquad \sup_{t\in[0,T]} |(\rho_a)_t(.,t)|_{L^2(\gamma_1,\gamma_2)} \leq \varrho_1^a.$$

Similarly, we define ρ_b to be a solution of (4.21) satisfying (4.47), with the space variable z being replaced by x, and we take $\varrho^b, \varrho_1^b > 0$ such that

$$\sup_{t\in[0,T]} |\rho_b(.,t)|_{L^2(\alpha_1,\alpha_2)} \leq \varrho^b, \quad \sup_{t\in[0,T]} |(\rho_b)_t(.,t)|_{L^2(\alpha_1,\alpha_2)} \leq \varrho_1^b$$

Finally, we define ϱ and ϱ_1 to be

$$\varrho = \max\{\varrho^a, \varrho^b\} \quad \varrho_1 = \max\{\varrho_1^a, \varrho_1^b\}. \tag{4.48}$$

Now we are able to state our stability result for the absorbers' centers.

Theorem 4.16. *Let p^k for $k = 1, 2$ be the solutions of (4.1) corresponding to the absorption domains $w_j^k = \mathbf{S}_j^k + \epsilon B_j^k, 1 \leq j \leq N_k$ characterized by the configurations $(\lambda_j^k, \mathbf{S}_j^k)_{1\leq j\leq N_k}$ with $\nu_{j,k}^{0,a} \neq 0$. Let $h^k := \frac{\partial p^k}{\partial \nu}\Big|_{\Sigma_T}$ for $k = 1, 2$ be the corresponding measurements on the boundary Σ_T. If we denote by $\mathbf{S}^k = \left(\mathbf{S}_j^k\right)_{1\leq j\leq N_k}$ for $k = 1, 2$, then assuming that $\mathbf{S}_j^k \in \Omega_\alpha$ and T satisfies*

$$T > 2\frac{\text{diam }\Omega}{c_s},$$

then the following estimate holds

$$d_H(\mathbf{S}^1, \mathbf{S}^2) \leq 2\max_{k=1,2}\left[\frac{(\varrho^2 + \varrho_1^2)^{\frac{1}{2}}\sqrt{T|\Gamma|}}{\delta^{N_{3-k}-1}c_0} d^{N_1+N_2-1} \left\| h^2 - h^1\right\|_{H^{-1}((0,T),L^2(\Gamma))} + O(\epsilon)\right]^{\frac{1}{N_k}}. \tag{4.49}$$

Remark 4.7. *We note from the previous estimate that the stability of the reconstruction of the centers depends on the separability of the projections as well as the distance of the centers from the boundary that are expressed by the coefficients δ and α defined in (4.42) and (4.40) respectively. In fact, one can easily check from (4.41) and (4.49) that the larger the values of δ and α are, the better stability estimates are obtained.*

The proof of Theorem 4.16 is based on the following lemma

Lemma 4.3. *Let $P^{r,k} = (P_j^{r,k})_{1\leq j\leq N_k}, r = a, b$ be respectively the corresponding projections on the xy and yz- planes of $\mathbf{S}^k$. Under the assumptions of Theorem 4.16, we have, for $r = a, b$ and $k = 1, 2$*

$$d_H(P^{r,1}, P^{r,2}) \leq \max_{k=1,2}\left[\frac{(\varrho^2 + \varrho_1^2)^{\frac{1}{2}}\sqrt{T|\Gamma|}}{\delta^{N_{3-k}-1}c_0} d^{N_1+N_2-1} \left\|h^2 - h^1\right\|_{H^{-1}((0,T),L^2(\Gamma))} + O(\epsilon)\right]^{\frac{1}{N_k}}. \tag{4.50}$$

Proof.

First we prove the inequality (4.50) for $r = a$. In fact, we note from the definition of the

Hausdorff distance given in (4.43) that it is enough to prove the following two inequalities

$$\max_{1\leq\ell\leq N_2;1\leq m\leq N_1}\min\left\|P_\ell^{a,2}-P_m^{a,1}\right\|\leq\left[\frac{(\varrho^2+\varrho_1^2)^{\frac{1}{2}}\sqrt{T|\Gamma|}}{c_0\delta^{N_2-1}}d^{N_1+N_2-1}\left\|h^2-h^1\right\|_{H^{-1}((0,T),L^2(\Gamma))}+O(\epsilon)\right]^{\frac{1}{N_1}}. \tag{4.51}$$

and

$$\max_{1\leq\ell\leq N_1;1\leq m\leq N_2}\min\left\|P_\ell^{a,1}-P_m^{a,2}\right\|\leq\left[\frac{(\varrho^2+\varrho_1^2)^{\frac{1}{2}}\sqrt{T|\Gamma|}}{c_0\delta^{N_1-1}}d^{N_1+N_2-1}\left\|h^2-h^1\right\|_{H^{-1}((0,T),L^2(\Gamma))}+O(\epsilon)\right]^{\frac{1}{N_2}}. \tag{4.52}$$

Then, taking the maximum between (4.51) and (4.52), we get (4.50) for $r=a$.

For this purpose, we consider for $1\leq\ell\leq N_2$ the following functions

$$\Phi_\ell(x,y)=\prod_{m=1}^{N_1}\left(x+iy-P_m^{a,1}\right)\prod_{m\neq\ell}^{N_2}\left(x+iy-P_m^{a,2}\right),$$

and

$$\Psi_\ell(\mathbf{x},t)=\rho_a(z,t)\Phi_\ell(x,y),$$

where ρ_a is a solution of (4.21) satisfying (4.46) and (4.47). Then, Ψ_ℓ is a solution of (4.13)-(4.15).

On the other hand, substituting Ψ_ℓ in (4.17) we get

$$\mathcal{R}(h^2,\Psi_\ell)=\sum_{j=1}^{N_2}\int_{w_j^2}\frac{1}{c_s^2}\lambda_j^2(\mathbf{x})\prod_{m=1}^{N_1}\left(x+iy-P_m^{a,1}\right)\prod_{m\neq\ell}^{N_2}\left(x+iy-P_m^{a,2}\right)d\mathbf{x}+O(\epsilon^\kappa).$$

Applying the change of variable $\mathbf{x}=\mathbf{S}_j^2+\epsilon\boldsymbol{\tau}$ we obtain

$$\begin{aligned}\mathcal{R}(h^2,\Psi_\ell)=&\epsilon^3\sum_{j=1}^{N_2}\int_{B_j^2}\frac{1}{c_s^2}\lambda_j^2(\mathbf{S}_j^2+\epsilon\boldsymbol{\tau})\prod_{m=1}^{N_1}\left(P_j^{a,2}-P_m^{a,1}+\epsilon(\tau_1+i\tau_2)\right)\\&\times\prod_{m\neq\ell}^{N_2}\left(P_j^{a,2}-P_m^{a,2}+\epsilon(\tau_1+i\tau_2)\right)d\boldsymbol{\tau}+O(\epsilon^\kappa).\end{aligned}$$

Since $\kappa>4$ we have

$$\begin{aligned}\mathcal{R}(h^2,\Psi_\ell)&=\epsilon^3\sum_{j=1}^{N_2}\int_{B_j^2}\frac{1}{c_s^2}\lambda_j^2(\mathbf{S}_j^2+\epsilon\boldsymbol{\tau})\prod_{m=1}^{N_1}\left(P_j^{a,2}-P_m^{a,1}\right)\prod_{m\neq\ell}^{N_2}\left(P_j^{a,2}-P_m^{a,2}\right)d\boldsymbol{\tau}+O(\epsilon^4)\\&=\prod_{m=1}^{N_1}\left(P_\ell^{a,2}-P_m^{a,1}\right)\prod_{m\neq\ell}^{N_2}\left(P_\ell^{a,2}-P_m^{a,2}\right)\nu_{\ell,2}^{0,a}+O(\epsilon^4).\end{aligned}$$

Similarly, one has

$$\begin{aligned}\mathcal{R}(h^1,\Psi_\ell) &= \sum_{j=1}^{N_1}\epsilon^3\int_{B_j^1}\frac{1}{c_s^2}\lambda_j^1(\mathbf{S}_j^1+\epsilon\boldsymbol{\tau})\prod_{m=1}^{N_1}\left(P_j^{a,1}-P_m^{a,1}\right)\prod_{m\neq\ell}^{N_2}\left(P_j^{a,1}-P_m^{a,2}\right)d\boldsymbol{\tau}+O(\epsilon^4)\\ &= O(\epsilon^4).\end{aligned}$$

Subtracting the two previous sums, we get

$$\mathcal{R}(h^2-h^1,\Psi_\ell) = \prod_{m=1}^{N_1}\left(P_\ell^{a,2}-P_m^{a,1}\right)\prod_{m\neq\ell}^{N_2}\left(P_\ell^{a,2}-P_m^{a,2}\right)\nu_{\ell,2}^{0,a}+O(\epsilon^4).$$

Therefore, from (4.16), (4.42) and (4.45), we obtain

$$c_0\min_{1\le m\le N_1}\left\|P_\ell^{a,2}-P_m^{a,1}\right\|^{N_1} \le \frac{1}{\delta^{N_2-1}}\left\|h^2-h^1\right\|_{H^{-1}((0,T),L^2(\Gamma))}\|\Psi_\ell\|_{H_0^1((0,T),L^2(\Gamma))}+O(\epsilon^4). \quad (4.53)$$

Moreover, from (4.48), one can easily check that

$$\|\Psi_\ell\|_{H_0^1((0,T),L^2(\Gamma))} \le (\varrho^2+\varrho_1^2)^{\frac{1}{2}}\sqrt{T|\Gamma|}d^{N_1+N_2-1}. \quad (4.54)$$

In fact,

$$\|\Psi_\ell\|^2_{H_0^1((0,T),L^2(\Gamma))} = |\Psi_\ell|^2_{L^2(\Sigma_T)}+\left|\frac{\partial\Psi_\ell}{\partial t}\right|^2_{L^2(\Sigma_T)}.$$

On the other hand, for every $\mathbf{x}\in\Gamma$ we have

$$|\Phi_\ell(x,y)| \le d^{N_1+N_2-1}.$$

Therefore

$$\begin{aligned}|\Psi_\ell|^2_{L^2(\Sigma_T)} &= \int_0^T\int_\Gamma|\rho_a(z,t)|^2|\Phi_\ell(x,y)|^2d\xi dt\\ &\le d^{2(N_1+N_2-1)}T|\Gamma|\sup_{t\in[0,T]}|\rho_a(.,t)|^2_{L^2(\gamma_1,\gamma_2)}\\ &\le d^{2(N_1+N_2-1)}T|\Gamma|\varrho^2,\end{aligned}$$

and

$$\begin{aligned}\left|\frac{\partial\Psi_\ell}{\partial t}\right|^2_{L^2(\Sigma_T)} &= \int_0^T\int_\Gamma\left|\frac{\partial\rho_a}{\partial t}(z,t)\right|^2|\Phi_\ell(x,y)|^2d\xi dt\\ &\le d^{2(N_1+N_2-1)}T|\Gamma|\sup_{t\in[0,T]}\left|\frac{\partial\rho_a}{\partial t}(.,t)\right|^2_{L^2(\gamma_1,\gamma_2)}\\ &\le d^{2(N_1+N_2-1)}T|\Gamma|\varrho_1^2.\end{aligned}$$

Combining together all the previous estimates we get (4.54). Finally, we note from (4.45) that $c_0 = O(\epsilon^3)$. Now, substituting (4.54) in (4.53) we end up with (4.51).

Similarly, by considering, first

$$\widetilde{\Phi}_\ell(x,y) = \prod_{m\neq\ell}^{N_1}\left(x+iy-P_m^{a,1}\right)\prod_{m=1}^{N_2}\left(x+iy-P_m^{a,2}\right),$$

and then,

$$\widetilde{\Psi}_\ell(\mathbf{x},t) = \rho_a(z,t)\widetilde{\Phi}_\ell(x,y),$$

and following the same steps, one can prove (4.52).

Taking the maximum between (4.51) and (4.52), we get (4.50) for $r = a$. To prove the inequality (4.50) for $r = b$, we consider the following functions

$$\Psi_\ell(\mathbf{x},t) = \rho_b(x,t)\Phi_\ell(y,z), \quad \widetilde{\Psi}_\ell(\mathbf{x},t) = \rho_b(x,t)\widetilde{\Phi}_\ell(y,z),$$

where ρ_b is a solution of (4.21) satisfying (4.46) and (4.47), with the space variable z being replaced by x. Then, following the same steps as in case $r = a$, one can obtain the inequality (4.50) for $r = b$. ■

Proof of Theorem 4.16.
Using the fact that

$$\max_{1\leq n\leq N_1;1\leq j\leq N_2}\min\left\|\mathbf{S}_n^1-\mathbf{S}_j^2\right\| \leq \max_{1\leq n\leq N_1;1\leq j\leq N_2}\min\left\|P_n^{a,1}-P_j^{a,2}\right\| + \max_{1\leq n\leq N_1^1;1\leq j\leq N_1^2}\min\left\|P_n^{b,1}-P_j^{b,2}\right\|$$

and

$$\max_{1\leq n\leq N_2;1\leq j\leq N_1}\min\left\|\mathbf{S}_n^2-\mathbf{S}_j^1\right\| \leq \max_{1\leq n\leq N_2;1\leq j\leq N_1}\min\left\|P_n^{a,2}-P_j^{a,1}\right\| + \max_{1\leq n\leq N_2;1\leq j\leq N_1}\min\left\|P_n^{b,2}-P_j^{b,1}\right\|$$

we have

$$d_H(\mathbf{S}^1,\mathbf{S}^2) \leq d_H(P_1^a,P_2^a) + d_H(P_1^b,P_2^b).$$

Using the previous lemma, we get the desired result.

2.2.3 Stability estimate for partial boundary measurements

In this subsection, we assume that we have partial boundary observations on a non-empty subset Γ_0 of Γ, as given in (4.4), and we establish the corresponding stability result.

We assume the same situation of the previous subsection, then the following stability estimate holds for the absorbers' centers.

Theorem 4.17. *Let* $\mathbf{S}^k = \left(\mathbf{S}_j^k\right)_{1\leq j\leq N_k}$ *for* $k = 1, 2$*, be two absorbers' configurations defined as in the previous subsection. Assuming that* Γ_0 *satisfies the observability condition*

$$\Gamma_0 = \Gamma(\mathbf{x}_0) = \{\mathbf{x} \in \Gamma, \quad \textit{such that} \quad (\mathbf{x} - \mathbf{x}_0).\nu > 0\},$$

for some $\mathbf{x}_0 \in \mathbb{R}^n$*, and*

$$T > \max\left\{\frac{2R(\mathbf{x}_0)}{c_s}, \frac{2\text{diam }(\Omega)}{c_s}\right\},$$

where

$$R(\mathbf{x}_0) = \sup_{\mathbf{x}\in\bar{\Omega}} |\mathbf{x} - \mathbf{x}_0|,$$

then the following stability estimate holds

$$d_H(\mathbf{S}^1, \mathbf{S}^2) \leq 2\max_{k=1,2}\left[\frac{(\varrho^2 + \varrho_1^2)^{\frac{1}{2}}\sqrt{T|\Gamma|}}{\delta^{N_{3-k}-1}c_0}\ \hat{c}\ d^{N_1+N_2-1}\left\|\ h^2 - h^1\right\|_{H^{-1}((0,T),L^2(\Gamma_0))} + O(\epsilon)\right]^{\frac{1}{N_k}},$$

for some positive constant $\hat{c}$*.*

Proof.

The proof is similar to that done in case of total observation. However, it depends on the stability of the reconstruction of the initial pressure given in section 2.1.1. In fact, following the same steps as in the previous subsection, one can obtain the same stability estimate as that obtained in Theorem 4.16. Moreover, from the regularity of wave equation, see [60], one has

$$\|h^2 - h^1\|_{H^{-1}((0,T),L^2(\Gamma))} \leq \tilde{c}\ |p_0^2 - p_0^1|_{L^2(\Omega)}, \tag{4.55}$$

for some $\tilde{c} > 0$, where $p_0^i(\mathbf{x}) = p^i(\mathbf{x}, 0)$ for $i = 1, 2$. This estimate can be obtained by following the context of Lemma 2.4 in Chapter 2 with constant speed. On the other hand, taking $\varphi = p_0$ in (4.11), one gets

$$|p_0|^2_{L^2(\Omega)} = c_s^2 \int_{\Sigma_T^0} h(\xi, t)w(\xi, t)\ d\xi dt.$$

However, using the stability of the exact controllability problem of (4.12) with $\varphi = p_0$, as explained in [60], we infer that for some $\tilde{c}_1 > 0$ we have

$$\|w\|_{H_0^1((0,T),L^2(\Gamma^0))} \leq \tilde{c}_1 |p_0|_{L^2(\Omega)}.$$

Thus,

$$\begin{aligned} |p_0|^2_{L^2(\Omega)} &\leq c_s^2 \|h\|_{H^{-1}((0,T),L^2(\Gamma_0))} \|w\|_{H_0^1((0,T),L^2(\Gamma_0))} \\ &\leq c_s^2 \tilde{c}_1 |p_0|_{L^2(\Omega)} \|h\|_{H^{-1}((0,T),L^2(\Gamma_0))}. \end{aligned}$$

Therefore,

$$|p_0|_{L^2(\Omega)} \leq c_s^2 \tilde{c}_1 \|h\|_{H^{-1}((0,T),L^2(\Gamma_0))}. \tag{4.56}$$

Substituting (4.56) in (4.55) we get

$$\|h^2 - h^1\|_{H^{-1}((0,T),L^2(\Gamma))} \leq \hat{c}\|h^2 - h^1\|_{H^{-1}((0,T),L^2(\Gamma_0))},$$

where $\hat{c} = c_s^2 \tilde{c} \tilde{c}_1$.

Finally, the result is obtained by substituting this approximation in the stability estimate with total boundary measurements given in Theorem 4.16. ■

3 Case of variable acoustic speed

Our goal in this section is to study the PAT problem in case of spatially variant acoustic speed $c_s = c_s(\mathbf{x})$, on which we prove the validity of our reconstruction algorithm in this case also. The acoustic pressure $p(\mathbf{x}, t)$ is now assumed to satisfy the following wave equation

$$\begin{cases} \dfrac{1}{c_s^2(\mathbf{x})} p_{tt}(\mathbf{x}, t) - \Delta p(\mathbf{x}, t) = 0 & \text{in } \Omega \times]0, T[, \\ p(\mathbf{x}, 0) = p_0(\mathbf{x}) & \text{in } \Omega, \\ p_t(\mathbf{x}, 0) = 0 & \text{in } \Omega, \\ p(\xi, t) = 0 & \text{on } \Gamma \times]0, T[, \end{cases} \tag{4.57}$$

equipped with the observation

$$\frac{\partial p}{\partial \nu}(\xi, t) = h(\xi, t) \text{ on } \Sigma_T^0 = \Gamma_0 \times (0, T), \tag{4.58}$$

where, Γ_0 satisfies the observability condition (4.5). As in section 2.1, our reconstruction method is based on the idea of the *reciprocity gap functional* and on special solutions of the wave equation (4.13) with $c_s = c_s(\mathbf{x})$.

However, functions of the form (4.20) don't work in this case. In fact, one cannot take ρ, a function of one space variable z, to be a solution of (4.21) while $c_s = c_s(x, y, z)$. For this purpose, we opt in this section to reconstruct the final pressure $p(., T)$, on which the controllability condition (4.15) is no longer required. Moreover, as in case of constant speed, the resolution of the problem requires the knowledge of $\frac{\partial p}{\partial \nu}$ on the whole boundary Γ, so we provide also the data completion of $\frac{\partial p}{\partial \nu}\Big|_{\Gamma_1}$.

First, we assume that $c_s \in C^1(\bar{\Omega})$ and satisfies

$$0 < c_{\min} \leq c_s(\mathbf{x}) \leq c_{\max}, \tag{4.59}$$

for some $c_{\min}, c_{\max} > 0$. Moreover, we define $s_1 > 0$ by

$$s_1 = \|\nabla c_s\|_{L^\infty(\bar{\Omega})}. \tag{4.60}$$

Data Completion

Now, we move to the reconstruction of $p(.,T)$ and $\frac{\partial p}{\partial \nu}\Big|_{\Sigma_T^1}$. As in case of constant speed, the idea is based on the reconstruction, first, of the initial pressure p_0 from the boundary observations, by means of exact controllability. Then, the data completion can be done by solving (4.57).

In fact, as $c_s \in C^1(\bar{\Omega})$, and satisfies (4.59), then referring to Lemma 2.4 in Chapter 2, we note that for every $p_0 \in L^2(\Omega)$ (4.57) admits a unique solution

$$p \in C((0,T), L^2(\Omega)) \cap C^1((0,T), H^{-1}(\Omega)),$$

with

$$\frac{\partial p}{\partial \nu} \in H^{-1}((0,T), L^2(\Gamma)).$$

Moreover, as explained in Chapter 2, Theorem 2.10, for T large enough, in particular,

$$T > \frac{2(s_1+1)}{c_{\min}} R(\mathbf{x}_0),$$

where $R(\mathbf{x}_0)$ is taken as that in (4.7), then the exact controllability for wave equation implies that there exists $w \in H_0^1((0,T), L^2(\Gamma_0))$ such that the solution ψ of (4.12), with $c_s = c_s(\mathbf{x})$, satisfies $\psi(.,T) = \psi_t(.,T) = 0$. Now, arguing in the same manner as in case of constant speed, one can obtain the initial pressure p_0.

The values of $p(.,T)$ and $\frac{\partial p}{\partial \nu}\Big|_{\Sigma_T^1}$ can then be obtained by solving (4.57).

Again, we denote by $h(\xi,t)$ the value of $\frac{\partial p}{\partial \nu}(\xi,t)$ on the whole boundary Σ_T.

3.1 Reconstruction Algorithm

We give in this subsection a reconstruction algorithm similar to that given in section 2.1, based on the idea of the *reciprocity gap functional*, and special solutions of the wave equation

$$\frac{1}{c_s^2(\mathbf{x})} v_{tt}(\mathbf{x},t) - \Delta v(\mathbf{x},t) = 0. \tag{4.61}$$

Then, multiplying (4.57) by v and integrating by parts we get

$$R(h,v) = \sum_{j=1}^{N} \int_{w_j} \frac{1}{c_s^2(\mathbf{x})} \lambda_j(\mathbf{x}) v_t(\mathbf{x},0)\, d\mathbf{x} + O(\epsilon^\kappa), \tag{4.62}$$

where

$$R(h,v) := \int_\Omega \frac{1}{c_s^2(\mathbf{x})}(p(\mathbf{x},T)v_t(\mathbf{x},T) - p_t(\mathbf{x},T)v(\mathbf{x},T))d\mathbf{x} + \int_0^T \int_\Gamma h(\xi,t)v(\xi,t)d\xi dt,$$

and λ_j is as defined in (4.18). We proceed in 4 steps as in the case of constant speed. First, we take for $\mathbf{x} = (x,y,z) \in \Omega$ and $n \in \mathbb{N}$

$$v_n^a(\mathbf{x},t) = (t-T)(x+iy)^n.$$

Then, v_n^a is a solution of (4.61) satisfying $v_n^a(.,T) = 0$. Thus

$$R(h,v_n^a) := \int_\Omega \frac{1}{c_s^2(\mathbf{x})} p(\mathbf{x},T)\frac{\partial v_n^a}{\partial t}(\mathbf{x},T)d\mathbf{x} + \int_0^T \int_\Gamma h(\xi,t)v_n^a(\xi,t)d\xi dt.$$

Moreover, substituting v_n^a in (4.62) we get

$$\begin{aligned} R(h,v_n^a) &= \sum_{j=1}^N \int_{w_j} \frac{1}{c_s^2(\mathbf{x})}\lambda_j(\mathbf{x})(x+iy)^n d\mathbf{x} + O(\epsilon^\kappa) \\ &= \sum_{j=1}^N \sum_{k=0}^n \binom{n}{k} \nu_j^{k,a}(P_j^a)^{n-k} + O(\epsilon^\kappa), \end{aligned}$$

where $\nu_j^{k,a}$ is as defined in (4.24), with $c_s = c_s(\mathbf{x})$.

Now, arguing as in steps 1,2 and 3 in section 2.1, we can reconstruct the number of sources N, the projections P_j^a and the coefficients $\nu_j^{k,a}$. Finally, to reconstruct the third components z_j we adopt the following wave functions for every $1 \le \ell \le N$,

$$v_\ell(\mathbf{x},t) = (t-T)z\prod_{m\neq\ell}^N (x+iy-P_m^a).$$

Then, we have the following result.

Theorem 4.18. *Assuming that, for every $1 \le \ell \le N$, $\nu_\ell^{0,a} \neq 0$, then the third component z_ℓ of $\mathbf{S}_\ell$ is given by*

$$z_\ell = \frac{\mathcal{R}(h,v_\ell)}{\nu_\ell^{0,a}\prod_{m\neq\ell}(P_\ell^a - P_m^a)} + O(\epsilon).$$

Proof.
Substituting v_ℓ in (4.62), we get

$$\mathcal{R}(h,v_\ell) = \sum_{j=1}^N \int_{w_j} \frac{1}{c_s^2(\mathbf{x})}\lambda_j(\mathbf{x})z\prod_{m\neq\ell}(x+iy-P_m^a)d\mathbf{x} + O(\epsilon^\kappa),$$

and applying the change of variable $\mathbf{x} = \mathbf{S}_j + \epsilon\boldsymbol{\tau}$, we obtain

$$\mathcal{R}(h, v_\ell) = \sum_{j=1}^{N} \epsilon^3 \int_{B_j} \frac{1}{c_s^2(\mathbf{S}_j + \epsilon\boldsymbol{\tau})} \lambda_j(\mathbf{S}_j + \epsilon\boldsymbol{\tau})(z_j + \epsilon\tau_3) \prod_{m\neq\ell} \Big(P_j^a - P_m^a + \epsilon(\tau_1 + i\tau_2)\Big)\, d\boldsymbol{\tau} + O(\epsilon^\kappa).$$

Since $\kappa > 4$, we get

$$\begin{aligned}\mathcal{R}(h, v_\ell) &= \sum_{j=1}^{N} \epsilon^3 \int_{B_j} \frac{1}{c_s^2(\mathbf{S}_j + \epsilon\boldsymbol{\tau})} \lambda_j(\mathbf{S}_j + \epsilon\boldsymbol{\tau}) z_j \prod_{m\neq\ell} \Big(P_j^a - P_m^a\Big)\, d\boldsymbol{\tau} + O(\epsilon^4) \\ &= \epsilon^3 \int_{B_\ell} \frac{1}{c_s^2(\mathbf{S}_\ell + \epsilon\boldsymbol{\tau})} \lambda_\ell(\mathbf{S}_\ell + \epsilon\boldsymbol{\tau}) z_\ell \prod_{m\neq\ell} (P_\ell^a - P_m^a)\, d\boldsymbol{\tau} + O(\epsilon^4) \\ &= z_\ell \nu_\ell^{0,a} \prod_{m\neq\ell} (P_\ell^a - P_m^a) + O(\epsilon^4).\end{aligned}$$

Therefore, since $\nu_\ell^{0,a} \neq 0$ we get

$$z_\ell = \frac{\mathcal{R}(h, v_\ell)}{\nu_\ell^{0,a} \prod_{m\neq\ell} (P_\ell^a - P_m^a)} + O(\epsilon).$$

■

Thus, we were able to reconstruct z_ℓ up to $O(\epsilon)$.

3.2 Stability estimates with partial boundary measurements

Our goal in this subsection is to study the stability of reconstruction of the centers $\mathbf{S}_j$ of the absorbers from the boundary measurements (4.58) in case of variable sound speed. We follow the same method used in section 2.2, on which we adopt the same definitions used, and we obtain the following stability result.

Theorem 4.19. *Let p^k for $k = 1, 2$ be the solutions of (4.57) corresponding to the absorption domains $w_j^k = \mathbf{S}_j^k + \epsilon B_j^k, 1 \leq j \leq N_k$ characterized by the configurations $(\lambda_j^k, \mathbf{S}_j^k)_{1\leq j\leq N_k}$ with $\nu_{j,k}^{0,a} \neq 0$. Let $h^k := \frac{\partial p^k}{\partial \nu}\Big|_{\Sigma_T^0}$ for $k = 1, 2$ be the corresponding measurements on the boundary Σ_T^0. Let $\mathbf{S}^k = \left(\mathbf{S}_j^k\right)_{1\leq j\leq N_k}$ for $k = 1, 2$. Assuming that $\mathbf{S}_j^k \in \Omega_\alpha$, Γ_0 satisfies the observability condition*

$$\Gamma_0 = \Gamma(\mathbf{x}_0) = \{\mathbf{x} \in \Gamma, \quad \textit{such that} \quad (\mathbf{x} - \mathbf{x}_0).\nu > 0\},$$

for some $\mathbf{x}_0 \in \mathbb{R}^n$, and

$$T > \frac{2(s_1 + 1)}{c_{\min}} R(\mathbf{x}_0),$$

where $c_{\min}$ *and* s_1 *are defined in* (4.59) *and* (4.60) *respectively, and*

$$R(\mathbf{x}_0) = \sup_{\mathbf{x}\in\bar{\Omega}} |\mathbf{x} - \mathbf{x}_0|,$$

then the following estimate holds

$$d_H(\mathbf{S}^1, \mathbf{S}^2) \leq 2 \max_{k=1,2} \left[\frac{C(c_s, \Omega, T)}{c_0 \delta^{N_{3-k}-1}} d^{N_1+N_2-1} \left\| h^2 - h^1 \right\|_{H^{-1}((0,T),L^2(\Gamma_0))} + O(\epsilon) \right]^{\frac{1}{N_k}},$$

where $C(c_s, \Omega, T)$ is a positive constant to be determined.

The proof of Theorem 4.19 is based on the following lemma

Lemma 4.4. *Let* $P^{r,k} = (P_j^{r,k})_{1\leq j\leq N_k}, r = a, b$ *be respectively the corresponding projections on the* xy *and* yz*- planes of* $\mathbf{S}^k$*. Under the assumptions of Theorem 4.19, we have, for* $r = a, b$ *and* $k = 1, 2$

$$d_H(P_1^r, P_2^r) \leq \max_{k=1,2} \left[\frac{C(c_s, \Gamma, T)}{c_0 \delta^{N_{3-k}-1}} d^{N_1+N_2-1} \left\| h^2 - h^1 \right\|_{H^{-1}((0,T),L^2(\Gamma_0))} + O(\epsilon) \right]^{\frac{1}{N_k}}. \tag{4.63}$$

Proof.
First, we prove the inequality for $r = a$. For this purpose, we consider for $1 \leq \ell \leq N_2$ the following functions

$$\Phi_\ell(x, y) = \prod_{m=1}^{N_1} \left(x + iy - P_{m,1}^a \right) \prod_{m\neq\ell}^{N_2} \left(x + iy - P_{m,2}^a \right)$$

and

$$\Psi_\ell(\mathbf{x}, t) = (t - T)\Phi_\ell(x, y),$$

Then, Ψ_ℓ is a solution of (4.61), with $\Psi_\ell(., T) = 0$. Thus, substituting Ψ_ℓ in (4.62), we get

$$\mathcal{R}(h^2, \Psi_\ell) = \sum_{j=1}^{N_2} \int_{w_j^2} \frac{1}{c_s^2(\mathbf{x})} \lambda_j^2(\mathbf{x}) \prod_{m=1}^{N_1} \left(x + iy - P_m^{a,1} \right) \prod_{m\neq\ell}^{N_2} \left(x + iy - P_m^{a,2} \right) d\mathbf{x} + O(\epsilon^\kappa).$$

Applying the change of variable $w_j^2 = \mathbf{S}_j^2 + \epsilon B_j^2$ we obtain

$$\begin{aligned} \mathcal{R}(h^2, \Psi_\ell) =& \epsilon^3 \sum_{j=1}^{N_2} \int_{B_j^2} \frac{1}{c_s^2(\mathbf{S}_j^2 + \epsilon\boldsymbol{\tau})} \lambda_j^2(\mathbf{S}_j^2 + \epsilon\boldsymbol{\tau}) \prod_{m=1}^{N_1} \left(P_j^{a,2} - P_m^{a,1} + \epsilon(\tau_1 + i\tau_2) \right) \\ & \times \prod_{m\neq\ell}^{N_2} \left(P_j^{a,2} - P_m^{a,2} + \epsilon(\tau_1 + i\tau_2) \right) d\boldsymbol{\tau} + O(\epsilon^\kappa). \end{aligned}$$

Since $\kappa > 4$ we have

$$\mathcal{R}(h^2, \Psi_\ell) = \epsilon^3 \sum_{j=1}^{N_2} \int_{B_j^2} \frac{1}{c_s^2(\mathbf{S}_j^2 + \epsilon\boldsymbol{\tau})} \lambda_j^2(\mathbf{S}_j^2 + \epsilon\boldsymbol{\tau}) \prod_{m=1}^{N_1} \left(P_j^{a,2} - P_m^{a,1}\right) \prod_{m\neq\ell}^{N_2} \left(P_j^{a,2} - P_m^{a,2}\right) d\boldsymbol{\tau}$$
$$+ O(\epsilon^4) = \prod_{m=1}^{N_1} \left(P_\ell^{a,2} - P_m^{a,1}\right) \prod_{m\neq\ell}^{N_2} \left(P_\ell^{a,2} - P_m^{a,2}\right) \nu_{\ell,2}^{0,a} + O(\epsilon^4).$$

Similarly, one has

$$\mathcal{R}(h^1, \Psi_\ell) = \sum_{j=1}^{N_1} \epsilon^3 \int_{B_j^1} \frac{1}{c_s^2(\mathbf{S}_j^1 + \epsilon\boldsymbol{\tau})} \lambda_j^1(\mathbf{S}_j^1 + \epsilon\boldsymbol{\tau}) \prod_{m=1}^{N_1} \left(P_j^{a,1} - P_m^{a,1}\right) \prod_{m\neq\ell}^{N_2} \left(P_j^{a,1} - P_m^{a,2}\right) d\boldsymbol{\tau}$$
$$+ O(\epsilon^4) = O(\epsilon^4).$$

Subtracting the two previous sums, we get

$$\mathcal{R}(h^2 - h^1, \Psi_\ell) = \prod_{m=1}^{N_1} \left(P_\ell^{a,2} - P_m^{a,1}\right) \prod_{m\neq\ell}^{N_2} \left(P_\ell^{a,2} - P_m^{a,2}\right) \nu_{\ell,2}^{0,a} + O(\epsilon^4).$$

Therefore

$$\begin{aligned} &\prod_{m=1}^{N_1} \left(P_\ell^{a,2} - P_m^{a,1}\right) \prod_{m\neq\ell}^{N_2} \left(P_\ell^{a,2} - P_m^{a,2}\right) \nu_{\ell,2}^{0,a} \\ &= \int_\Omega \frac{1}{c_s^2(\mathbf{x})} (p^2(x,T) - p^1(\mathbf{x},T)) \Phi_\ell(x,y) d\mathbf{x} - \int_0^T \int_\Gamma (h^2 - h^1) \Psi_\ell \, d\xi dt + O(\epsilon^4). \end{aligned} \tag{4.64}$$

Moreover, using Holder inequality and regularity of the solution of the wave equation, we get

$$\begin{aligned} &\left| \int_\Omega \frac{1}{c_s^2(\mathbf{x})} (p^2(\mathbf{x},T) - p^1(\mathbf{x},T)) \Phi_\ell(x,y) d\mathbf{x} - \int_0^T \int_\Gamma (h^2 - h^1) \Psi_\ell \, d\xi dt + O(\epsilon^4) \right| \\ &\leq \frac{1}{c_{\min}^2} |p^2(.,T) - p^1(.,T)|_{L^2(\Omega)} |\Phi_\ell|_{L^2(\Omega)} + \|h^2 - h^1\|_{H^{-1}((0,T),L^2(\Gamma))} \|\Psi_\ell\|_{H_0^1((0,T),L^2(\Gamma))} \\ &\quad + O(\epsilon^4). \end{aligned} \tag{4.65}$$

On the other hand, one an easily check that

$$|\Phi_\ell|_{L^2(\Omega)} \leq \sqrt{|\Omega|} d^{N_1+N_2-1}.$$

Also,

$$\|\Psi_\ell\|_{H_0^1((0,T),L^2(\Gamma))} = \left(|\Psi_\ell|^2_{L^2(\Sigma_T)} + \left| \frac{\partial \Psi_\ell}{\partial t} \right|^2_{L^2(\Sigma_T)} \right)^{\frac{1}{2}},$$

and

$$|\Psi_\ell|^2_{L^2(\Sigma_T)} \leq \frac{T^3}{3}|\Gamma| d^{2(N_1+N_2-1)},$$

$$\left|\frac{\partial \Psi_\ell}{\partial t}\right|^2_{L^2(\Sigma)} \leq T|\Gamma| d^{2(N_1+N_2-1)}.$$

Therefore

$$\|\Psi_\ell\|_{H_0^1((0,T),L^2(\Gamma))} \leq \left(\frac{T^2}{3}+1\right)^{\frac{1}{2}} \sqrt{T|\Gamma|} d^{N_1+N_2-1}. \tag{4.66}$$

Moreover, using the regularity of wave equation (4.57), and as explained in Lemma 2.4 in Chapter 2, we have

$$\|h^2 - h^1\|_{H^{-1}((0,T),L^2(\Gamma))} \leq c|p_0^2 - p_0^1|_{L^2(\Omega)}.$$

Furthermore, using the stability of the exact controllability problem given Theorem 2.10 and Lemma 2.4 in Chapter 2, one can see, as in section 2.2, that

$$|p_0^2 - p_0^1|_{L^2(\Omega)} \leq c\|h^2 - h^1\|_{H^{-1}((0,T),L^2(\Gamma_0))}. \tag{4.67}$$

Therefore, we deduce that

$$\|h^2 - h^1\|_{H^{-1}((0,T),L^2(\Gamma))} \leq c_1\|h^2 - h^1\|_{H^{-1}((0,T),L^2(\Gamma_0))}, \tag{4.68}$$

for some $c_1 > 0$. Similarly, from the regularity of the wave equation (4.57) we have

$$|p^2(.,T) - p^1(.,T)|_{L^2(\Omega)} \leq c|p_0^2 - p_0^1|_{L^2(\Omega)},$$

for some $c > 0$. Moreover, using (4.67) one gets

$$|p^2(.,T) - p^1(.,T)|_{L^2(\Omega)} \leq c_2\|h^2 - h^1\|_{H^{-1}((0,T),L^2(\Gamma_0))} \tag{4.69}$$

Now we return back to our estimation where we deduce from equations (4.64) and (4.65) and from the estimates (4.66), (4.68) and (4.69) that

$$\nu_{\ell,2}^{0,a} \prod_{m=1}^{N_1}\left(P_\ell^{a,2} - P_m^{a,1}\right) \prod_{m\neq\ell}^{N_2}\left(P_\ell^{a,2} - P_m^{a,2}\right) \leq C(c_s,\Omega,T) d^{N_1+N_2-1}\|h^2 - h^1\|_{H^{-1}((0,T),L^2(\Gamma_0))} + O(\epsilon^4),$$

where

$$C(c_s,\Omega,T) = \frac{c_2\sqrt{|\Omega|}}{c_{\min}^2} + c_1\left(\frac{T^2}{3}+1\right)^{\frac{1}{2}}\sqrt{T|\Gamma|}.$$

Therefore,

$$c_0 \min_{1\le m\le N_1} \|P^a_{\ell,2} - P^a_{m,1}\|^{N_1} \le \frac{C(c_s,\Omega,T)}{\delta^{N_2-1}} d^{N_1+N_2-1} \|h^2 - h^1\|_{H^{-1}((0,T),L^2(\Gamma_0))} + O(\epsilon^4).$$

Thus, noting that $c_0 = O(\epsilon^3)$ we get

$$\max_{1\le \ell\le N_2} \min_{1\le m\le N_1} \|P^a_{\ell,2} - P^a_{m,1}\| \le \left[\frac{C(c_s,\Omega,T)}{c_0\delta^{N_2-1}} d^{N_1+N_2-1} \|h^2 - h^1\|_{H^{-1}((0,T),L^2(\Gamma_0))} + O(\epsilon)\right]^{\frac{1}{N_1}}. \tag{4.70}$$

Similarly, by considering, first

$$\widetilde{\Phi}_\ell(x,y) = \prod_{m\neq\ell}^{N_1} \left(x + iy - P^{a,1}_m\right) \prod_{m=1}^{N_2} \left(x + iy - P^a_{m,2}\right)$$

and then,

$$\widetilde{\Psi}_\ell(\mathbf{x},t) = (t-T)\widetilde{\Phi}_\ell(x,y),$$

we get

$$\max_{1\le \ell\le N_1} \min_{1\le m\le N_2} \left\|P^a_{\ell,1} - P^a_{m,2}\right\| \le \left[\frac{C(c_s,\Omega,T)}{c_0\delta^{N_1-1}} d^{N_1+N_2-1} \|h^2 - h^1\|_{H^{-1}((0,T),L^2(\Gamma_0))} + O(\epsilon)\right]^{\frac{1}{N_2}}. \tag{4.71}$$

Taking the maximum between (4.70) and (4.71), we get (4.63) for $r = a$. To prove the result for $r = b$, we consider the following functions

$$\Psi_\ell(\mathbf{x},t) = (t-T)\Phi_\ell(y,z), \quad \widetilde{\Psi}_\ell(\mathbf{x},t) = (t-T)\widetilde{\Phi}_\ell(y,z).$$

Then, following the same previous steps one can obtain the desired result. ■

Proof of Theorem 4.19

The proof is similar to that of Theorem 4.16. ■

4 Conclusion

This chapter investigates the inverse PAT problem, in which we consider the problem of reconstruction of small absorbers in the wave equations (4.1) and (4.57) from the boundary measurements. Unlike prior methods, our method doesn't follow the quantitative photo-acoustic tomography approach. However, in our work we give a direct reconstruction process based on the algebraic algorithm proposed in [35]. In fact, our method allows us directly from the wave equation, and using only one Cauchy data on part of the boundary ($\Gamma_0 \subset \Gamma$) and the exact controllability problem for wave equation explained in Chapter 2, to reconstruct, modulo ϵ^{K+4},

the number of absorbers N, their centers $\mathbf{S}_j$, and some information about the absorption coefficient in both cases of constant and variable sound speed. In addition to that, we reconstruct the absorbed electromagnetic energy by each absorber in case of constant sound speed. The observation boundary Γ_0 is chosen to satisfy certain geometric conditions so that the controllability results are valid. Moreover, our algorithm doesn't require the knowledge of the *Grüneisen* coefficient $\beta(\mathbf{x})$, which is supposed throughout this chapter to be variable and unknown. Finally we end up with the corresponding stability results.

Part II

Radial solutions for semilinear elliptic equations

5

Radial and asymptotically constant solutions for nonautonomous elliptic equations

Pure mathematics is, in its way, the poetry of logical ideas.

– Albert Einstein

The second part of this thesis is dedicated to the study of semi-linear elliptic equations. In this chapter we study the existence of radial solutions of the equation $\Delta u + g(|x|, u) = 0$ on $\mathbb{R}^N$, with a prescribed limit $u(\infty) = z$ satisfying $g(r, z) = 0,\ \forall r \in \mathbb{R}^+$. The existence of such solutions was studied in [49] with equations of the form $\Delta u + g(u) = 0$ in $\mathbb{R}^N$. In this chapter we give a generalization of their result to nonautonomous equations.

This chapter is organized as follows:

- **Section 1** introduces the problem and states the main result of this chapter.
- **Section 2** is intended to the proof of the main theorem.

1 Introduction

Let $N \geq 2$. We discuss the existence of radial solutions u of the problem

$$\Delta u + g(|x|, u) = 0 \quad \text{in} \quad \mathbb{R}^N, \tag{5.1}$$

with a prescribed limit $z = u(\infty) > 0$ satisfying $g(r, z) = 0, \forall r \in \mathbb{R}^+$. Radial solutions of (5.1) have been studied in connection with many questions of mathematical physics like the existence of solitary waves and the nonlinear field equations [16, 17, 79]. The idea of having symmetric solutions for semilinear elliptic equations on general symmetric domains is now well understood by the moving plane method (see Section 2.3 in Chapter 1 and [18, 40]). If, for example, we consider a ball $B = B_R(0)$, a suitable nonlinearity f and a sufficiently regular positive solution

u of

$$\begin{cases} \Delta u + f(|x|, u) = 0 & \text{in} \quad B, \\ u = 0 & \text{on} \quad \partial B \end{cases} \tag{5.2}$$

then u is radially symmetric $u = u(r = |x|)$ and $u'(r) \leq 0$. The proof of this result has the maximum principle for elliptic equations as its principal ingredient. When the radius $R \to \infty$, it then becomes natural to ask about the existence of radially symmetric solutions of (5.1) that vanish at infinity. This question attracted a lot of attention (see [16, 17, 19, 28, 49, 68, 74] and the references therein) where variational and topological methods have been used in order to establish the existence of positive radial solutions of (5.1) with $u(\infty) = 0$. However, and up to our knowledge, none of the aforementioned works investigates the case with a prescribed limit different from 0.

The aim of this chapter is to provide an ODE-based proof for the existence of positive radial solutions of (5.1) with a prescribed nonzero limiting behavior related to the nonlinearity g. This approach combines a type of a shooting argument together with the resolution of (5.2) with a particular f, and for sufficiently large $R > 0$. The radial solution $u = u(r)$ of (5.1) satisfies:

$$\begin{cases} -u'' - \dfrac{N-1}{r} u' = g(r, u) \quad \text{for} \quad 0 < r < \infty \\ u(0) = \xi, \quad u'(0) = 0, \end{cases} \tag{5.3}$$

where ξ has to be determined so that

$$\lim_{r \to \infty} u(r) = z, \tag{5.4}$$

with $z > 0$ that we will make precise hereafter.

A similar problem on autonomous systems was considered by the authors in [49], on which they study the existence of non-vanishing solutions of the equation

$$\Delta u + g(u) = 0 \quad \text{in } R^N,$$

satisfying

$$\lim_{r \to \infty} u(r) = z.$$

In this chapter we revisit the work of [49] with $g = g(r, u)$. The dependence of g on r forces us to take some conditions on the function g and its behavior at $r = \infty$. Let us describe our conditions on g. We assume that $g : \mathbb{R}^+ \times \mathbb{R}^+ \longrightarrow \mathbb{R}$ is locally Lipschitz for the second variable and increasing in the first variable, and suppose

$$\lim_{r \to \infty} g(r, s) = g_\infty(s) \text{ exists } \forall s \in [0, \infty) \tag{5.5}$$

and $g(r,0) = g(r,z) = 0, \forall r \in \mathbb{R}^+$ and for some $z > 0$. We also assume, for all $r \geq 0$, the following:

$$\text{There exists } \alpha_r \in]0,z[\text{ such that } g(r,s) < 0 \text{ for } 0 < s < \alpha_r \text{ and } g(r,s) > 0 \text{ for } \alpha_r < s < z. \tag{5.6}$$

$$\text{There exists } \alpha_\infty \in]0,z[\text{ such that } g_\infty(s) < 0 \text{ for } 0 < s < \alpha_\infty \text{ and } g_\infty(s) > 0 \text{ for } \alpha_\infty < s < z. \tag{5.7}$$

$$\text{There exists } \eta_r > 0 \text{ such that } G(r,\eta_r) > G(r,z), \text{ where } G(r,t) = \int_0^t g(r,s)ds. \tag{5.8}$$

$$\text{There exists } \eta_\infty > 0 \text{ such that } G_\infty(\eta_\infty) > G_\infty(z), \text{ where } G_\infty(t) = \int_0^t g_\infty(s)ds. \tag{5.9}$$

Having (5.8) and (5.9), we define for each $r \geq 0$

$$\xi_r = \sup\{\eta_r > 0;\, G(r,\eta_r) > G(r,z)\}, \tag{5.10}$$

and

$$\xi_\infty = \sup\{\eta_\infty > 0;\, G_\infty(\eta_\infty) > G_\infty(z)\}, \tag{5.11}$$

then, in view of (5.6)–(5.11), the sequence ξ_r and ξ_∞ exist in $\mathbb{R}$ satisfying $\xi_r < \alpha_r$ and $\xi_\infty < \alpha_\infty$. Moreover the sequences $(\alpha_r)_r$ and $(\xi_r)_r$ are decreasing to $\alpha_\infty > 0$ and $\xi_\infty > 0$ as $r \to \infty$ respectively, and for every $r \geq 0$, we have

$$G(r,z) \geq G(r,\xi) \quad \text{for every} \quad \xi \in [\xi_r, \alpha_r[, \tag{5.12}$$

and

$$G_\infty(z) \geq G_\infty(\xi) \quad \text{for every} \quad \xi \in [\xi_\infty, \alpha_\infty[. \tag{5.13}$$

We finally assume

$$\liminf_{s \nearrow \alpha_\infty} \frac{g_\infty(s)}{s - \alpha_\infty} > 0. \tag{5.14}$$

We prove the following existence result.

Theorem 5.20. *Let g be a function defined on $\mathbb{R}^+ \times \mathbb{R}^+ = [0,\infty[\times[0,\infty[$, locally Lipschitz for the second variable and increasing for the first variable, satisfying (5.5), such that $g(r,0) = g(r,z) = 0,\ \forall r \geq 0$ where $z > 0$ satisfying the conditions (5.6)–(5.14), see figure 5.1. Then there exists $\xi \in]0,\xi_0[$ and a solution $u \in C^2(\mathbb{R}_+)$ of (5.3) and (5.4), with $u(r) < z$ for $r \in [0,\infty[$ and $u'(r) > 0$ for $r \in]0,\infty[$.*

Example 5.1. *The assumptions of Theorem 5.20 are satisfied for $g(r,s) = s(s-z)(\alpha_r - s)$, where*

$$\alpha_r = \frac{z}{2}\left(1 + \frac{1}{r+2}\right).$$

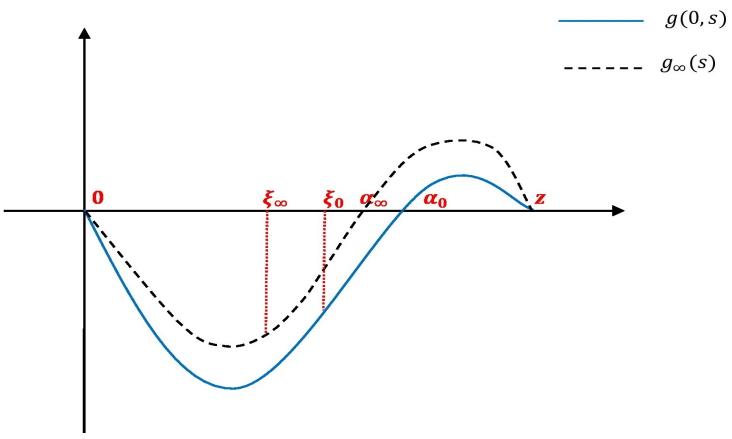

Figure 5.1: *Sketch of the nonlinearity g*

Then, $\alpha_r \searrow \alpha_\infty = \frac{z}{2}$, and $\lim_{r\longrightarrow\infty} g(r,s) = g_\infty(s) = s(s-z)(\alpha_\infty - s)$.

Remark 5.1. *The short time existence of (5.3) follows from a classical fixed point argument associated to the integral equation. In fact, multiplying the first equation in (5.3) by r^{N-1} and integrating it we obtain*

$$\begin{aligned} &-(r^{N-1}u')' = g(r,u)r^{N-1} \\ &-r^{N-1}u'(r) = \int_0^r g(s,u(s))s^{N-1}ds \quad since \quad u'(0) = 0, \\ &u'(r) = -\frac{1}{r^{N-1}}\int_0^r g(s,u(s))s^{N-1}ds, \\ &u(r) - \xi = -\int_0^r \frac{1}{s^{N-1}}\int_0^s g(\sigma,u(\sigma))\sigma^{N-1}d\sigma ds, \end{aligned} \tag{5.15}$$

where we extend g to $\tilde{g}$ on $\mathbb{R}^+\times\mathbb{R}$ by setting $g(r,s) = 0$ if $s < 0$. Indeed, since we are interested in solutions $0 < u < z$, and since $g(r,z) = 0$, we will furthermore adjust the extended g and replace it with

$$\tilde{g} = \begin{cases} g & on \quad]0,z[, \\ 0 & elsewhere. \end{cases}$$

However, in all what follows and for the sake of clarity, we always keep the notation g for our nonlinearity.

Remark 5.2. *For $r > 0$, the equation (5.15) is no longer singular, so that the solution u can be extended, by the usual method, to be defined on a maximal interval $[0, r_\xi[$ upon which it satisfies the blow up alternative. In our work, we prove that $r_\xi = \infty$ for all $\xi \in]0,\alpha_0[, \forall r \geq 0$.*

Let us finally mention that a similar problem of existence of solutions, with a prescribed limit, for semilinear elliptic problems over a quarter-plane has been treated in [50,51]. In those papers, the

solution is not necessarily radial and the existence is based on Perron's method after constructing suitable sub- and super-solutions.

2 Proof of Theorem 5.20

The proof will follow from several Lemmas. As a first step we observe that for small values of r, namely on a maximal interval $[0, r_\xi[$, the existence of a solution of (5.3) is ensured by classical arguments (see Remarks 5.1 and 5.2). The first lemma shows the existence of $u(r)$ for all $r \geq 0$, whenever $u(0) = \xi \in]0, \alpha_0[$, i.e. $r_\xi = \infty$ for any $\xi \in]0, \alpha_0[$. We begin first by defining the function

$$f(r, s) = -g(r, z - s).$$

Since g is increasing in r then f is decreasing in r. Now, we define the function

$$F(r, t) = \int_0^t f(r, s)ds = -\int_0^t g(r, z - s)ds,$$

then F is also decreasing in r, and $F'_t(r, t) = -g(r, z - t)$ which means

$$F'_u(r, z - u) = -g(r, u). \tag{5.16}$$

Substituting (5.16) in (5.3) we obtain

$$-u'' - \frac{N-1}{r}u' = -F'_u(r, z - u). \tag{5.17}$$

Multiplying (5.17) by u' we obtain:

$$-\frac{1}{2}((u')^2)' - \frac{N-1}{r}(u')^2 = -F'_u(r, z - u)u'.$$

Moreover,

$$(F(r, z - u(r)))' = F'_r(r, z - u(r)) + F'_u(r, z - u(r))(-u'(r)),$$

hence

$$-\frac{1}{2}\left(u'(r)^2\right)' - \frac{N-1}{r}(u'(r))^2 = (F(r, z - u(r))' - F'_r(r, z - u(r)). \tag{5.18}$$

Integrating (5.18) between 0 and r, we obtain the following fundamental equality:

$$F(r, z - u(r)) + \frac{1}{2}(u'(r))^2 + (N-1)\int_0^r \frac{(u'(s))^2}{s}ds - \int_0^r F'_r(s, z - u(s))ds = F(0, z - \xi), \tag{5.19}$$

which is satisfied as long as u exists. We have

Lemma 5.1. *(Existence on $\mathbb{R}$)*

If $\xi \in]0, \alpha_0[$ *then* (5.3) *admits a unique solution* $u \in C^2(\mathbb{R}^+)$.

Proof. Let $\xi \in]0, \alpha_0[$. First of all, it is worth mentioning that, as $g(0, \xi) < 0$ (see (5.6)), the solution u will be increasing in a small neighborhood of 0, thus $u(r) > u(0) = \xi$ there. This is a consequence of the equation $u''(0) + g(0, \xi) = 0$ that results from (5.3) computed at $r = 0$. Since u satisfies the blow up alternative, we need to show that u and u' are bounded for r bounded. However, thanks to (5.19) and the Lipschitz property of g, it will be enough only to show that u remains bounded. We claim that

$$u \text{ is bounded from below for all } r \geq 0.$$

Indeed, if this is not true,

$$r_1 = \inf\{r \geq 0;\ u'(r) = 0, \text{ and } u''(r) < 0\},$$

then $0 < r_1 < r_\xi$ and

$$0 < g(r_1, u(r_1)) = -u''(r_1). \tag{5.20}$$

Now, for all $r > r_1$ integrating (5.18) between r_1 and r we obtain

$$F(r, z-u(r)) + \frac{1}{2}(u'(r))^2 + (N-1)\int_{r_1}^{r} \frac{(u'(s))^2}{s} ds - \int_{r_1}^{r} F'_r(s, z-u(s)) ds = F(r_1, z-u(r_1)). \tag{5.21}$$

Using the positivity of the terms in the left hand side of (5.21) we obtain

$$F(r, z - u(r)) \leq F(r_1, z - u(r_1)) = \int_z^{u(r_1)} g(r_1, t) dt,$$

thanks to (5.20) we have $\alpha_{r_1} < u(r_1) < z$ and

$$F(r, z - u(r)) \leq \int_z^{u(r_1)} g(r_1, t) dt < 0, \quad \forall r > r_1. \tag{5.22}$$

On the other hand, since u is not bounded from below then there exists $r_2 > r_1 > 0$ such that $u(r_2) > 0$ and $u(r_2)$ is very small and thanks to (5.8)

$$\int_z^{u(r_2)} g(r_2, t) dt > 0,$$

and this leads to a contradiction with (5.22).

We now show that u remains bounded from above by examining the values of $u \geq z$. In fact, if for some $r_0 > 0$, $u(r_0) = z$ and $u'(r_0) > 0$, then, because $g(r, s) = 0$ if $s \geq z$ (see Remark 5.1),

we have

$$u''(r) + \frac{N-1}{r}u'(r) = 0 \quad \text{for} \quad r \geq r_0,$$

then

$$u'(r) = u'(r_0)\left(\frac{r_0}{r}\right)^{N-1} \leq u'(r_0) =: \beta > 0,$$

thus

$$u(r) \leq z + \beta(r - r_0),$$

hence $u(r)$ remains bounded from above for r bounded. ■

Remark 5.3. *For $\xi \in]0, \alpha_0[$, we occasionally denote the solution of (5.3) by $u = u(r, \xi)$ if we want to show the dependence on the initial data. In this case u' denotes $u'_r(r, \xi)$.*

Let us observe that for $\xi \in]0, \alpha_0[$, $g(0, \xi) < 0$ and hence $u''(0, \xi) = -g(0, \xi) > 0$. This implies that

$$u'(r, \xi) > 0 \quad \text{and} \quad u(r, \xi) < z \quad \text{for small } r > 0. \tag{5.23}$$

Now let

$$S^+ = \{\xi \in]0, \alpha_0[;\ u(r_0, \xi) = z \ \text{ for some } \ r_0 = r_0(\xi) > 0\},$$

$$S^- = \{\xi \in]0, \alpha_0[;\ u'(r_0, \xi) = 0 \ \text{ for some } \ r_0 = r_0(\xi) > 0 \ \text{ and } \ u(r, \xi) < z \ \text{ for all } \ r \geq 0\},$$

$$S^z = \{\xi \in]0, \alpha_0[;\ u'(r, \xi) > 0 \ \text{ for all } \ r > 0 \ \text{ and } \ u(r, \xi) < z \ \text{ for all } \ r \geq 0\}.$$

Owing to (5.23), we can easily see that the sets S^+, S^- and S^z are mutually disjoint and cover the interval $]0, \alpha_0[$. The idea of the proof of the main theorem then goes as follows: we first show that if $\xi \in S^z$ then $u = u(r, \xi)$ is the required solution of Theorem 5.20, and next we indirectly prove that $S^z \neq \emptyset$.

Lemma 5.2. *($\xi \in S^z \implies \lim_{r\to\infty} u(r, \xi) = z$)*
Let $\xi \in S^z$. Then the number $l = \lim_{r\to\infty} u(r, \xi)$ satisfies $g_\infty(l) = 0$, i.e. $l = \alpha_\infty$ or $l = z$. Moreover, if g_∞ satisfies (5.14), then $l = z$.

Proof. Let $\xi \in S^z$. The solution $u(r) = u(r, \xi)$, being increasing and bounded from above by z, satisfies $u(r) \nearrow l \in]\xi, z]$ as $r \to \infty$. The boundedness of u and the regularity of F imply, thanks to (5.19), that $\int_0^r \frac{(u'(s))^2}{s} ds$ and $\int_0^r F'_r(s, z - u(s)) ds$ are bounded for $r \geq 0$, hence

$$\int_0^\infty \frac{(u'(s))^2}{s} ds < \infty \quad \text{and} \quad \int_0^\infty F'_r(s, z - u(s)) ds < \infty,$$

and by the Lebesgue dominated convergence theorem we obtain $\lim_{r\to\infty} F(r, z - u(r))$ exists. Indeed

$$F(r, z - u(r)) = -\int_{u(r)}^z g(r, t) dt = -\int_{\mathbb{R}} \mathbb{1}_{[u(r), z]}(t) g(r, t) dt,$$

where $L(r,t) = \mathbb{1}_{[u(r),z]}(t)g(r,t) \to \mathbb{1}_{[l,z]}(t)g_\infty(t)$ as $r \to \infty$ and

$$|L(r,t)| \leq |g(r,t)| \leq \max\{\|g(0,t)\|_\infty, \|g_\infty(t)\|_\infty\}.$$

Therefore,

$$\lim_{r\to\infty} F(r, z-u(r)) = -\int_{\mathbb{R}} \mathbb{1}_{[l,z]}(t)g_\infty(t)dt. \tag{5.24}$$

Then, passing to the limit $r \to \infty$ in (5.19) shows $u'(r)$ converges as $r \to \infty$ and the limit should be

$$\lim_{r\to\infty} u'(r) = 0$$

since u is bounded. We claim now that $\lim_{r\to\infty} g(r, u(r))$ exists. In fact,

$$\lim_{r\to\infty} g(r, u(r)) = g_\infty(l). \tag{5.25}$$

This result is a consequence of the Lipschitz condition on g and (5.5). We may now pass to the limit $r \to \infty$ in (5.3) in order to obtain, using the boundedness of u' and (5.25),

$$\lim_{r\to\infty} u''(r) = 0,$$

hence

$$\lim_{r\to\infty} g(r, u(r)) = g_\infty(l) = 0,$$

and therefore

$$l = \alpha_\infty \quad \text{or} \quad l = z.$$

We now assume g_∞ satisfies (5.14) and we claim that $l \neq \alpha_\infty$.

To understand the idea of the proof, we show the result for sufficiently regular g and u, and for (5.14) replaced by $g'_\infty(\alpha_\infty) > 0$. Differentiating (5.3) with respect to r, we get

$$-u''' - \frac{N-1}{r}u'' + \frac{N-1}{r^2}u' = g'_r(r,u) + g'_u(r,u)u'.$$

Multiplying by $r^{\frac{N-1}{2}}$ and noting that

$$\left(r^{\frac{N-1}{2}}u'\right)'' = r^{\frac{N-1}{2}}u''' + r^{\frac{N-1}{2}}\left(\frac{N-1}{r}\right)u'' + r^{\frac{N-1}{2}}\left(\frac{(N-1)(N-3)}{4r^2}\right)u'$$

we obtain

$$-\left(r^{\frac{N-1}{2}}u'\right)'' = r^{\frac{N-1}{2}}\left(g'_u(r,u) - \left(\frac{N-1}{r^2} + \frac{(N-1)(N-3)}{4r^2}\right)\right)u' + r^{\frac{N-1}{2}}g'_r(r,u). \tag{5.26}$$

Let

$$v = r^{\frac{N-1}{2}} u'$$

since $r^{\frac{N-1}{2}} g'_r(r,u) \geq 0$, then (5.26) becomes

$$-v'' \geq \left(g'_u(r,u) - \frac{(N-1)(N+1)}{4r^2} \right) v, \tag{5.27}$$

with $v > 0$ on $]0,\infty[$. We now assume by contradiction that $u(r) \nearrow \alpha_\infty$ as $r \to \infty$. Then $g'(r,u(r)) \to g'_\infty(\alpha_\infty) > 0$ as $r \to \infty$. On the other hand, we have $\dfrac{(N-1)(N+1)}{4r^2} \to 0$ as $r \to \infty$. These arguments ensure the existence of $R_1 > 0$ and $\omega_1 > 0$ such that

$$g'_u(r,u(r)) - \frac{(N-1)(N+1)}{4r^2} \geq \omega_1 \quad \text{for} \quad r \geq R_1,$$

therefore, by (5.27), we finally get

$$-v''(r) \geq \omega_1 v(r) \quad \text{for} \quad r \geq R_1. \tag{5.28}$$

Thus $v'' < 0$ for $r \geq R_1$, which implies that $v'(r) \searrow L \in [-\infty,\infty[$ as $r \to \infty$. If $L < 0$ then $v(r) \to -\infty$ as $r \to \infty$ and this is impossible by the positivity of v. If $L \geq 0$ then $v' > 0$ and v increases on $[R_1,\infty[$, thus $v(r) \geq v(R_1) > 0$ for $r \geq R_1$. Again by (5.28) we get $v''(r) \leq -\omega_1 v(R_1) < 0$ and consequently $v'(r) \to -\infty$ as $r \to \infty$ and this is also impossible by the positivity of v'. This contradiction shows that $l \neq \alpha_\infty$ as required.

We turn back to the general case where u is only C^2 and g is a locally Lipschitz function with respect to the second variable and increasing for the first variable satisfying (5.14). Arguing in a similar manner, we assume $u(r) \nearrow \alpha_\infty$ as $r \to \infty$ and we set

$$v(r) = r^{\frac{N-1}{2}} (\alpha_\infty - u(r)),$$

then $v > 0$ on $[0,\infty[$. By differentiating the above equation twice in r, and using (5.3), we end up with an equation, similar to (5.27), that reads

$$-v'' = \left(\frac{g(r,u)}{u - \alpha_\infty} - \frac{(N-1)(N-3)}{4r^2} \right) v. \tag{5.29}$$

Since $u(r) \nearrow \alpha_\infty$ as $r \to \infty$, we use condition (5.14) to deduce the existence of ε_0 and $\beta > 0$ such that

$$\frac{g_\infty(s)}{s - \alpha_\infty} > \beta, \quad \text{over} \quad [\alpha_\infty - \varepsilon_0, \alpha_\infty[,$$

and the existence of R_{ε_0}, such that $\forall R \geq R_{\varepsilon_0}$

$$u(r) \in [\alpha_\infty - \varepsilon_0, \alpha_\infty[.$$

Now, the monotonicity of g leads to

$$\frac{g(r,u(r))}{u(r)-\alpha_\infty} \geq \frac{g_\infty(u(r))}{u(r)-\alpha_\infty} > \beta > 0, \quad \text{for} \quad u(r) \in [\alpha_\infty - \varepsilon_0, \alpha_\infty[. \tag{5.30}$$

The fact that $\dfrac{(N-1)(N-3)}{4r^2} \to 0$ as $r \to \infty$ together with (5.30) give the existence of $R_2 > 0$ and $\omega_2 > 0$ such that

$$\frac{g(r,u)}{u-\alpha_\infty} - \frac{(N-1)(N-3)}{4r^2} \geq \omega_2 \quad \text{for} \quad r \geq R_2.$$

From (5.29) we are lead to

$$-v''(r) \geq \omega_2 v(r) \quad \text{for} \quad r \geq R_2.$$

Arguing in a similar manner as above, we reach our contradiction and therefore $l \neq \alpha_\infty$. ■

Lemma 5.2 indicates that it is sufficient to show $S^z \neq \emptyset$ in order to terminate the proof of Theorem 5.20. Having

$$]0,\alpha_0[= S^+ \cup S^- \cup S^z \tag{5.31}$$

with S^+, S^- and S^z mutually disjoint, we can easily see (using the connectedness of $]0,\alpha_0[$) that $S^z \neq \emptyset$ if $S^\pm$ are both nonempty open subsets of $]0,\alpha_0[$. This will be the goal of the following lemmas.

Lemma 5.3. *(S^- is nonempty)*
Let ξ_0 be given by (5.10). Then $[\xi_0,\alpha_0[\subset S^-$.

Proof. Let $\xi \in [\xi_0,\alpha_0[\subset]0,\alpha_0[= S^+ \cup S^- \cup S^z$. Assume to the contrary that $\xi \notin S^-$, then $\xi \in S^+ \cup S^z$.

If $\xi \in S^+$ then there exists $r_0 > 0$ such that $u(r_0) = z$. Using (5.19) for $r = r_0$, we get

$$F(r_0,0) + \frac{1}{2}(u'(r_0))^2 + (N-1)\int_0^{r_0} \frac{(u'(s))^2}{s} ds - \int_0^{r_0} F'_r(s, z-u(s)) ds = F(0, z-\xi).$$

Note that $u'(r_0) \neq 0$ since otherwise $u = z$ on $[0,\infty[$ by the uniqueness of the solution of the ODE (5.3), which is impossible. This simple observation used in the above equation gives

$$0 = F(r_0,0) < F(0,z-\xi)$$

then

$$F(0,z-\xi) > 0. \tag{5.32}$$

On the other hand,

$$F(0,z-\xi) = -\int_\xi^z g(0,t)dt > 0,$$

then

$$\int_{\xi}^{z} g(0,t)dt < 0,$$

in contradiction with (5.12).

If $\xi \in S^z$ then, by Lemma 5.2, we have $\lim_{r\to\infty} u(r) = z$. Passing to the limit $r \to \infty$ in (5.19) we obtain

$$\lim_{r\to\infty} F(r, z-u(r)) + (N-1)\int_0^\infty \frac{(u'(s))^2}{s}ds - \int_0^\infty F'_r(s, z-u(s))ds = F(0, z-\xi),$$

where $\int_0^\infty \frac{(u'(s))^2}{s}ds - \int_0^\infty F'_r(s, z-u(s))ds > 0$ as u increases from ξ to z with $\xi < z$. Moreover, using (5.24) we deduce that

$$\lim_{r\to\infty} F(r, z-u(r)) = 0.$$

This again leads to (5.32) and hence a contradiction with (5.12). This shows that $\xi \in S^-$ as required. ■

Lemma 5.4. *(S^+ is nonempty)*
There exists a sequence $(\xi^n)_{n\geq 1} \subset S^+$ such that $\lim_{n\to\infty} \xi^n = 0$.

The proof of this lemma is based on the following existence result for semilinear elliptic equations on $B = B_R(0) \subset \mathbb{R}^N$ with Dirichlet conditions. Let $h : [0,\infty[\longrightarrow \mathbb{R}$ be a locally Lipschitz function with $h(0) = 0$ and $h(\theta) = 0$ for some $\theta > 0$. We may always identify h with its extension

$$\tilde{h} = \begin{cases} h & \text{on } \ ]0,\theta[, \\ 0 & \text{elsewhere,} \end{cases}$$

since we are interested in solutions ranging between 0 and θ. We assume the following conditions on h that are similar to (5.6) and (5.8).

$$\text{There exists } \gamma \in]0,\theta[\text{ such that } h(u) < 0 \text{ for } 0 < u < \gamma \text{ and } h(u) > 0 \text{ for } \gamma < u < \theta. \tag{5.33}$$

$$\text{There exists } \zeta > 0 \text{ such that } H(\zeta) > 0, \text{ where } H(t) = \int_0^t h(s)ds. \tag{5.34}$$

Theorem 5.21. *(Existence of semilinear elliptic equations [16, 72])*
Let $h : [0,\infty[\longrightarrow \mathbb{R}$ be a locally Lipschitz function with $h(0) = 0$ and $h(\theta) = 0$ for some $\theta > 0$. Assume also that h satisfies (5.33) and (5.34). Then, for some R large enough, there exists a positive solution u of

$$\begin{cases} \Delta u + h(u) = 0 & \text{in } \ B, \\ u = 0 & \text{on } \ \partial B \end{cases} \tag{5.35}$$

satisfying $0 \leq u \leq \theta$ and

$$\int_B H(u)dx > 0. \tag{5.36}$$

Remark 5.4. *By the moving plane method [18, 40], the solution u in Theorem 5.21 is radially symmetric whose maximum is attained at 0, i.e.* $\max_B u = u(0)$. *Moreover, if we define*

$$\zeta_* := \inf\{\zeta > 0;\ H(\zeta) > 0\},$$

then in view of (5.33) (5.34) and (5.36), $\zeta_* > 0$ exists in $\mathbb{R}$ and

$$\max_B u = u(0) > \zeta_*.$$

In fact, if $\max_B u \le \zeta_*$ then $0 \le u \le \zeta_*$, hence $H(u) \le 0$ on B which violates (5.36).

Thanks to Theorem 5.21 we have the following result.

Theorem 5.22. *Let $f : \mathbb{R}^+ \times [0, \infty[\longrightarrow \mathbb{R}$ be a locally Lipschitz function with respect to the second variable with $f(r, 0) = f(r, \theta) = 0$ for some $\theta > 0$. We also assume that f is decreasing with respect to the first variable with*

$$f_\infty(s) = \lim_{r\to\infty} f(r, s) \ge h(s)$$

for all $s \in \mathbb{R}^+$, for some function h satisfying (5.33) and (5.34). Then, for some $R > 0$ large enough, there exists a positive solution u of

$$\begin{cases} \Delta u + f(|x|, u) = 0 & \text{in} \quad B, \\ u = 0 & \text{on} \quad \partial B \end{cases} \tag{5.37}$$

satisfying $0 \le u \le \theta$ and $u(0) > \zeta_*$.

Proof. Since $f(r, s) \ge h(s)$ then the solution u_1 of (5.35) is a subsolution of (5.37) and satisfies

$$u_1(0) = \max_B u(x) > \zeta_*.$$

Note that $f(r, \theta) = 0$ and $u_1 \le \theta$ and consequentely the constant θ is a supersolution of (5.37). Therefore, by applying Perron's method, we infer the existence of radial symmetric positive solution u such that

$$u_1(x) \le u(x) \le \theta, \quad \max_B u = u(0) \ge u_1(0) > \zeta_*.$$

This terminates the proof. ■

Remark 5.5. *If g is the function given by Theorem 5.20 then the function $f(r, s) := -g(r, z - s)$ satisfies the assumptions of Theorem 5.22 with $\theta = z$ and $h(s) := \lim_{r\to\infty} f(r, s)$.*

We are now ready to prove Lemma 5.4.

Proof of Lemma 5.4. Throughout the proof, h may represent several functions satisfying (5.33) and (5.34). Set

$$f(r,s) := -g(r, z-s), \tag{5.38}$$

Let

$$\zeta_n = z - \frac{\xi_\infty}{n}, \tag{5.39}$$

then

$$\zeta_1 \leq \zeta_n < z \quad \text{and} \quad \lim_{n\to\infty} \zeta_n = z.$$

For $h := f_\infty$ with $\theta = z$, $\gamma = z - \alpha_\infty$ and $\zeta_* = z - \xi_\infty$, we can construct a locally Lipschitz function $f_n : \mathbb{R}^+ \longrightarrow \mathbb{R}$ satisfying

$$f_n(s) = f_\infty(s) \text{ on }]-\infty, z-\alpha_\infty] \cup [z, \infty[\quad \text{and} \quad f_n(s) < f_\infty(s) \text{ on }]z-\alpha_\infty, z[.$$

In fact, if $h := f_n$ then $\theta = z$, $\gamma = z - \alpha_\infty$ and

$$\zeta_* = \zeta_n < z.$$

Applying Theorem 5.21 with $h = f_n$, there exists, for R sufficiently large, a radially symmetric positive solution v_n of

$$\begin{cases} \Delta u + f_n(u) = 0 & \text{in} \quad B, \\ u = 0 & \text{on} \quad \partial B \end{cases} \tag{5.40}$$

with

$$0 < v_n < z \quad \text{on} \quad B.$$

However, by Remark 5.4, we deduce that

$$\max_B v_n = v_n(0) > \zeta_* = \zeta_n. \tag{5.41}$$

Since

$$f_n \leq f_\infty$$

then v_n is a subsolution of

$$\begin{cases} \Delta u + f_\infty(u) = 0 & \text{in} \quad B, \\ u = 0 & \text{on} \quad \partial B, \end{cases}$$

therefore, by applying Theorem 5.22, we infer the existence of a radially symmetric positive solution w_n of

$$\begin{cases} \Delta u + f(|x|, u) = 0 & \text{in} \quad B, \\ u = 0 & \text{on} \quad \partial B, \end{cases} \tag{5.42}$$

such that

$$\max_B w_n = w_n(0) > \zeta_n. \tag{5.43}$$

Being a radial solution of (5.42), and by (5.38), the function w_n satisfies

$$\begin{cases} -w_n''(r) - \dfrac{N-1}{r} w_n'(r) = -g(r, z - w_n(r)) \quad \text{for} \quad 0 < r < \infty \\ w_n(0) > \zeta_n, \quad w_n(R) = 0 \quad \text{and} \quad w_n'(0) = 0. \end{cases}$$

We take

$$u_n = z - w_n,$$

then u_n clearly satisfies

$$\begin{cases} -u_n''(r) - \dfrac{N-1}{r} u_n'(r) = g(r, u_n(r)) \quad \text{for} \quad 0 < r < \infty \\ 0 < u_n(0) < z - \zeta_n, \quad u_n(R) = z \quad \text{and} \quad u_n'(0) = 0. \end{cases}$$

For every integer $n \geq 1$, let

$$\xi_n = u_n(0)$$

then the previous equation leads

$$\xi_n \in S^+$$

and, by (5.39),

$$\xi_n < z - \zeta_n = \frac{\xi_\infty}{n},$$

hence

$$\lim_{n \to \infty} \xi_n = 0,$$

and this terminates the proof. ■

Remark 5.6. *The question about whether the solution $u(\cdot, \xi)$, $\xi \in S^+$, will converge (or oscillate) around z remains open. This could be interpreted as a kind of attractiveness towards the equilibrium. Similar problems in this context on open balls can be found in [21–23].*

At last it remains to show that S^+ and S^- are both open. This is done by using the continuous dependence of $u(r, \xi)$ and $u'(r, \xi)$ on the initial data ξ. More precisely we prove

Lemma 5.5. *The sets $S^\pm$ are open in $\mathbb{R}$.*

Proof. We only show the openness of S^- as the proof that S^+ is open is quite identical. Let $\xi \in S^-$, then

$$r_* = \inf\{r > 0;\, u'(r, \xi) = 0\} > 0$$

and

$$u'(r,\xi) > 0 \quad \text{for all} \quad r \in]0, r_*[.$$

From (5.3) we deduce that $u''(r_*,\xi) = -g(r_*, u(r_*,\xi))$. We claim that $u''(r_*,\xi) \neq 0$. If not, then as u is bounded from below and $u(r_*,\xi) < z$, we get

$$u(r_*,\xi) = \alpha_* \quad \text{and} \quad u'(r_*,\xi) = 0,$$

and hence, by a uniqueness argument: $u = \alpha_*$, which is impossible. Since $u'(r,\xi) \searrow 0$ when $r \nearrow r_*$, then $u''(r_*,\xi) < 0$ and therefore there exists a number $r_1 > r_*$ such that

$$u(r,\xi) < u(r_*,\xi) \quad \text{for all} \quad r \in]r_*, r_1].$$

Now by a continuity argument, we can easily see that for η near ξ we have

$$\begin{cases} u(r_1,\eta) < u(r_*,\eta), \\ \eta < u(r,\eta) < z \quad \text{for all} \quad r \in]0, r_1]. \end{cases}$$

This points out that $\eta \in S^-$ and hence S^- is open. ■

Proof of Theorem 5.20. Directly follows from (5.31) together with Lemma 5.2, Lemma 5.3, Lemma 5.4 and Lemma 5.5. ■

6

Conclusion

We are what we repeatedly do. Excellence then is not an act but a habit.

– Will Durant

Our work in this thesis is divided into two main parts. In the first part, we study the inverse source problem for wave equation and its application to medical imaging. We mainly concentrate our work on the photo-acoustic and thermo-acoustic tomography problems (PAT and TAT). The purpose of this thesis is to reconstruct small inhomogeneities (tumor cells) in the imaged biological tissues. We give a direct reconstruction method based on the algebraic algorithm developed first in [34], which enables us to localize the tumors and provides us by some diagnostic information.

PAT and TAT are two medical imaging techniques based on the photo-acoustic effect (generation of sound from light). In both models, the object is illuminated by an optical wave, which is absorbed by the biological tissues and converted into heat, causing thermal expansion of the tissues and generation of acoustic waves. These waves are then measured by transducers located at the boundary of the object, and an image is produced. The main difference between the two imaging techniques is in the type of the optical pulse used, which makes some differences in the mathematical modeling of the problem. In PAT, a high frequency radiation is delivered into the biological tissues to be imaged, while in TAT a low frequency radiation is used. The main tool of such imaging techniques is the difference in energy absorption between healthy tissues and cancerous ones.

The inverse problem we are interested in consists in locating the absorbers (tumors) from the measured acoustic signals at the boundary. Different methods are used in literature for solving the problem, which mostly follow the so called quantitative photo-acoustic tomography approach (qPAT). The idea behind this approach is to divide the inverse problem into two inversions: the acoustic inversion, and the optical inversion. However, this approach involves many difficulties leading to the ill-posedness of the inverse map.

In our work, we don't follow the qPAT approach, however, we develop a new reconstruction

method based on the algebraic algorithm. This algorithm was first developed in [34]. It provides us by useful algebraic relations between the boundary observations and the unknowns, which permits us to reconstruct the number of the absorbers and their locations using only a single Cauchy data. This algorithm is based on the idea of the *reciprocity gap functional*, and special solutions of the adjoint wave equation, which are the main tools used throughout this thesis to solve the both PAT and TAT inverse problems. Moreover, an important tool used in our work throughout this thesis is the exact controllability for wave equation. For this purpose, we recall in Chapter 2 the work of J.L. Lions in [60] on the exact controllability for wave equation with constant speed. Moreover, we follow the same algorithm followed by Lions to study the case of variable speed.

In Chapter 3, we concentrate our work on the TAT problem. In this case, a low frequency radiation is delivered into the biological tissue to be imaged, at which a high difference in conductivity between healthy tissues and cancerous ones is detected. The inverse problem we are interested in consists in determining the conductivity coefficient σ from the measurement of the acoustic pressure at the boundary. More precisely, we assume that the conductivity coefficient is defined piece-wisely in sub-domains w_j that denote the tumors, which is relatively higher than that in the background medium. We assume that $w_j = \mathbf{S}_j + \epsilon B_j$, where $\mathbf{S}_j$ are the centers, B_j represent background mediums containing the origin, and ϵ is the diameter, assumed to be smaller than 1. We establish a direct algebraic algorithm that allows us to determine the number of the sub-domain w_j, their centers $\mathbf{S}_j$, and some information related to the conductivity coefficient. These unknowns are all recovered up to an estimation error $O(\epsilon^{K+4})$. The main idea of this algorithm is the projection of the problem onto well-chosen test functions. Moreover,we provide a Hölder stability estimate of the reconstruction of the centers $\mathbf{S}_j$. The reconstruction algorithm is affected by several factors. First, it is necessary to have a priori information on the number of sources, in particular, we assume that we know an upper bound of the number of sources. Moreover, the reconstruction algorithm depends on the conductivity of the background medium, in particular, on how much σ_0 is small. Also, we realize that the conductivity of the background medium plays an important role on the generalization of the problem to higher dimensions. Furthermore, the separability coefficient of the centers $\mathbf{S}_j$ defined in (3.55) highly contributes in the resolution of the problem, in particular, in the stability of the reconstruction algorithm. Finally, this algorithm is also affected by the closeness of the centers $\mathbf{S}_j$ to the boundary Γ.

In Chapter 4, we study the PAT problem. Unlike the TAT, in PAT a high frequency radiation is used, which is characterized by its high speed compared to that of the acoustic waves. These radiations are known to satisfy the so called *stress confinement condition* (the complete energy is assumed to be deposited instantaneously compared to the travel time of the acoustic waves), which leads to some differences in the mathematical context of the problem. First, the high

frequency radiation used in this case corresponds to the absorption spectrum of hemoglobin, which is known to be an important absorbing molecule in human body. In fact, in our body there are certain molecules that are responsible for energy absorption such as hemoglobin and melanin, and medically speaking, tumors are known to be highly saturated with hemoglobin which enhances energy absorption in such tissues. The inverse problem we are interested in is thus the reconstruction of the absorption coefficient which highly differs between healthy tissues and cancerous ones. Furthermore, the stress confinement condition satisfied in this case allows us to assume that the acoustic pressure is generated initially, which facilitates the inversion procedure and enables us to consider the problem in a more general case. In other words, we give our results in both cases of constant variable acoustic speed, and with partial boundary observations on a non-empty subset Γ_0 of the boundary Γ, which is chosen to satisfy certain geometric conditions. This can be done by means of the exact controllability problem explained in Chapter 2. We follow an algebraic algorithm similar to that used in the TAT problem in order to reconstruct the absorption coefficient μ_a defined piece wisely in sub-domains $w_j = \mathbf{S}_j + \epsilon B_j$. As in the previous problem, the algebraic algorithm allows us to directly reconstruct, up to an estimation error $O(\epsilon^{K+4})$, the number of the absorbers w_j and their centers $\mathbf{S}_j$. Moreover, we reconstruct the absorbed electromagnetic energy by each absorber in case of constant acoustic speed. Again, the reconstruction algorithm relies on the knowledge of an upper bound of the number of absorbers, in addition to the absorption coefficient in the background medium, which is chosen to be relatively small compared to that of the tumors. Finally, we end up with the corresponding stability estimate.

The second part of this thesis is dedicated to the study of semilinear elliptic equations of the form $\Delta u + g(|x|, u) = 0$ in $\mathbb{R}^N$. In particular, we study, under some conditions on the nonlinearity g, the existence of radial solutions with prescribed limit $z = u(\infty) > 0$, satisfying $g(|x|, z) = 0$ for every $x \in \mathbb{R}^n$. The existence of radial solutions for semilinear elliptic equations was highly discussed in literature, in particular solutions that vanish at ∞. However, the existence of non vanishing solutions at ∞, in particular solutions satisfying $\lim\limits_{|x|\to\infty} u(x) = z < \infty$ $(z \neq 0)$ was rarely discussed. In [70], the authors have addressed this idea with equations of the form $\Delta u + g(u) = 0$. They proved, for specific functions g, the existence of oscillating solutions that converge to a positive root α of g. In [49], the authors have developed an ODE based method to prove, under some conditions on g, the existence of monotonically increasing, radial solutions with prescribed limiting behavior. In this thesis, we revisit the work of [49] to prove the existence of such solutions for $g = g(|x|, u)$. We develop an ODE based method, in particular we rewrite the equation in the form

$$\begin{cases} -u'' - \dfrac{N-1}{r}u' = g(r,u) \quad \text{for} \quad 0 < r < \infty \\ u(0) = \xi, \quad u'(0) = 0, \end{cases}$$

and we prove that for specific functions g (see figure 5.1) there exists $\xi > 0$ such that the solution u satisfies

$$\lim_{|x|\to\infty} u(x) = z,$$

where $z > 0$ is chosen such that $g(r, z) = 0$ for every $r > 0$.

The presented work in this thesis has been realized as a part of Multi-Ondes project receiving financial support from ANR-France

Bibliography

[1] Abdelaziz, B., El Badia, A., and El Hajj, A. (2015). Direct algorithm for multipolar sources reconstruction. *Journal of Mathematical Analysis and Applications*, **428**(1), 306–336.

[2] Abdelaziz, B., El Badia, A., and El Hajj, A. (2017). Some remarks on the small electromagnetic inhomogeneities reconstruction problem. *Inverse Problems & Imaging*, **11**(6), 1027–1046.

[3] B. Abdelaziz, Algorithmes directs pour résoudre quelques problèmes inverses de sources (Doctoral Dissertation), (2014) Université de Technologie de Compiègne, France.

[4] Agranovsky, M. and Kuchment, P. (2007). Uniqueness of reconstruction and an inversion procedure for thermoacoustic and photoacoustic tomography with variable sound speed. *Inverse Problems*, **23**(5), 2089.

[5] Ammari, H., Asch, M., Bustos, L. G., Jugnon, V., and Kang, H. (2011). Transient wave imaging with limited-view data. SIAM Journal on Imaging Sciences, 4(4), 1097-1121.

[6] Ammari, H., Bossy, E., Jugnon, V., and Kang, H. (2010). Mathematical modeling in photoacoustic imaging of small absors. *SIAM review*, **52**(4), 677–695.

[7] Ammari, H., Bossy, E., Jugnon, V., and Kang, H. (2011). Reconstruction of the optical absorption coefficient of a small absorber from the absorbed energy density. *SIAM Journal on Applied Mathematics*, **71**(3), 676–693.

[8] Ammari, H., Bretin, E., Jugnon, V., and Wahab, A. (2012). Photoacoustic imaging for attenuating acoustic media. In *Mathematical modeling in biomedical imaging II*, pages 57–84. Springer.

[9] Bal, G. and Ren, K. (2011). Multi-source quantitative photoacoustic tomography in a diffusive regime. *Inverse Problems*, **27**(7), 075003.

[10] Bal, G., and Ren, K. (2012). On multi-spectral quantitative photoacoustic tomography in diffusive regime. Inverse Problems, 28(2), 025010.

[11] Bal, G., Jollivet, A., and Jugnon, V. (2010). Inverse transport theory of photoacoustics. *Inverse Problems*, **26**(2), 025011.

[12] Bal, G., and Uhlmann, G. (2010). Inverse diffusion theory of photoacoustics. Inverse Problems, 26(8), 085010.

[13] Bal, G., Ren, K., Uhlmann, G., and Zhou, T. (2011). Quantitative thermo-acoustics and related problems. *Inverse Problems*, **27**(5), 055007.

[14] Bardos, C., Lebeau, G., and Rauch, J. (1992). Sharp sufficient conditions for the observation, control, and stabilization of waves from the boundary. *SIAM journal on control and optimization*, **30**(5), 1024–1065.

[15] Belhachmi, Z., Glatz, T., and Scherzer, O. (2016). A direct method for photoacoustic tomography with inhomogeneous sound speed. *Inverse Problems*, **32**(4), 045005.

[16] Berestycki, H. and Lions, P.-L. (1978). Existence d'ondes solitaires dans des problèmes non-linéaires du type Klein-Gordon. *C. R. Acad. Sci. Paris Sér. A-B*, **287**(7), A503–A506.

[17] Berestycki, H. and Lions, P.-L. (1980). Existence of a ground state in nonlinear equations of the Klein-Gordon type. In *Variational inequalities and complementarity problems (Proc. Internat. School, Erice, 1978)*, pages 35–51. Wiley, Chichester.

[18] Berestycki, H. and Nirenberg, L. (1991). On the method of moving planes and the sliding method. *Boletim da Sociedade Brasileira de Matemática-Bulletin/Brazilian Mathematical Society*, **22**(1), 1–37.

[19] Berger, M. S. (1972). On the existence and structure of stationary states for a nonlinear Klein-Gordon equation. *J. Functional Analysis*, **9**, 249–261.

[20] Bergounioux, M., Bonnefond, X., Haberkorn, T., and Privat, Y. (2014). An optimal control problem in photoacoustic tomography. *Mathematical Models and Methods in Applied Sciences*, **24**(12), 2525–2548.

[21] Bonheure, D., Grossi, M., Noris, B., and Terracini, S. (2016a). Multi-layer radial solutions for a supercritical neumann problem. *Journal of differential equations*, **261**(1), 455–504.

[22] Bonheure, D., Grumiau, C., and Troestler, C. (2016b). Multiple radial positive solutions of semilinear elliptic problems with neumann boundary conditions. *Nonlinear Analysis: Theory, Methods & Applications*, **147**, 236–273.

[23] Boscaggin, A., Colasuonno, F., and Noris, B. (2018). Multiple positive solutions for a class of p-laplacian neumann problems without growth conditions. *ESAIM: Control, Optimisation and Calculus of Variations*, **24**(4), 1625–1644.

[24] Cazenave, T. (2006). An introduction to semilinear elliptic equations. *Editora do IM-UFRJ, Rio de Janeiro*.

[25] Chung, Y.-S. and Chung, S.-Y. (2009). Identification of the combination of monopolar and dipolar sources for elliptic equations. *Inverse problems*, **25**(8), 085006.

[26] Chung, Y.-S., Kim, J., and Chung, S.-Y. (2012). Identification of multipoles via boundary measurements. *European Journal of Applied Mathematics*, **23**(2), 289–313.

[27] Clason, C. and Klibanov, M. V. (2008). The quasi-reversibility method for thermoacoustic tomography in a heterogeneous medium. *SIAM Journal on Scientific Computing*, **30**(1), 1–23.

[28] Coffman, C. V. (1972). Uniqueness of the ground state solution for $\Delta u - u + u^3 = 0$ and a variational characterization of other solutions. *Arch. Rational Mech. Anal.*, **46**, 81–95.

[29] Cox, B., Laufer, J., and Beard, P. (2009). The challenges for quantitative photoacoustic imaging. In *Photons Plus Ultrasound: Imaging and Sensing 2009*, volume 7177, page 717713. International Society for Optics and Photonics.

[30] Cox, B. T., Arridge, S. R., Köstli, K. P., and Beard, P. C. (2006). Two-dimensional quantitative photoacoustic image reconstruction of absorption distributions in scattering media by use of a simple iterative method. *Applied Optics*, **45**(8), 1866–1875.

[31] Cox, B. T., Laufer, J. G., Beard, P. C., and Arridge, S. R. (2012). Quantitative spectroscopic photoacoustic imaging: a review. *Journal of biomedical optics*, **17**(6), 061202.

[32] Ding, T., Ren, K., and Vallélian, S. (2015). A one-step reconstruction algorithm for quantitative photoacoustic imaging. *Inverse Problems*, **31**(9), 095005.

[33] El Badia, A. and El Hajj, A. (2013). Stability estimates for an inverse source problem of helmholtz's equation from single cauchy data at a fixed frequency. *Inverse Problems*, **29**(12), 125008.

[34] El Badia, A. and Ha-Duong, T. (2000). An inverse source problem in potential analysis. *Inverse Problems*, **16**(3), 651.

[35] El Badia, A. and Ha-Duong, T. (2001). Determination of point wave sources by boundary measurements. *Inverse Problems*, **17**(4), 1127.

[36] Evans, L. C. (2010). *Partial differential equations*, volume 19. American Mathematical Soc.

[37] Finch, D. and Patch, S. K. (2004). Determining a function from its mean values over a family of spheres. *SIAM journal on mathematical analysis*, **35**(5), 1213–1240.

[38] Finch, D., Haltmeier, M., and Rakesh (2007). Inversion of spherical means and the wave equation in even dimensions. *SIAM Journal on Applied Mathematics*, **68**(2), 392–412.

[39] Gao, H., Osher, S., and Zhao, H. (2012). Quantitative photoacoustic tomography. In *Mathematical Modeling in Biomedical Imaging II*, pages 131–158. Springer.

[40] Gidas, B., Ni, W.-M., and Nirenberg, L. (1979). Symmetry and related properties via the maximum principle. *Communications in Mathematical Physics*, **68**(3), 209–243.

[41] Glowinski, R., Li, C.-H., and Lions, J.-L. (1990). A numerical approach to the exact boundary controllability of the wave equation (i) dirichlet controls: description of the numerical methods. *Japan Journal of Applied Mathematics*, **7**(1), 1.

[42] Grün, H., Paltauf, G., Haltmeier, M., and Burgholzer, P. (2007). Photoacoustic tomography using a fiber based fabry-perot interferometer as an integrating line detector and image reconstruction by model-based time reversal method. In *European Conference on Biomedical Optics*, page 6631_6. Optical Society of America.

[43] Gusev, V. E., and Karabutov, A. A. (1991). Laser optoacoustics. STIA, 93, 16842.

[44] Haemmerich, D., Staelin, S. T., Tsai, J.-Z., Tungjitkusolmun, S., Mahvi, D. M., and Webster, J. G. (2003). In vivo electrical conductivity of hepatic tumours. *Physiological measurement*, **24**(2), 251.

[45] Haltmeier, M., Scherzer, O., Burgholzer, P., and Paltauf, G. (2004). Thermoacoustic computed tomography with large planar receivers. *Inverse problems*, **20**(5), 1663.

[46] Haltmeier, M., Scherzer, O., Burgholzer, P., Nuster, R., and Paltauf, G. (2007). Thermoacoustic tomography and the circular radon transform: exact inversion formula. *Mathematical Models and Methods in Applied Sciences*, **17**(04), 635–655.

[47] Hristova, Y. (2009). Time reversal in thermoacoustic tomography—an error estimate. *Inverse Problems*, **25**(5), 055008.

[48] Hristova, Y., Kuchment, P., and Nguyen, L. (2008). Reconstruction and time reversal in thermoacoustic tomography in acoustically homogeneous and inhomogeneous media. *Inverse Problems*, **24**(5), 055006.

[49] Ibrahim, H. (2020). Radial solutions of semilinear elliptic equations with prescribed asymptotic behavior. *Mathematische Nachrichten*, page to appear in.

[50] Ibrahim, H. and Nasreddine, E. (2016). Existence of semilinear elliptic equations with prescribed limiting behaviour. *Mathematical Methods in the Applied Sciences*, **39**(14), 4129–4138.

[51] Ibrahim, H. and Nasreddine, E. (2018). On the existence of nonautonomous ode with application to semilinear elliptic equations. *Mediterranean Journal of Mathematics*, **15**(2), 64.

[52] Jacques, S. L. (2013). Optical properties of biological tissues: a review. *Physics in Medicine & Biology*, **58**(11), R37.

[53] Vincent, J. (2010), Modélisation et Simulation en Photo-acoustique, (Doctoral dissertation, École Polytechnique)

[54] Kuchment, P. (2013). *The Radon transform and medical imaging*. SIAM.

[55] Kuchment, P. and Kunyansky, L. (2008). Mathematics of thermoacoustic tomography. *European Journal of Applied Mathematics*, **19**(2), 191–224.

[56] Kunyansky, L. A. (2007). Explicit inversion formulae for the spherical mean radon transform. *Inverse problems*, **23**(1), 373.

[57] Lasiecka, I., Lions, J.-L., and Triggiani, R. (1986). Non homogeneous boundary value problems for second order hyperbolic operators.

[58] Leff, D. R., Warren, O. J., Enfield, L. C., Gibson, A., Athanasiou, T., Patten, D. K., Hebden, J., Yang, G. Z., and Darzi, A. (2008). Diffuse optical imaging of the healthy and diseased breast: a systematic review. *Breast cancer research and treatment*, **108**(1), 9–22.

[59] Li, C., Pramanik, M., Ku, G., and Wang, L. V. (2008). Image distortion in thermoacoustic tomography caused by microwave diffraction. *Physical Review E*, **77**(3), 031923.

[60] Lions, J.-L. (1988). Controlabilité exacte, perturbations et stabilisation de systèmes distribués.

[61] Mehnati, P., Tirtash, M. J., Zakerhamidi, M. S., and Mehnati, P. (2016). Assessing absorption coefficient of hemoglobin in the breast phantom using near-infrared spectroscopy. *Iranian Journal of Radiology*, **13**(4).

[62] Miklavčič, D., Pavšelj, N., and Hart, F. X. (2006). Electric properties of tissues. *Wiley encyclopedia of biomedical engineering*.

[63] Morse, P. M. (1968). Ku ingard, theoretical acoustics. *Princeton University Press, 949p*, **4**, 150.

[64] Naetar, W. and Scherzer, O. (2014). Quantitative photoacoustic tomography with piecewise constant material parameters. *SIAM Journal on Imaging Sciences*, **7**(3), 1755–1774.

[65] Nara, T. (2008). An algebraic method for identification of dipoles and quadrupoles. *Inverse Problems*, **24**(2), 025010.

[66] Nara, T. (2012). Algebraic reconstruction of the general-order poles of a meromorphic function. *Inverse problems*, **28**(2), 025008.

[67] Natterer, F. (2012). Photo-acoustic inversion in convex domains. *Inverse Probl. Imaging*, **6**(2), 1–6.

[68] Nehari, Z. (1963). On a nonlinear differential equation arising in nuclear physics. *Proc. Roy. Irish Acad. Sect. A*, **62**, 117–135 (1963).

[69] Nguyen, L. V. (2009). A family of inversion formulas in thermoacoustic tomography. *arXiv preprint arXiv:0902.2579*.

[70] Ni, W.-M. (1982). On the positive radial solutions of some semilinear elliptic equations on $\mathbb{R}^n$. *Applied Mathematics and Optimization*, **9**(1), 373–380.

[71] Ohe, T., Inui, H., and Ohnaka, K. (2011). Real-time reconstruction of time-varying point sources in a three-dimensional scalar wave equation. *Inverse problems*, **27**(11), 115011.

[72] Pohozaev, S. (1965). Eigenfunctions of the equation δu+ f (u)= 0. In *Dokl. Akad. Nauk SSSR*, volume 165, pages 33–36.

[73] Prost, A., Poisson, F., and Bossy, E. (2015). Photoacoustic generation by a gold nanosphere: From linear to nonlinear thermoelastics in the long-pulse illumination regime. Physical Review B, 92(11), 115450.

[74] Ryder, G. H. (1967). Boundary value problems for a class of nonlinear differential equations. *Pacific J. Math.*, **22**, 477–503.

[75] Scherzer, O. (2010). *Handbook of mathematical methods in imaging*. Springer Science & Business Media.

[76] Smith, S. R., Foster, K. R., and Wolf, G. L. (1986). Dielectric properties of vx-2 carcinoma versus normal liver tissue. *IEEE transactions on biomedical engineering*, (5), 522–524.

[77] Stefanov, P. and Uhlmann, G. (2009). Thermoacoustic tomography with variable sound speed. *Inverse Problems*, **25**(7), 075011.

[78] Stefanov, P. and Uhlmann, G. (2012). Instability of the linearized problem in multiwave tomography of recovery both the source and the speed. *arXiv preprint arXiv:1211.6217*.

[79] Strauss, W. A. (1977). Existence of solitary waves in higher dimensions. *Communications in Mathematical Physics*, **55**(2), 149–162.

[80] Surowiec, A. J., Stuchly, S. S., Barr, J. R., and Swarup, A. (1988). Dielectric properties of breast carcinoma and the surrounding tissues. *IEEE Transactions on Biomedical Engineering*, **35**(4), 257–263.

[81] Triki, F., and Vauthrin, M. (2018). Mathematical modeling of the Photoacoustic effect generated by the heating of metallic nanoparticles.

[82] Vauthrin, M. (2017), Etude de quelques modèles en imagerie photoacoustique (Doctoral dissertation, Université Grenoble Alpes,)

[83] Wang, L. V., and Wu, H. I. (2012). Biomedical optics: principles and imaging. John Wiley and Sons.

[84] Widlak, T. and Scherzer, O. (2015). Stability in the linearized problem of quantitative elastography. *Inverse problems*, **31**(3), 035005.

[85] Xu, M. and Wang, L. V. (2005). Universal back-projection algorithm for photoacoustic computed tomography. *Physical Review E*, **71**(1), 016706.

[86] Xia, J., Yao, J., and Wang, L. V. (2014). Photoacoustic tomography: principles and advances. Electromagnetic waves (Cambridge, Mass.), 147, 1.

[87] Xu, M., and Wang, L. V. (2002). Pulsed-microwave-induced thermoacoustic tomography: Filtered backprojection in a circular measurement configuration. Medical physics, 29(8), 1661-1669.

[88] Yamamoto, M. (1995). Stability, reconstruction formula and regularization for an inverse source hyperbolic problem by a control method. *Inverse problems*, **11**(2), 481.

[89] Yamamoto, M. (1999). Uniqueness and stability in multidimensional hyperbolic inverse problems. *Journal de mathématiques pures et appliquées*, **78**(1), 65–98.

[90] Yao, P.-F. (1999). On the observability inequalities for exact controllability of wave equations with variable coefficients. *SIAM Journal on Control and Optimization*, **37**(5), 1568–1599.

[91] Yao, D. K., Zhang, C., Maslov, K. I., and Wang, L. V. (2014). Photoacoustic measurement of the Grüneisen parameter of tissue. Journal of biomedical optics, 19(1), 017007.

[92] Zhou, Y., Yao, J., and Wang, L. V. (2016). Tutorial on photoacoustic tomography. Journal of biomedical optics, 21(6), 061007.